Identification and characterization of a genomic region involved in *Drosophila* gastrulation

Inaugural-Dissertation

zur

Erlangung des Doktorgrades
der Mathematisch-Naturwissenschaftlichen Fakultät

der Universität zu Köln

vorgelegt von

Sam Jacob Mathew

aus Kerala, Indien

Köln, Dezember 2005

1. Berichterstatter:

Prof. Dr. Maria Leptin

2. Berichterstatter:

Prof. Dr. Diethard Tautz

Tag der mündlichen Prüfung: 07 Februar 2006

Table of Contents

Table of contents

1. Introduction

1.1 Gastrulation: An overview

Early embryonic development in various members of the animal kingdom, from sponges to higher vertebrates begins from the single celled zygote, which undergoes cell division to give rise to a hollow ball of cells, the blastula (Stern, 2004). This hollow ball of cells are remodelled to give rise to the three germ layers (two in sponges), the ectoderm, endoderm and mesoderm by the process of gastrulation. Although this is a generalized view, gastrulation essentially is the process by which the germ layers are established (Leptin, 2005). This involves a combination of different processes involving axes determination, fate specification, cell movements and cytoskeletal rearrangements, cell signalling, cell cycle regulation and so on.

1.2 Gastrulation in *Drosophila*

The process of gastrulation has been extensively investigated in *Drosophila*. It is relevant to understand the processes preceding gastrulation to appreciate gastrulation itself. After fertilization, the single celled zygote undergoes thirteen rounds of nuclear division resulting in a syncytial blastoderm (Campos-Ortega and Hartenstein, 1985). The syncytial blastoderm is converted into a cellular blastoderm by the process of cellularization, during which the plasma membrane invaginates between individual nuclei (reviewed by Lecuit, 2004). It is at this stage, about 3 hours after fertilization that the process of gastrulation begins. The initial step in gastrulation is the invagination of the mesoderm by forming a furrow on the ventral side, the ventral furrow. The already specified mesodermal cells migrate into the embryo and make up part of a tubular structure called the germ band, which then undergoes characteristic elongation and retraction movements. The germ band is composed of ectodermal as well as mesodermal cells (Sonnenblick, 1950). Later on, the mesodermal cells start dividing and migrate out on the underlying

ectoderm and give rise to mesodermal structures, namely somatic and visceral muscles, dorsal vessel and fat body (Campos-Ortega and Hartenstein, 1985).

Gastrulation also includes the invagination of the endoderm. The endoderm invagination happens in two regions of the embryo almost immediately after ventral furrow formation has started, one at the anterior ventral part and the other at the posterior pole (Campos-Ortega and Hartenstein, 1985). The primordia that invaginate in these two regions later on contact each other and fuse to give rise to the midgut (Campos-Ortega and Hartenstein, 1985).

The work discussed here will focus on the first step in gastrulation namely ventral furrow invagination.

1.3 Ventral furrow formation- the mechanism

Ventral furrow formation, the first step in gastrulation, starts after the process of cellularization has been completed. The first sign of ventral furrow formation is a flattened zone of cells, about 18 cells wide and 60 cells long, the prospective mesodermal cells, on the ventral side of the embryo (Leptin and Grunewald, 1990; Sweeton *et al*., 1991). Within this domain, cells lose their 'cobblestone' appearance and become more closely apposed along their entire length (Sweeton *et al*., 1991). More pronounced changes commence over a period of 10-15 minutes. The cells constrict their apical sides to become wedge shaped and then shorten along their apical-basal axis (Figure 1F, G, J and K). The mid-ventral cells (approximately 12 cells in width) also begin to form membranous blebs or ruffles on the surface when the apices of these cells constrict, indicating that the apical surface area lost is displaced into these blebs (Sweeton *et al*., 1991). It has been shown that not all ventral cells constrict their surfaces simultaneously, but individual cells begin to constrict stochastically, followed by others over a period of about 10 minutes (Kam et al., 1991; Oda and Tsukita, 2001; Sweeton *et al*., 1991). This is restricted to the more ventral part of the embryo (blue region in Figure 1 E, F, G), with the lateral parts never undergoing constriction (yellow region in Figure 1 E, F, G), indicating a subdivision of the mesoderm into two populations (Leptin and Grunewald,

1990). As a result of these changes, the blastoderm epithelium invaginates to form the ventral furrow, which is then completely internalized and forms the germ band (reviewed by Leptin, 1999).

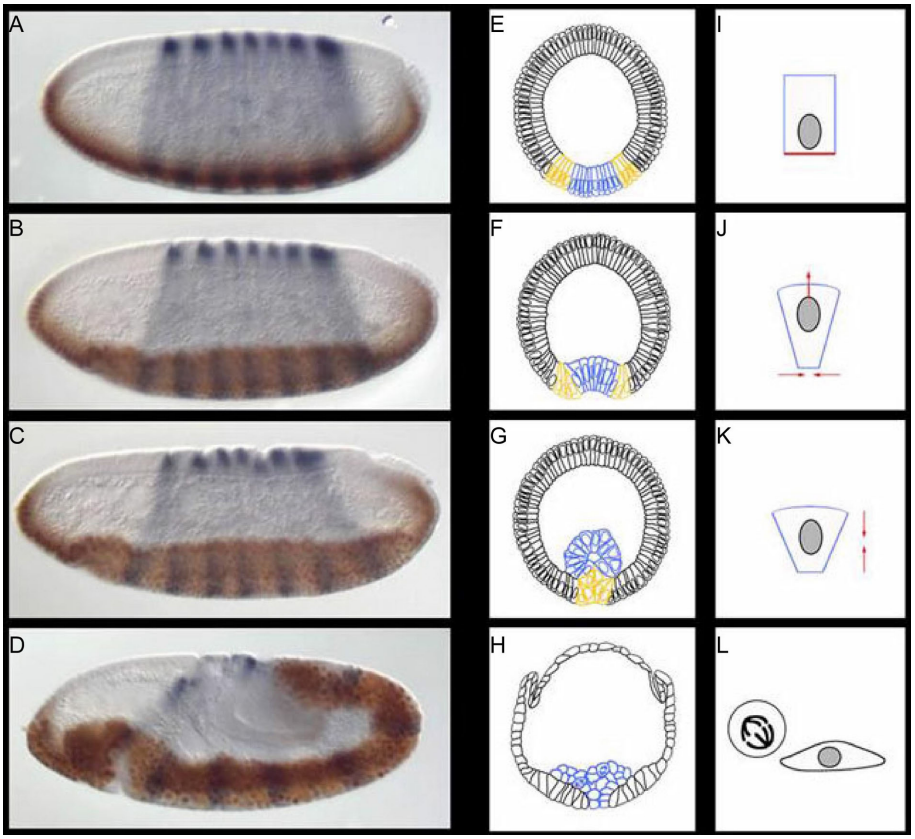

Figure 1: Figure representing progressive stages of gastrulation in *Drosophila* and the changes associated with each stage at the cellular level. A, B, C and D are Drosophila embryos stained with anti-Twist (brown) and anti-Even skipped (blue stripes) antibodies. Twist marks the mesoderm and the embryos shown here represent pre-gastrulation (A), ventral furrow forming (B and C) and germ band extending (D) embryos. E, F, G and H are schematic representations of cross sections through embryos of each stage shown in A, B, C and D. The blue and yellow shaded regions correspond to the Twist positive ventral region of the embryos with the blue part expressing higher Twist levels and the yellow part lower levels. The ventral indentation signalling ventral furrow formation can be clearly seen in F and the germ band in G (blue and yellow tubular structure). The germ band has started spreading (blue part) on the ectoderm in H. The events happening at the cellular level in a ventral cell is exemplified in the schematic I, J, K and L. Prior to gastrulation, the ventral cells undergo flattening on their apical side, indicated by the red border in I. Then, constriction of the apical sides happen (arrows pointing at each other), pushing the previously apically placed nucleus basally (arrow) as shown in J. This force helps in invagination of the mesoderm. Afterwards, the cells contract in an apico-basal manner (arrows pointing at each other in K) and become shortened (K). These changes are sufficient to allow these cells to migrate into the embryo and form the germ band. Later on, they lose their epithelial structure, start dividing and migrate on the ectoderm (L). Figure courtesy of Leptin (Leptin, 1999).

Mathematical modelling has indicated that apical constriction resulting in the cell shape changes described above is sufficient to drive the formation of the invagination (Odell *et al*., 1981). Once inside the embryo, the mesoderm primordium loses its epithelial structure and disperses into single cells which divide, attach to the ectoderm and subsequently migrate out on the ectoderm as a single cell layer (Beiman *et al*., 1996; Vincent *et al*., 1998).

1.4 Genes involved in ventral furrow formation

Both maternal and zygotic molecules are required for the processes described above to happen in a temporally and spatially controlled manner. Maternal molecules refer to the gene products, either RNA or protein, deposited in the embryo during oogenesis by the mother. These molecules are sufficient for early events in development (about 2 hours AEL in *Drosophila*), after which the zygotic transcriptional machinery becomes active (reviewed in Leptin, 1999). The maternally contributed molecules known to play a role in gastrulation as well as the zygotic components involved are discussed below.

1.4.1 Maternal genes

Several known maternal effect genes are required for normal patterning of the embryo so as to generate proper cell fates. These include genes like *dorsal* and *toll* which are essential to maintain proper dorso-ventral cell fates by activating zygotic genes such as *twist* and *snail* (discussed in the next section). Mutations have been isolated in the *toll-dorsal* signalling cascade, which dorsalize or ventralize the entire embryo, depending on the nature of the mutation and the function of the particular molecule in the pathway (reviewed by Moussian and Roth, 2005). Thus, these molecules function by restricting transcription of the zygotic fate determining genes to specific domains in the embryo.

The second category of maternally provided molecules include the components of the actin cytoskeleton and associated regulatory molecules. These molecules are required

during oogenesis as well as for processes like cellularization. Therefore, mutations in such molecules disrupt earlier processes where they are required, making it difficult to study their exact role in ventral furrow formation. Actin isoforms as well as actin binding proteins have been shown to be present in the early embryo (Miller *et al*., 1989). Myosin, which regulates cell shape changes in a wide variety of organisms, has been shown to be dynamically localized during gastrulation (Young *et al*., 1991; Dawes-Hoang *et al*., 2005). Studies suggest that the cell shape changes necessary for ventral furrow formation might be accomplished through regulating myosin and thereby the actin cytoskeleton. Evidence in this regard has been accumulating in recent years which suggested a pathway regulating myosin during gastrulation. Two such regulatory molecules were the small GTP binding protein Rho1 and its exchange factor RhoGEF2, reported to be required for normal gastrulation (Barrett *et al*., 1997; Hacker and Perrimon, 1998). Recently, the Rho effector, Rho-kinase or *Drok* has also been shown to be required for gastrulation (Dawes-Hoang *et al.,* 2005).

Another maternal effect gene identified several years ago and shown to be involved in gastrulation is *concertina* (*cta*), the alpha subunit of a heterotrimeric G protein (Parks and Wieschaus, 1991). *cta* has been shown to affect cell shape changes and function downstream of a zygotic gene, *folded gastrulation* or *fog* (discussed in the next section). A pathway had been proposed for activation of Cta by Fog, through an as yet unidentified receptor (Costa *et al*., 1994). Recently, an interaction partner of the Gα-subunit of heterotrimeric G proteins, Ric-8 was identified and also shown to be involved in gastrulation (Hampoelz *et al*., 2005). Results from recent studies support a model for dynamic myosin localization during ventral furrow formation according to which signalling by Fog through the unidentified G protein coupled receptor would activate the Gα-subunit Concertina (Morize *et al*., 1998; Dawes-Hoang *et al.,* 2005). This signal is then relayed to Rho1 through RhoGEF2 and myosin localization or activation is achieved through the effector Drok (Dawes-Hoang *et al.,* 2005). However, the phenotype exhibited by embryos lacking *cta* is weaker compared to that of embryos lacking RhoGEF2,

suggesting that multiple signalling inputs might converge at the level of RhoGEF2 (Dawes-Hoang *et al.,* 2005).

Other maternally provided components that might be required for actin cytoskeleton remodelling would be junctional components like Armadillo (β-Catenin), other Catenins, Cadherins and actin binding proteins such as Diaphanous and Spectrin (Hunter and Wieschaus, 2000; Wang *et al*., 2004; Dawes-Hoang *et al.,* 2005).

1.4.2 Zygotic genes

Two zygotic genes identified several years ago, essential for ventral furrow formation are *twist* and *snail* (Grau *et al*., 1984; Nusslein-Volhard *et al*., 1984; Thisse *et al*., 1987). Both of these genes are transcriptionally activated by the nuclear gradient of the maternal gene product Dorsal, and are expressed on the ventral side of the embryo (reviewed by Reuter and Casal, 1994). *snail* (*sna*) encodes a zinc-finger protein that represses ectodermal fates in the mesoderm primordium whereas *twist* (*twi*) encodes a bHLH protein that acts as an activator of genes in the mesoderm (Kosman *et al*., 1991; Leptin, 1991; Kasai *et al.,* 1992; Nibu *et al.,* 1998). In other words, *twist* and *snail* are the two zygotic mesodermal fate determining genes.

Embryos mutant for either *twi* or *sna* exhibit severe gastrulation defects, detectable at the earliest stages of cell shape changes. Instead of the normal succession of apical flattening and constriction, displacement of nuclei and cell shortening along the apical-basal axis, only some of these processes occur in mutant embryos. In *sna* mutants, the ventral epithelium becomes very thin suggesting that shortening of cells occur, but no apical constriction is seen at all and only rudiments of a furrow forms (reviewed by Leptin, 1999). In *twi* mutants, ventral cells become narrow at their apical ends and nuclei move away from the apical side. As a result, a narrow and shallow furrow is formed. However, neither strong apical constriction nor cell shortening occurs, and the furrow fails to invaginate fully (reviewed by Leptin, 1999). Since Twist is required for the maintenance of *sna* expression in the mesoderm, the defects in *twi* mutants might in part be due to a reduction in Snail function. Indeed, when additional Snail is provided in the prospective mesoderm, the *twi* mutant phenotype is alleviated (Ip *et al*., 1994). However, the ventral

furrow is not restored to a normal appearance, suggesting that *twi* also has *sna* independent functions. This was confirmed by the analysis of embryos mutant for both genes. In such embryos, no processes characteristic of mesodermal cells occur at all and the gene expression patterns of the ventral cells are identical to those in the neighbouring neural ectoderm. Thus, Twist and Snail jointly control the activation of the molecules that mediate cell-shape changes in the ventral furrow (reviewed by Leptin, 1999).

The lateral borders of *sna* but not of *twi* expression precisely mark the lateral boundaries of the mesoderm primordium (Leptin, 1991). In *sna* mutants, expression of several ectodermal genes extend into the mesoderm, indicating that Snail is required to repress ectodermal fates (Leptin, 1991). However, there are a few examples of genes that require Snail for their expression in the mesoderm, such as *zfh1* (Casal and Leptin, 1996). Twist, on the other hand is thought to activate genes such as *fog* in the mesoderm in order to maintain mesodermal identity (Leptin, 1991).

The anterior and posterior borders of the mesoderm primordium are not directly defined by the expression of *twi* or *sna* but are established by the activity of the terminal gap gene, *huckebein* (*hkb*) (Reuter and Leptin, 1994). *hkb* is expressed at both termini of the blastoderm. Within the posterior region of the embryo, *hkb* determines the border of the mesoderm by repressing *sna* expression whereas at the anterior region of the embryo, *hkb* does not repress *sna* because the maternal morphogen *bicoid* counteracts the repressive effect of *hkb* on *sna* (Reuter and Leptin, 1994). Nevertheless *hkb* antagonizes the effect of *sna* and *twi* on mesodermal target genes and thereby establishes the anterior border of the mesoderm primordium (Reuter and Casal, 1994).

Several target genes of Twist have been identified previously and one such target, *folded gastrulation* (*fog*), is known to be involved in gastrulation (Zusman and Wieschaus, 1985). *fog*, which codes for a secreted protein, is first expressed transiently in the prospective ventral furrow and a few minutes later in the posterior pole of the embryo (Costa *et al*., 1994). Embryos mutant for *fog* show the same phenotype as those lacking functional Concertina protein, where cell shape changes during ventral furrow formation are disorganized and proceed in an uncoordinated manner (Costa *et al*., 1994). Further, it

has been shown that activating the *fog*/*cta* pathway results in ectopic cell shape changes (Morize *et al*., 1998). Evidence from recent work has led to a model for cell shape changes during gastrulation wherein Fog induced activation of Concertina leads to myosin localization or activation, suggesting that *fog* is an important member in the cascade triggering the cell shape changes responsible for ventral furrow formation (Dawes-Hoang *et al*., 2005). However, although delayed and disrupted, the ventral furrow does form in *fog* mutant embryos, indicating the presence of at least one parallel pathway controlling cell shape changes during ventral furrow formation (Costa *et al*., 1994; Dawes-Hoang *et al*., 2005; personal communication from Koelsch, V).

Another category of zygotic genes that are involved in ventral furrow formation are the cell cycle regulators, *tribbles* (*trbl*), *fruhstart* (*frs*) and *held out wings* (*how*) (Grosshans and Wieschaus 2000; Mata *et al*., 2000; Seher and Leptin, 2000; Grosshans *et al*., 2003; Nabel-Rosen *et al*., 2005). Although the gene product of *how* is supplied maternally, zygotic mutant embryos exhibit similar defects as embryos lacking the maternal *how* gene product (Nabel-Rosen et al., 2005) and hence it is included in the category of zygotic genes. In embryos mutant for any of these three genes, ventral furrow formation is delayed and uncoordinated. This is because these three genes function to block cell division in the mesoderm during the process of ventral furrow invagination by regulating the activity of the mitotic inducer *cdc25* or *string* (*stg*). In accordance with this, it has been shown that embryos mutant for these genes enter mitosis prematurely (Grosshans and Wieschaus 2000; Mata *et al*., 2000; Seher and Leptin, 2000; Grosshans *et al*., 2003; Nabel-Rosen *et al*., 2005). One reason why morphogenesis and cell division might be mutually exclusive events might be because both processes require reorganization of the actin cytoskeleton.

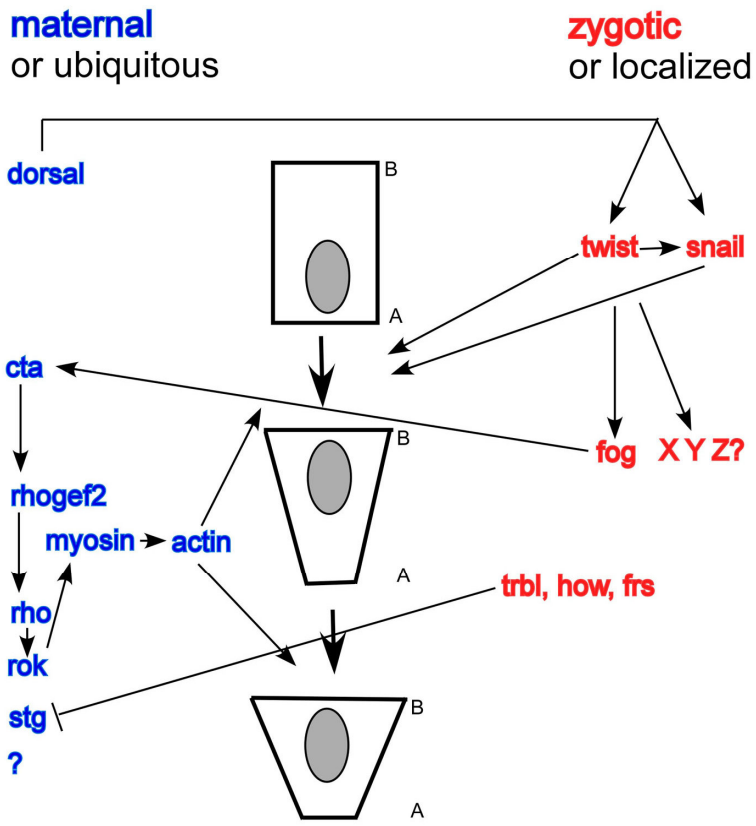

Figure 2: A schematic representing the known maternal and zygotic molecules involved in ventral furrow formation: A ventral cell undergoing cell shape changes in the process of furrow formation is represented, with the grey oval being the nucleus. The apical and basal poles are represented by A and B respectively adjacent to the cell. The maternal factors are shown in blue and the zygotic, in red. The initial step is Dorsal mediated activation of Twist and Snail, the zygotic cell fate determinants. Twist maintains *snail* expression and also activates other targets, notably the secreted molecule Fog, which binds an unidentified G protein coupled receptor activating Cta, the α subunit of a heterotrimeric G protein. This activates a Rho signalling cascade mediated by RhoGEF2, Rho1 and ROK, which in turn activates or localizes myosin, thought to mediate actin cytoskeletal movements culminating in the cell shape changes. However, a fog independent pathway must exist, as fog mutants can generate a ventral furrow, components of which are represented by the X, Y, Z notations. The other molecules represented are *trbl*, *how* and *frs*, which help in regulating cell cycle during ventral furrow formation by preventing the action of *stg*. Figure modified from Leptin, 1999.

A model representing most of the molecules involved in ventral furrow formation mentioned so far is depicted in Figure 2. The initial event of activation of the zygotic determinants *twi* and *sna* is achieved by a nuclear gradient of Dorsal. Twist maintains the expression of *sna* and also activates downstream targets such as *fog*. Fog is a secreted

protein which activates a G protein signalling cascade through the Gα subunit Concertina. Concertina is maternally provided and is thought to trigger a Rho signalling cascade mediated by RhoGEF2, Rho1 and ROK, culminating in myosin localization or activation (Dawes-Hoang *et al*., 2005). However, a *fog* independent pathway for ventral furrow formation must exist as *fog* mutants generate a ventral furrow, albeit delayed. Components of such a pathway are represented by the X, Y, Z notations in Figure 2. These are most likely *twist* targets because the known *twist* targets are unable to reproduce the *twist* loss of function phenotype (Seher and Leptin, unpublished). Zygotic factors such as *trbl*, *frs* and *how* are known to block cell division during ventral furrow formation, by negatively regulating the activity of *stg* (Figure 2). Other factors such as junctional components and actin binding proteins have not been represented in this model.

1.5 Genetic screens to identify genes involved in early development

Most of the genes described above, both maternal and zygotic, affecting ventral furrow formation and gastrulation were identified in large-scale screens for loss of function phenotypes (Nusslein-Volhard *et al*., 1980; Nusslein-Volhard and Wieschaus, 1980; Simpson, 1983; Nusslein-Volhard *et al*., 1984; Zusman and Wieschaus, 1985). Some of the early studies on genes such as *fog*, located on the X chromosome were done using an unstable ring X chromosome to generate gynandromorphs (Zusman and Wieschaus, 1985).

It was clear that some loci required during early embryonic development would have been missed in the large scale mutagenesis screens, as evidenced by earlier observations that embryos lacking the entire X chromosome become abnormal prior to cellularization (Poulson, 1940). Wieschaus and Sweeton, in a modification of the genetic technique used to generate gynandromorphs (Zusman and Wieschaus, 1985), utilized the availability of X chromosome to Y translocations and generate embryos that lacked the entire X chromosome (Wieschaus and Sweeton, 1988). Further, they were able to generate embryos deficient for smaller overlapping regions of the X chromosome, thereby

narrowing down the genomic stretch responsible for the defects, culminating in identification of the locus (Wieschaus and Sweeton, 1988).

In a further refinement of the aforementioned strategy, a genetic screen was designed and carried out in order to identify early requirements for autosomal zygotic gene activity, obtaining maximum coverage of the genome as possible at that time (Merrill *et al*., 1988). The strategy was novel and simple, using compound autosomes and autosome -Y translocations, in order to generate embryos deficient for overlapping regions of each autosome until the entire chromosome arm was covered (Merrill *et al*., 1988). The advantage of this technique was that maternal effects would not skew the nature of the embryonic defects observed, as the mothers used (compound autosome stocks) have the complete chromosomal complement (Rasmussen, 1960).

A schematic representing how the chromosomal segregation pattern occurs in a compound autosomal stock is shown in Figure 3. The left arms of the chromosome are represented in blue and the right arms in red, with the centromere depicted as a black dot in between. Unlike normal stocks where one left arm is attached to one right arm, in the compound stock, both left arms are attached to each other, as are the two right arms (Rasmussen, 1960). However, the individuals have the normal genetic complement. Segregation analysis indicated that females from these stocks produce two types of gametes, either both left arms attached to each other or the two right arms attached to each other, whereas males can produce gametes with all four arms attached to each other as well as no arms at all, in addition to the two produced by females (Figure 3) (Merrill *et al*., 1988). The columns marked in grey show the chromosomal combination that will give rise to viable, fertile progeny so as to maintain the stock. The columns marked in green are the gametes that would be helpful in generating deletions of autosomal arms.

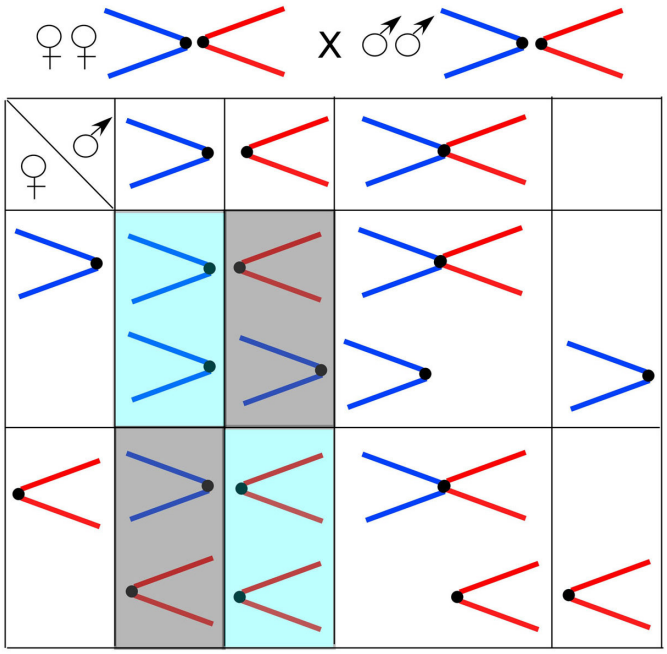

Figure 3: Schematic representing chromosomal segregation in a compound autosomal stock. The blue lines represent the left arms of the autosome and the red lines the right arms. The black dot attaching the chromosomal arms is the centromere. Unlike normal chromosomes where one left arm is joined to one right arm by the centromere, in the compound autosomal stock the two left arms are attached to each other as are the two right arms. However, these individuals contain the normal genetic complement. Their gametes however contain either two left or two right arms of the attached autosome or all four arms or none. Segregational analysis from previous studies indicate that virtually all the female gametes are either attached right arms or attached left arms whereas male gametes in addition include the category of all four arms attached to each other as well as none. The boxes marked in grey indicate the progeny from the stock that have the full chromosomal complement and help in maintaining the stock. The boxes marked in green are the ones lacking entire right arms or left arms, useful in studying zygotic gene function. Figure modified from Merrill *et al*., 1988.

When such compound stock females are crossed to males carrying autosomal translocations, one eighth of the progeny lack the genomic stretch uncovered by the translocation. However, since the mothers (compound stock) have the complete chromosomal complement, they do not exhibit any maternal effect. Thus, by using overlapping translocations that cover the entire chromosome arm, one could screen for zygotic loci required during early embryonic development (Merrill *et al*., 1988). Many of the zygotic genes involved in cellularization were identified during the course of this screen.

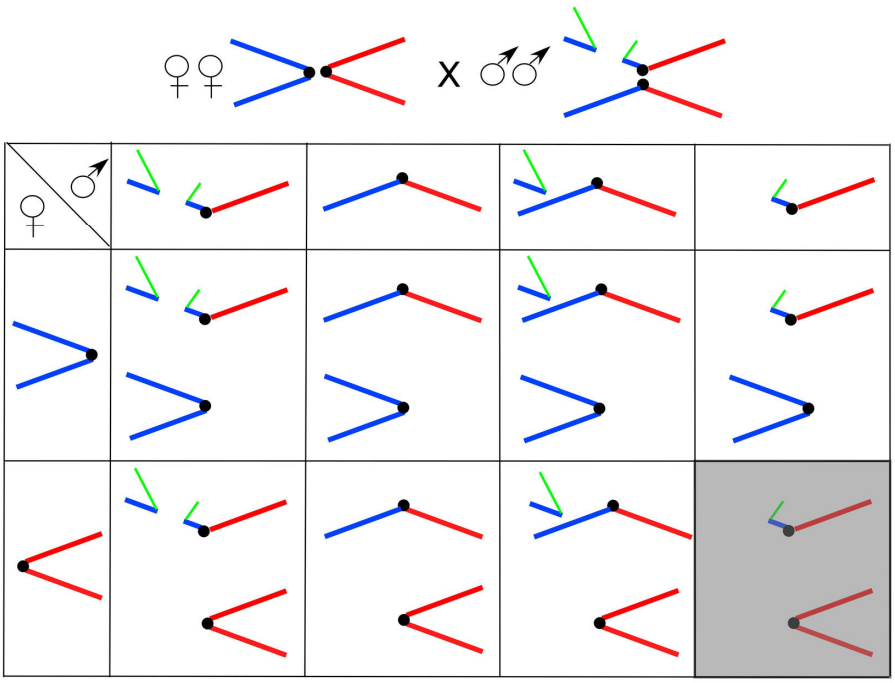

Figure 4: Schematic showing the chromosomal segregation pattern in a cross between the compound stock females and a translocation stock. The blue lines represent the left arms of the chromosome, the red lines the right arms and the black dots, the centromere. In this instance, part of the genomic stretch from the left arm is translocated, represented by the break flanked by the green lines on one of the left arms. One-eighth of the progeny would exhibit any zygotic effects due to deletion of genes uncovered by the translocated segment (grey column). However, only zygotic effects would be manifest in such embryos, as the mothers have the complete chromosomal complement. By screening overlapping sets of translocations covering the entire chromosomal arm, one would be able to identify zygotic loci which are required early in development. Figure modified from Merrill *et al*., 1988.

This strategy of generating synthetic deficiencies by using chromosomal aberrations were used later on to screen for zygotic loci involved in *wingless* signalling (Muller *et al*., 1999), as well as to find genes involved in ventral furrow formation (Grosshans and Wieschaus 2000). The latter screen led to the identification of two zygotic cell cycle regulators during gastrulation, *trbl* and *frs* (Grosshans and Wieschaus 2000).

However, independent screens which employed other strategies also led to identification of both or one of these loci (Mata *et al*., 2000; Seher and Leptin, 2000). Mata *et al* identified *trbl* in a modular misexpression screen (Mata *et al*., 2000; Rorth, 1996), whereas Seher and Leptin identified *trbl* and *frs* in a deficiency screen (Seher and Leptin, 2000; thesis, Seher). The latter screen was performed to identify target loci of *twist* that

are involved in gastrulation. This was because the *twist* loss of function phenotype was not reproduced by loss of function of the known *twist* targets, implying that unidentified loci might have a role. This screen was performed using deficiency stocks so that a quarter of the embryos derived by crossing deficiency males to females would be homozygous mutant for all the genes uncovered by the deficiency (thesis, Seher). Thus, zygotic effects as well as dominant maternal effects on gastrulation would be manifest in these embryos. Genomic regions uncovered by such deficiencies exhibiting gastrulation defects were ear marked for further analysis so as to facilitate mapping of the gene or genes within the uncovered stretch responsible for the defects.

In this screen, about 80% of the genome of *Drosophila* was scanned using deficiencies for early gastrulation phenotypes (Seher and Leptin, 2000; thesis, Seher, T). Four independent genomic regions, in addition to the known loci involved in gastrulation were identified by this screen. One such genomic region was the 24-25 cytogenetic region, uncovered by the deficiency Df(2L)sc-19-8. Later on, embryos from an overlapping deficiency, Df(2L)ed-dp which uncovers the cytogenetic region 24C3-25A2, was also shown to be defective in gastrulation (thesis, Seher, T). The work described here will focus on the characterization of the 24-25 cytogenetic region in order to identify the gene or genes responsible for the gastrulation defects exhibited by deficiencies in the region.

1.6 Aim

The aim of this work is to map, clone and characterize the gene or genes responsible for the gastrulation defects exhibited by embryos derived from deficiency stocks in the 24-25 cytogenetic region in *Drosophila melanogaster*.

2. Materials and Methods

2.1 Materials

2.1.1 Reagents

Tween20, tRNA, RNase and amino acids were purchased from Sigma. New England Biolabs supplied acetylated Bovine Serum Albumen (BSA), IKB ladder, 10KB ladder, restriction enzymes or other DNA modifying enzymes and their buffers. Proteinase K was purcahsed from Qiagen. Expand High Fidelity PCR system, ssDNA (salmon sperm DNA), Nitroblue tetrazolium (NBT), 5'-bromo-4-chloro-indoxylphosphate (BCIP), unlabelled nucleotides, hexanucleotide mix and anti-DIG antibody were supplied by Roche Diagnostics GmbH. Araldite and heparin were bought from Serva. Agarose electrophoresis grade was from Gibco BRL. The Vectastain-ABC-kit was purchased from Vector Laboratories. Unless otherwise mentioned, all the other chemicals were purchased from Amersham, Invitrogen, Merck, Roth or Sigma. Drosophila EST and cDNA clones were obtained from Resgen (Invitrogen), BACPAC Resources (http://bacpac.chori.org/drosocDNA.htm) or DGRC (http://dgrc.cgb.indiana.edu/).

2.1.2 *Drosophila melanogaster* stocks

The following *Drosophila* stocks were used in this study. The genotype of the stock, the stock number if it was obtained from a stock center or the source in other cases, as well as the references (where avaiable) are provided.

Stock Genotype	Stock No./Source	Original Reference
Deficiencies 24-25 cytogenetic region		
Df(2L) M24 F-B/SM1	Bl-744	Szidonya and Reuter, 1988
Df(2L) sc 19-11/In(2L) Cy,Roi	Sz	Szidonya and Reuter, 1988
Df(2L)dp-h25/In(2L)Cy[L]t[R], In(2R)Cy, amos[Roi-1]	Bl-3081	Szidonya and Reuter, 1988
Df(2L)dp-h19/SM1	Sz	Szidonya and Reuter, 1988
Df(2L)dp-h28/SM1	Sz	Szidonya and Reuter, 1988
Df(2L)M24F11/Dp(2;2)B3, ed1 dpo2 cl1	Bl-3080	Szidonya and Reuter, 1988
Df(2L) sc 19-11/In(2L) Cy,Roi	Sz	Szidonya and Reuter, 1988
Df(2L)sc19-9/In(2L)CyLtR In(2R)Cy, Cy1 amosRoi-1	Bl-3815	Szidonya and Reuter, 1988

Df(2L)sc19-8/SM6b; Dp(2;1)B19, y1, ed1 dpo2 cl1	Bl-693	Szidonya and Reuter, 1988
Df(2L)sc19-4/In(2L)CyLtR In(2R)Cy, Cy1 amosRoi-1	Bl-3813	Szidonya and Reuter, 1988
Df(2L)sc19-3/In(2L)CyLtR In(2R)Cy, Cy1 amosRoi-1	Bl-3812	Szidonya and Reuter, 1988
Df(2L)sc19-7/In(2L)CyLtR In(2R)Cy, Cy1 amosRoi-1	Bl-3814	Szidonya and Reuter, 1988
Df(2L)ed1/CyO; P{ry+t7.2=ftz/lacC}1	Bl-5330	Szidonya and Reuter, 1988
Df(2L)dp-h24/SM6b	Bl-1070	Szidonya and Reuter, 1988
Df(2L) sc 19-10/In(2L) Cy,Roi	Sz	Szidonya and Reuter, 1988
Df(2L) ed dp/SM1	Bl-702	Szidonya and Reuter, 1988
Df(2L) sc 19-5/In(2L) Cy,Roi	Sz	Szidonya and Reuter, 1988
Df(2L)sc19-1/SM6b; Dp(2;1)B19	Bl-615	Szidonya and Reuter, 1988
Df(2L)dp-cl-h3/Dp(2;2)B3, ed1 dpo2 cl1	Bl-1185	Szidonya and Reuter, 1988
EP Insertions and excisions		
EP(2)578	Sz	Rorth, 1996
y1 w67c23; P{w+mC y+mDint2=EPgy2}EY9771	Bellen lab	Bellen *et al*., 2004
Traf1EP578^{ex1}/Cyo	Chung lab	Cha *et al*., 2003
Traf1EP578^{ex1}/ Traf1EP578^{ex1}(floating balancer)	ML	unpublished
DTraf2EP(X)1516/Basc	Chung lab	Cha *et al*., 2003
Drosdel P element stocks		
y w iso; P{FRT, w+}RS5-SZ-4048; 3iso	Drosdel	Ryder *et al*., 2004
y w iso; P{FRT, w+}RS5-SZ-3590; 3iso	Drosdel	Ryder *et al*., 2004
y w iso; P{FRT, w+}RSCB-0544-3; 3iso	Drosdel	Ryder *et al*., 2004
y w iso; P{FRT, w+}RS5-HA-1531; 3iso	Drosdel	Ryder *et al*., 2004
y w iso; P{FRT, w+}RSCB-5668-3; 3iso	Drosdel	Ryder *et al*., 2004
y w iso; P{FRT, w+}RS5-HA-1707; 3iso	Drosdel	Ryder *et al*., 2004
y w iso; P{FRT, w+}RSCB-5717-3; 3iso	Drosdel	Ryder *et al*., 2004
y w iso; P{FRT, w+}RSUM-8380-3; 3iso	Drosdel	Ryder *et al*., 2004
y w iso; P{FRT, w+}RSCB-0621-3; 3iso	Drosdel	Ryder *et al*., 2004
y w iso; P{FRT, w+}RS5-HA-1621; 3iso	Drosdel	Ryder *et al*., 2004
y w iso; P{FRT, w+}RS5-HA-1035; 3iso	Drosdel	Ryder *et al*., 2004
y w iso; P{FRT, w+}RS5-HA-1043; 3iso	Drosdel	Ryder *et al*., 2004
y w iso; P{FRT, w+}RSCB-0110-3; 3iso	Drosdel	Ryder *et al*., 2004
y w iso; P{FRT, w+}RSCB-0383-3; 3iso	Drosdel	Ryder *et al*., 2004
y w iso; P{FRT, w+}RS5-HA-1420; 3iso	Drosdel	Ryder *et al*., 2004
y w iso; P{FRT, w+}RS5-SZ-3156; 3iso	Drosdel	Ryder *et al*., 2004
y w iso; P{FRT, w+}RSCB-0211-3; 3iso	Drosdel	Ryder *et al*., 2004
y w iso; P{FRT, w+}RSCB-0494-3; 3iso	Drosdel	Ryder *et al*., 2004
Isogenized stocks for generating deletions		
y w 70FLPiso; Sco/SM6a; 3iso	Bl6416	Ryder *et al*., 2004
w1118 iso; Sco/SM6a; 3iso	Bl5907	Ryder *et al*., 2004
Drosdel deletions constructed		
P{FRT, w+}CB-0621-3r--5-HA-1621r/SM1	ED260/ML	unpublished
P{FRT, w+}CB-0211-3r--5-HA-1621r/SM1	ED256/ML	unpublished
P{FRT, w+}CB-0494-3r--5-HA-1621r/SM1	ED258/ML	unpublished
P{FRT, w+}CB-0383-3r--5-SZ-4048r/SM1	ED247/ML	unpublished
P{FRT, w+}CB-5668-3r--5-HA-1531r/SM1	ED250/ML	unpublished
P{FRT, w+}CB-5668-3r--5-HA-1035r/SM1	Df(2L)1035/ML	unpublished

P{FRT, w+}CB-5668-3r--5-SZ-3156r/SM1	ED251/ML	unpublished
P{FRT, w+}CB-5668-3r--5-HA-1043r/SM1	ED262/ML	unpublished
P{FRT, w+}CB-0110-3r--5-HA-1707r/SM1	ED252/ML	unpublished
P{FRT, w+}CB-0544-3-3r--5-HA-1420r/SM2	ED270/ML	unpublished
Stocks used for complementation		
cn1 P{ry+t7.2=PZ}l(2)0670806708/CyO;ry506	Bl12320	BDGP
y1 w67c23; P{w+mC=lacW}edk01102/CyO	Bl10490	BDGP
l(2)SH0479/CyO (CG3714)	Steven Hou lab	Oh *et al*., 2003
ft[G-rv]/SM5	Bl1894	Bryant *et al*., 1988
y1 w67c23; P{w+mC=lacW}tutlk14703/CyO	Bl10451	BDGP
l(2)SH0805/CyO (CG18013)	Steven Hou lab	Oh *et al*., 2003
y1 w67c23; P{w+mC=lacW}Tps1k08903/CyO	Bl10838	BDGP
dw-24E1 l(2)cg1 cg1/SM5	Bl292	Curry, 1941
y^{1}; $P\{y^{+mDint2}\ w^{BR.E.BR}$=SUPor-P}mRpL27^{KG01128}/SM6a; ry^{506}	Bl14881	BDGP
l(2)SH0840/CyO (CG15442-RpL27A)	Steven Hou lab	Oh *et al*., 2003
dplv1 b1/SM5	Bl278	Grace, 1980
l(2)SH1525/CyO (CG2937-mRpS2)	Steven Hou lab	Oh *et al*., 2003
slf1 cn1 bw1 sp1/CyO	Bl3265	Nusslein-Volhard *et al*., 1984
y1 w67c23; P{w+mC=lacW}l(2)k10004k10004/CyO	Bl10964	BDGP
y1 w67c23; P{w+mC=lacW}l(2)k10217k10217/CyO	Bl10983	BDGP
y1 w67c23; P{w+mC=lacW}vkgk00236/CyO	Bl10473	BDGP
y1 w67c23; P{w+mC=lacW}l(2)k10127k10127/CyO	Bl10973	BDGP
y1 w67c23; P{w+mC=lacW}l(2)k11206k11206/CyO	Bl11017	BDGP
EMS alleles in 24-25 cytogenetic region		
l(2)jf2a6/In(2L)CyLtR In(2R)Cy, Cy1 amosRoi-1	Sz	Szidonya and Reuter, 1988
l(2)jf2b8/In(2L)CyLtR In(2R)Cy, Cy1 amosRoi-1	Sz	Szidonya and Reuter, 1988
l(2)jf3b25/In(2L)CyLtR In(2R)Cy, Cy1 amosRoi-1	Sz	Szidonya and Reuter, 1988
l(2)jf3sz11/In(2L)CyLtR In(2R)Cy, Cy1 amosRoi-1	Sz	Szidonya and Reuter, 1988
l(2)jf3sz49/In(2L)CyLtR In(2R)Cy, Cy1 amosRoi-1	Sz	Szidonya and Reuter, 1988
l(2)jf3sz56/In(2L)CyLtR In(2R)Cy, Cy1 amosRoi-1	Sz	Szidonya and Reuter, 1988
l(2)jf4b11/In(2L)CyLtR In(2R)Cy, Cy1 amosRoi-1	Sz	Szidonya and Reuter, 1988
l(2)jf5a18/In(2L)CyLtR In(2R)Cy, Cy1 amosRoi-1	Sz	Szidonya and Reuter, 1988
l(2)jf5a19/In(2L)CyLtR In(2R)Cy, Cy1 amosRoi-1	Sz	Szidonya and Reuter, 1988
l(2)jf5b2/In(2L)CyLtR In(2R)Cy, Cy1 amosRoi-1	Sz	Szidonya and Reuter, 1988
l(2)jf5h10/In(2L)CyLtR In(2R)Cy, Cy1 amosRoi-1	Sz	Szidonya and Reuter, 1988
l(2)jf5sz31/In(2L)CyLtR In(2R)Cy, Cy1 amosRoi-1	Sz	Szidonya and Reuter, 1988
l(2)jf6sz3/In(2L)CyLtR In(2R)Cy, Cy1 amosRoi-1	Sz	Szidonya and Reuter, 1988
l(2)jf7h32/In(2L)CyLtR In(2R)Cy, Cy1 amosRoi-1	Sz	Szidonya and Reuter, 1988
l(2)jf7h36/In(2L)CyLtR In(2R)Cy, Cy1 amosRoi-1	Sz	Szidonya and Reuter, 1988
l(2)jf7h39/In(2L)CyLtR In(2R)Cy, Cy1 amosRoi-1	Sz	Szidonya and Reuter, 1988
l(2)jf13sz18/In(2L)CyLtR In(2R)Cy, Cy1 amosRoi-1	Sz	Szidonya and Reuter, 1988
l(2)jf14h7/In(2L)CyLtR In(2R)Cy, Cy1 amosRoi-1	Sz	Szidonya and Reuter, 1988
l(2)jf15h12/In(2L)CyLtR In(2R)Cy, Cy1 amosRoi-1	Sz	Szidonya and Reuter, 1988

Translocation stocks		
T(Y;2)A183, y[+]/SM1; C(1)RM, y[1]/C(1;Y)1,y[1]	Bl2628	
T(Y;2)B184, B[S], y[+]/SM1; C(1)RM, y[1]/C(1;Y)1,y[1]	Bl2645	
T(Y;2)G100, y[+]/SM1; C(1)RM, y[1]/C(1;Y)1,y[1]	Bl2685	
T(Y;2)L110, B[S], y[+]/SM1; C(1)RM, y[1]/C(1;Y)1,y[1]	Bl2739	
T(Y;2)H158,y[+]/SM1; C(1)RM, y[1]/C(1;Y)1,y[1]	Bl3683	
T(Y;2)B110, B[S], y[+]/SM1; C(1)RM, y[1]/C(1;Y)1,y[1]	Bl2640	
T(Y;2)B190, y[+]/SM1; C(1)RM, y[1]/C(1;Y)1,y[1]	Bl2647	
T(Y;2)B251, B[S], y[+]/SM1; C(1)RM, y[1]/C(1;Y)1,y[1]	Bl2661	
T(Y;2)J30, y[+]/SM1; C(1)RM, y[1]/C(1;Y)1,y[1]	Bl2711	
T(Y;2)R50, B[S], y[+]/SM1; C(1)RM, y[1]/C(1;Y)1,y[1]	Bl2763	
T(Y;2)B24, y[+]/SM1; C(1)RM, y[1]/C(1;Y)1,y[1]	Bl2631	
T(Y;2)B63, B[S], y[+]/SM1; C(1)RM, y[1]/C(1;Y)1,y[1]	Bl2633	
T(Y;2)B177, B[S], y[+]/SM1; C(1)RM, y[1]/C(1;Y)1,y[1]	Bl2644	
T(Y;2)B238, B[S], y[+]/SM1; C(1)RM, y[1]/C(1;Y)1,y[1]	Bl2659	
T(Y;2)B26, B[S], y[+]/SM1; C(1)RM, y[1]/C(1;Y)1,y[1]	Bl3682	
Tp(2;Y)G/b[1]pr[1]tk[1]	Bl4359	
UAS stocks		
w; UAS-eiger	Basler lab	Moreno *et al*., 2002
w; UAS-Traf1HA	Miura lab	Kuranaga *et al*., 2002
w; UAS-misshapen	Mlodzik lab	
w; UAS-basket	Mlodzik lab	
w; UAS-hemipterous	Mlodzik lab	
w; UAS-hemipterous	Mlodzik lab	
w; UAS-hemipterous(constitutively active)	Mlodzik lab	
w; UAS-Rho1dsRNA	Liqun Luo lab	Billuart *et al*., 2001
w; UAS-Traf1Fulllength(1-1466)	ML	Unpublished
w; UAS-Traf1ΔC-Trafdomain(1-1011)	ML	Unpublished
w; UAS-Traf1 ΔC-Trafdomain+Zincfingers(1-803)	ML	Unpublished
w; UAS-Traf1ΔN-Exon1(809-1466)	ML	Unpublished
w; UAS-Traf1ΔN-Exon1+Zincfingers(1011-1466)	ML	Unpublished
w; UAS-Wengen	ML	Unpublished
GAL4 stocks		
maternal Gal4	St.Johnston lab	
Twist Gal4	Akam lab	Greig and Akam, 1993
Scalloped Gal4	Klein lab	
w; UAS-puckered	Martinez-Arias lab	Martin-Blanco *et al*., 1998
Other stocks		
Df(2L)aldpbTE116(R)GW11cnsp/CyO	Rolf Reuter	Reuter and Leptin, 1994
w;twiEY53R12bw/SM1	Rolf Reuter	Reuter and Leptin, 1994

w,fog[4a6]/FM7/Ymal[106]	Wieschaus lab	Costa *et al*., 1994
Df(2L)TE116(R)GW11Df(2R)S60/SM1	Rolf Reuter	Reuter and Leptin, 1994
al1 dpov1 b1 pr1 Bl1 c1 px1 sp1/SM1	Bl213	
Orgeon R wild type	Bl5	
C(2)v	Wieschaus lab	Merrill *et al*., 1988
w; 2XPEe Traf1	ML	Unpublished

Abbreviations used

Bl- Bloomington stock centre

Sz- Szeged stock center

Drosdel- Drosdel consortium for generating deficiencies

ML- Maria Leptin lab

BDGP- Berkeley Drosophila Genome Project

2.1.3 Antibodies

The following primary antibodies were used:

Rabbit anti-Twist (kindly provided by S.Roth; Roth *et al*., 1989) at a dilution of 1:3000 and Rabbit anti-Eve (kindly provided by M. Frasch; Frasch and Levine, 1987) at a dilution of 1:5000.

The secondary antibody (anti-Rabbit biotinylated) was purchased from Dianova.

2.1.4 Oligonucleotides

Oligonucleotides were purchased from Eurogentec and Carl Roth GmbH. The lyophilised pellet was resuspended in water at a concentration of 100pmol/µl and stored at -80^0C. Aliquots of 15-20pmol/µl were made and used in the PCR reactions.

Oligo Name	**Purpose**	**Sequence**
dp1a	SEPCR	GCAATTACACATGCTCCTG
dp1b	SEPCR	GATTATCCTGACACTCGTTG
11929a	SEPCR	CTGGTCTACAATGCAGTAG
11929b	SEPCR	CAACCAAGCTACTAGTGAC
15631a	SEPCR	GGAATCAAACAGCTTCACG
15631b	SEPCR	CAGTTACACTCCTAGTGTC
3225a	SEPCR	CTGCTCAAGAAGATCCTTC
3225b	SEPCR	GATGGTTATGATCTCCTCG
CG15634F	SEPCR	GTTCTCCATTCGATGGAAC

CG15634R	SEPCR	GACTCTGCAGATTCTTGTTG
CG3702F	SEPCR	TCGATAGGTCCTCAACACT
CG3702R	SEPCR	TCAGCTCACCGAGCATATT
AtetF	SEPCR	ATATGCCGACTAATGCCGT
AtetR	SEPCR	TGTCCGCTTAGCGAATCAT
CG15429F	SEPCR	ACTATCTCAAGGACGAGGT
CG15429R	SEPCR	ATGTCGTCCGTGTAGTAGA
CG15431F	SEPCR	TAGCAATCGAGTCCAAGCA
CG15431R	SEPCR	AGTCCCAATTCTCGATGCT
CG15436F	SEPCR	AATGGCGGAAATATGCCGA
CG15436R	SEPCR	TGCTCAGCCGAAAAGTCTT
CG12677F	SEPCR	CCACACATTTCTGAAGAGG
CG12677R	SEPCR	GCGTTGAGTCAATATCGAG
Traf1 3'F	SEPCR	GTCTACATAAAGGTCCTGC
Traf1 3'R	SEPCR	GCTGCTCCGAATTTAACAC
Traf1 5'F	SEPCR	CTGTATCTGAAACTGAGCC
Traf1 5'R	SEPCR	CTCTAGATGGCCCTATTTG
CG3652F	SEPCR	CTACTAGATGTTCGAGGAC
CG3652R	SEPCR	CTAATCACTAAACGAGGCG
Tps1F	SEPCR	CACTGTCAACAAGCACTTC
Tps1R	SEPCR	GTAGTCATCGAAATCGTCC
T7	Sequencing	TAATACGACTCACTATAGGG
T3	Sequencing	ATTAACCCTCACTAAAGGGA
SP6	Sequencing	ATTTAGGTGACACTATAG
PUASTF	Sequencing	GAAGAGAACTCTGAATAGGGAATTGG
PUASTR	Sequencing	GGTAGTTTGTCCAATTATGTCAC
LEP1F	Excision mapping	CGAGTTGCTCGTTGTTTTC
LEP1R	Excision mapping	CTCTGGCATTGCACTTTAG
LEP2F	Excision mapping	CTAAAGTGCAATGCCAGAG
LEP3F	Excision mapping	GCACTATGAAACCTCCTTG
REP3R	Excision mapping	GGCTCAGTTTCAGATACAG
Traf5RR	Excision mapping	CGAGAACTTCCGTTTGTTC
TrafFBamH1	Cloning	ATAGGATCCCGCAAGCGGTTCGTATTCGTGAAGTTCGCA
TrafRXba1	Cloning	ATATCTAGACTAAGAAGTCAAACATACAATAAATGAAGTA
TrafBamH1mutF	Cloning	TGAAAGTGGACCCCAGCAAGATAGT
TrafBamH1mutR	RT-PCR+Cloning	ACTATCTTGCTGGGGTCCACTTTCA
TrafRXba1	Cloning	ATATCTAGATACTTCATTTATTGTATGTTTGACTTCTTAG
TrafFBH1	Cloning	ATAGGATCCATGGTTCGAAGTTTGGCCCAGTGGA
TrafFBH1RNA	Cloning	ATAGGATCCAATGGTTCGAAGTTTGGCCCAGTGGA
Traf1011XhR	Cloning	ATTCTCGAGTTAGCCGACCAGTCGGTG

TrafHind3F	Cloning	ATAAAGCTTATGGTTCGAAGTTTGGCCCA
HAbamF	Cloning	AATGGATCCCCATGGCCTACCCATATGAT
HAXbaR	Cloning	AACTCTAGATTAGCTCGCGTAATCTGG
Traf503RXh1	Cloning	AACCTCGAGGTTCCAGTTCCGTGATGGGCATG
TrfFXho1	Cloning	ATAACTCGAGCGCAAGCGGTTCGTATTCGTGAAGTTC
Traf1011XhF	Cloning	GACCTCGAGCACCGACTGGTCGGCTAA
TrafHind3Fnew	Cloning	ATAAAGCTTGCATGGTTCGAAGTTTGGCCCA
Traf804XhoIF	RT-PCR+Cloning	ACTCTCGAGATGCTAGCCGTGTCCTGCAGCTTC
Traf1009XhoIF	Cloning	ACTCTCGAGATGATCACCGACTGGTCGGCTAAG
HAXho1F	Cloning	AATCTCGAGCCATGGCCTACCCATATGAT
TrafRKpn1	Cloning	ACTGGTACCACTCCTTAGACGGCCACTATCTTGCT
Traf804KpnIR	Cloning	ACTGGTACCGAAGCTGCAGGACACGGCTAG
HANotIF	Cloning	AATGCGGCCGCATGGCCTACCCATATGATGTT
TrafRXhoI	Cloning	AATCTCGAGCCCTCCTTAGACGGCCACTATCTTGCT
Traf804XhoIR	Cloning	AATCTCGAGCCGAAGCTGCAGGACACGGCTAG
Act5cF	RT-PCR	TGAACCCCAAGGCCAACCG
Act5cR	RT-PCR	ATCCAGACAGAGTACTTGCG

2.1.5 *E.coli* strains

The DH5α and BL-21 strains were used. Selection was done using ampicillin, kanamycin or chloramphenicol.

2.1.6 Plasmids

pUAST	(Brand and Perrimon, 1993)
pBluescript KS(+) & KS(-)	(Stratagene)
pSP64	(Promega)
pFLC1	(BDGP)
pOT2	(BDGP)
2XPEe pCaSperAUGβGal	(Jiang and Levine, 1993)

2.1.7 Computer software, digital photography and sectioning

Digital pictures were taken using an Axiophot Photomikroscop (Zeiss) with the ProgRes 3008 (Kontron Elektronik) or Axiocam MRc5 (Zeiss) camera. The latter camera used the Axiovision Release 4.4 imaging software. Pictures were edited using Adobe Photoshop (Adobe Systems) software. Figures were drawn using Canvas 8.0 and 9.0 (Deneba Systems) software. DNA sequence alignments and analysis were carried out using the

DNA Strider 1.2 software while oligonucleotide design was done using Amplify 1.2 and Primer3. Embryos were sectioned on a Leica RM2065 microtome, using glass blades. In order to predict transcription factor binding sites, the genomatix matinspector software was used. The promoter prediction was done using the genomatix gene2promoter software.

2.2 Methods

All molecular biology techniques were according to Sambrook *et al*., 1989.

2.2.1 Genomic Sequence, EST, expression pattern and fly stock searches

Searches for annotated *Drosophila* genomic sequences, *Drosophila* ESTs and *Drosophila* deficiency and P-element insertion strains were conducted using Flybase (http://flybase.bio.indiana.edu/). EST and cDNA sequences were obtained from BDGP (http://www.fruitfly.org/EST/index.shtml). The mRNA expression pattern of genes were analysed from the BDGP *in situ* resource (http://www.fruitfly.org/cgi-bin/ex/insitu.pl).

2.2.2 Generating Drosdel deletions

Information on the crosses performed to construct deletions are given at the Drosdel website at http://131.111.146.35/~pseq/drosdel/ddinfo.html (Ryder *et al*., 2004) and is according to the method described by Golic and Golic, 1996. In summary, the respective forward and reverse FRT carrying P element fly stocks used to generate the deletion were crossed to each other, so as to bring both elements in the same individual. The cross was performed in a FLPase enzyme background, which facilitates recombination between the FRT sites. Embryos from such a cross were heat shocked at 37^0 C for 30 minutes to facilitate recombination. Such heat shocked embryos were allowed to develop and adult flies having mosaic eyes (indicating recombination) were crossed to isogenized balancer stocks. In the next generation, by selecting for the eye colour marker, recombinant events and thus deficiency or duplication events were recovered and stocks were established. The deficiencies were confirmed by complementation and at least five stocks were tested

for each individual deficiency. From these, one that did not complement lethal alleles in the region was selected and maintained as stock.

2.2.3 *Drosophila* nomenclature

All fly nomenclature used is according to Lindsley and Zimm, 1992.

Dp(2;2)B3 is a tandem duplication. Its break points include 23E2-3; 26E2-F1 on the cytological map (Lindsley and Zimm, 1992; Szidonya and Reuter, 1988). It was recovered as trans suppressor of *Df(2L)M24F11*.

Dp(2;1)B19 is an inversted insertional transposition. Its break points include 24D4; 25F2; 9B14-C1 on the cytological map (Lindsley and Zimm, 1992; Szidonya and Reuter, 1988). It is homozygous viable and female sterile.

2.2.4 Fly maintenance, embryo collection and fixation

The flies were maintained under standard conditions (Ashburner, 1989; Wieschaus and Nuesslein-Volhard, 1986).

To fix the embryos, properly staged embryos were collected on an apple juice – agar plate, dechorionated using 50% bleach and washed in tap water. Embryos were fixed in 4% Formaldehyde in PBS (Sambrook *et al.,* 1989): heptane = 1:1 solution at 37^0C for 20 minutes, with vigorous shaking followed by devitellinization with methanol:heptane = 1:1 solution by vortexing for half a minute. Embryos were washed several times in methanol and stored in methanol at -20^0C if not used immediately.

2.2.5 Antibody staining of embryos

The fixed embryos were rehydrated in PBST, followed by one hour blocking at room temperature using 5% BSA in PBST. The liquid phase was taken off and the primary antibody was added. The reaction was left at 4^0C overnight, on a rotating wheel. Embryos were washed with PBST several times, at room temperature followed by incubation in secondary antibody (biotin labeled) at room temperature for 90 minutes. The secondary antibody was washed away by PBST. In the mean time, the ABC mix (ABC kit, Linaris Biologische Produkte GmbH) was prepared to a dilution of 1:100 in PBST. After the

embryos were washed thoroughly, the ABC mix was added to the embryos and incubated on a rotating wheel. After 30 minutes, the reagent was washed away and the antibody was detected by adding 20% DAB (1mg/ml stock solution) and 0.3% H_2O_2 (30% stock). To remove the peroxidase, 3% H_2O_2 was added and incubated for 20 minutes. After the peroxidase was washed away, a second round of antibody staining was done, if needed, as described above.

2.2.6 *In situ* hybridization

RNA *in situ* hybridization was performed according to Tautz and Pfeifle, 1989. To generate probes, the plasmid containing the cDNA sequence was digested and purified. This was used as the template in an *in vitro* transcription reaction containing 2µl DIG 10X RNA labelling mix (Roche), 2µl transcription buffer, 2µl 0.1M DTT, 0.8µl RNasin (Promega), 2µl SP6, T7 or T3 RNA polymerase and incubated at 37^0C for 2 hours. The reaction was stopped by incubation on ice; 80µl of pre-hybridization mix (50% deionized formamide, 25% 20X SSC pH 7.0, 0.5% tRNA 20mg/ml, 1% ssDNA 10mg/ml, 0.05% heparin 100mg/ml, 0.1% Tween20 in water) was added to make a dilution of 1 in 5.

Fixed embryos were rehydrated in PBST (0.2% Tween20 in water), treated with formaldehyde to fix again, treated with proteinase K for 30 seconds to permeabilize and fixed once more. Several washes in PBST were performed at each step. Embryos were pre-hybridized in pre-hybridization mix for 2 hours at 56^0C, followed by overnight hybridization with the probe at 1:500 dilution, at 56^0C. After incubation, the free probe was washed away by incubating the embryos in a decreasing concentration of pre-hybridization mix, at 56^0C. The embryos were then washed and treated with the anti-DIG antibody conjugated with AP (1:500, Roche) for 1 hour at room temeperature. The antibody was discarded and the embryos washed several times in PBST. The signal was visualized using 1%NBT (10mg/ml Nitro blue tetrazolium in 70% Dimethylformamide) and 1% X-Phospate solution (10mg/ml 5-bromo-4-chloro-indoxylphosphate in Dimethylformamide) in staining buffer (100mM Na_2CO_3 pH 9.5 or 50mM Tris-Hcl pH9.5, 2mM $MgCl_2$, 0.1% Tween20).

2.2.7 Embedding and sectioning of stained embryos

Stained embryos were dehydrated in 30%, 50%, 70%, 80%, 90%, 95% and 100% (absolute ethanol treated with molecular Sieves, Sigma M-2010, 1/8 inch pellets) ethanol. After dehydration, 100% acetone (treated same as absolute ethanol) was added for 15 minutes, followed by a mixture of 50% acetone and 50% Araldite (57.4g CY212 Araldite with 48g HY964 Hardener were mixed thoroughly first and then 2ml 2,4,6- Tris (dimethylaminomethyl) phenol was added and mixed). The mixture containing the embryos was transferred to a shallow plastic lid and the acetone was allowed to evaporate under the hood.

Embryos were arranged in an araldite block for sectioning and the block was allowed to polymerize at 50^0C overnight. Sections were made on the Leica RM2065 microtome.

2.2.8 Single embryo PCR

Embryos were collected as described before on an apple juice-agar plate and fixed. Individual embryos were dispensed in 10µl volume of a solution containing 10mM Tris-HCl pH 8.2, 1mM EDTA and 25mM NaCl and frozen. After a minimum of 30 minutes, the embryos were thawed and added 0.2µl Proteinase K (200µg/ml stock solution). The embryos were incubated at 37^0C for 30 minutes followed by 95^0C for 2 minutes for heat inactivation of the Proteinase K. 1µl of this extract was used as the template for PCR reactions.

The PCR was carried out in a UNO Thermoblock (Biometra). The reaction components were: 20pmols of each primer, 10mM dNTP, 10X PCR buffer without Mg^{2+}(supplier), 2.5mM Mg^{2+} and 0.25µl of High Fidelity Taq Polymerase (Expand High Fidelity PCR system from Roche) in a 25µl PCR reaction mix. The PCR programme included a denaturation step of 3 minutes at 94^0C followed by 35 cycles: 30 seconds at 94^0C, 1 minute at 50^0C the annealing temperature, 3 minutes at 72^0C the extension temperature and ending with a final extension of 10 minutes at 72^0C. The PCR products were analysed on a 1% agarose gel.

2.2.9 Molecular cloning

The 2XPEe Traf1 construct was generated by PCR amplifying the Traf1 cDNA in pBSK (LD20987) using the primers TrafFBH1 and TrafRXb1, digesting with Xba1 and BamH1 and ligating into the same sites of the 2XPEe pCaSperAUGβGal vector.

The pUAST wengen construct was generated by digesting the wengen cDNA in pFLC1 (RE29502) with EcoR1 and BamH1. The resultant fragment was cloned into pUAST at the Bgl2 and EcoR1 sites.

Traf1 was subcloned into the pSP64 vector. This was done by digesting the PCR fragment generated by the primers TrafFBH1 and TrafRXb1 using Traf1 cDNA in pBSK as template, with BamH1 which digests only at the 3'. The resulting 5' blunt, 3' staggered fragment was cloned into the BamH1 and Sma1 sites of pSP64 and called pSP64Traf1FL1.

Using pSP64Traf1FL as template, PCR was performed with primers HABamF and TrafRXb1 and the resulting product digested with Xba1 and BamH1. This fragment was ligated into pUAST using the Bgl2 and Xba1 sites to generate full length Traf1 in pUAST.

Traf1 was again subcloned into the pSP64 vector by digesting the PCR fragment generated by the primers TrafHind3F and TrafRXb1 using Traf1 cDNA in pBSK as template, with Hind3 and BamH1. The resulting fragment was cloned into the Hind3 and BamH1 sites of pSP64 and called pSP64Traf1FL2.

Using pSP64Traf1FL2 as template, PCR was performed with Traf804Xho1F and HAXbaR primers. The resultant product was digested with Xho1 and Xba1 and ligated into the same sites in pUAST to generate Traf1ΔN-Exon1 in pUAST.

Using pSP64Traf1FL2 as template, PCR was performed with Traf1009Xho1F and HAXbaR primers. The resultant product was digested with Xho1 and Xba1 and ligated into the same sites in pUAST to generate Traf1ΔN-Exon1+Zincfingers in pUAST.

Traf1 was again subcloned into the pSP64 vector by digesting the Traf1 cDNA in pBSK with BamH1 and removing the protruding 5' terminus by Mung Bean Nuclease

treatment. Then it was cut with Xho1 and cloned into Sma1-Sal1 digested pSP64. This was called pSP64Traf1FL3.

Using pSP64Traf1FL3 as template, PCR was performed with primers HABamF and Traf1011XhR. The resultant product was digested with Xho1 and BamH1 and cloned into Xho1- Bgl2 digested pUAST, to generate pUASTΔC-Trafdomain.

Using pSP64Traf1FL as template, PCR was performed with primers HANot1F and Traf804Xho1R. The resulting product was digested with Not1 and Xho1. This fragment was ligated into pUAST using the Not1 and Xho1 sites to generate pUASTΔC-Trafdomain+Zincfingers.

2.2.10 Generating transgenic flies

Transgenic flies were generated by DNA microinjection into blastoderm stage embryos according to Spradling and Rubin (Rubin and Spradling, 1982; Spradling and Rubin, 1982). The injected embryos were allowed to develop into flies and these were crossed to balancer stocks which were w^-. In the next generation, flies with coloured eyes were selected and stocks were established from about 20-25 such insertions. Stocks were maintained balanced or homozygous.

2.2.11 DNA Sequencing

DNA sequencing was carried out on an ABI sequencer using Big Dye Terminator kit from Perkin Elmer.

2.2.12 RT-PCR

RNA was extracted from adult flies using the Trizol reagent (Invitrogen) as recommended by the manufacturer. First strand synthesis was carried out using the Cloned AMV First-Strand cDNA Synthesis Kit (Invitrogen) and PCR was performed as recommended by the manufacturer.

3. Results

3.1 The deficiency Df(2L)ed-dp embryos show gastrulation defects

In order to allow the mapping of the gene or genes responsible for gastrulation in the region identified by T.Seher (Seher and Leptin, 2000; thesis, Seher), embryos were collected from deficiencies in the region and the gastrulation phenotype observed. Embryos from a cross between Df(2L)ed-dp heterozygous males and females were collected, fixed and stained with anti-Twist and anti-Even skipped antibodies (Figure 5A-F). Twist stains the mesoderm and helps to track ventral furrow formation whereas Eve is a pair rule gene, expressed in seven stripes from the anterior to the posterior of the embryo which serves as a marker to determine the age of the embryo.

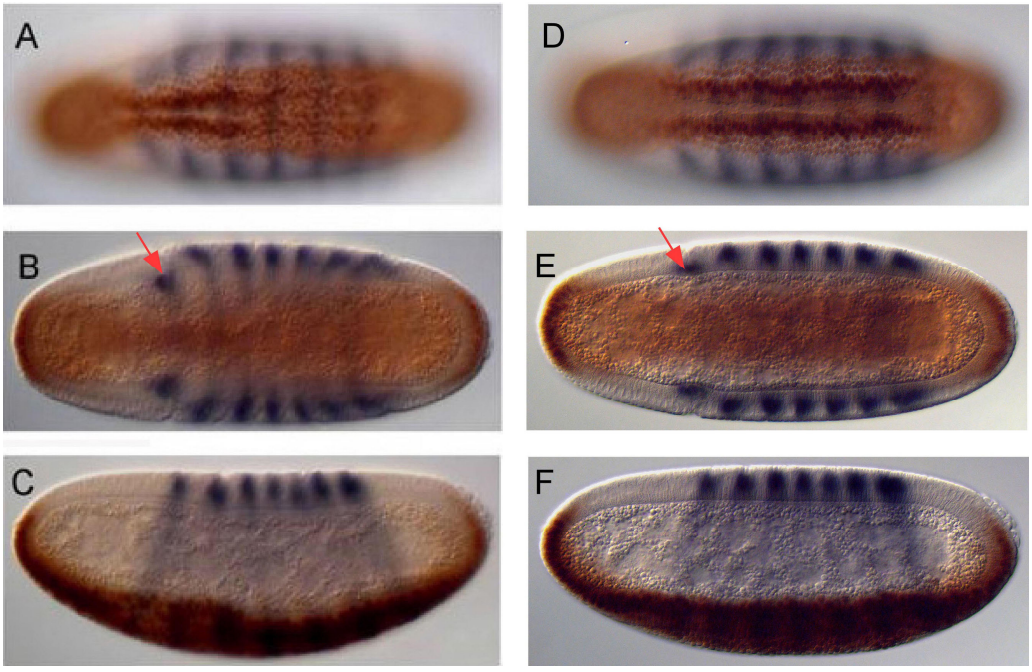

Figure 5: Whole mount preparations of stage 6 embryos stained with anti-Twi and anti-Eve antibodies. A, B and C – Df(2L)ed-dp embryo; D, E and F – wild type embryo of corresponding age. A, D- Ventral view of Df(2L)ed-dp embryo showing the delayed ventral furrow invagination (A) and wild type embryo showing fully formed furrow at the same stage (D). B, E- Ventral view of Df(2L)ed-dp (B) and wild type (E) embryos in a slightly different focal plane showing the cephalic furrow and the first Eve stripe (arrow heads). C, F- Lateral view of Df(2L)ed-dp (C) and wild type (F) embryos showing mesoderm invagination. Anterior is to the left in all embryos and dorsal is towards the top in C and F.

About a quarter of the embryos from a cross between Df(2L)ed-dp males and females exhibit a slow invagination of the ventral furrow as compared to wild type embryos (Figure 5A, D). Two criteria were used to determine the age of the embryos, the depth of the cephalic furrow invagination and the position of the pole cells at the posterior. The cephalic furrow is known to start invaginating at roughly the same time as the ventral furrow (Campos-Ortega and Hartenstein, 1985) and the first Eve stripe coincides with the cephalic furrow (Vincent *et al.,* 1997) thereby serving as a marker to age the embryo. In this instance, comparing the cephalic furrow invagination of Df(2L)ed-dp and wild type embryos (arrow heads in Figure 5B, E) shows that the Df(2L)ed-dp embryos are slightly older. This is also indicated by the position of the pole cells (Figure 5C, F). The delay in invagination of the mesoderm, as compared to wild type, is evident in the lateral view (Figure 5C, F). The general nature of invagination is also abnormal, in that the anterior half of the ventral furrow seems to invaginate earlier than the posterior half (Figure 5A), although the exact reasons behind this is unclear.

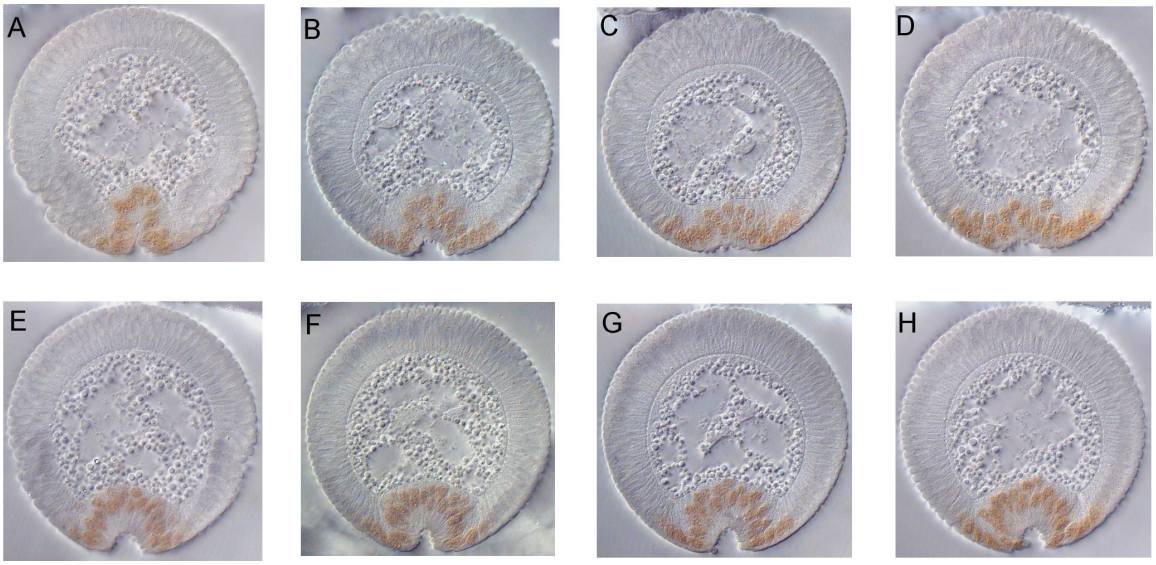

Figure 6: Serial sections through Df(2L)ed-dp (A,B,C and D) and wild type (E,F,G and H) embryos stained with anti-Twi and anti-Eve antibodies. The sections are from the anterior end of the embryo (A and E) to the posterior end (D and H), with B, F, C and G being from the mid region of the corresponding embryos. Towards the posterior end in Df(2L)ed-dp sections (C and D), the mesoderm primordium has hardly invaginated.

One possibility might be that the forces generated for normal cephalic furrow invagination pushes some of the mesodermal cells close to itself, inwards. This phenotype is also evident in serial sections from the anterior end to the posterior end of mutant embryos (Figure 6A-D). Defects in cell shape changes, which are known to lead to gastrulation delays, are not detectable at this level of resolution although this possibility cannot be ruled out as a cause for the observed phenotype unless further investigations at a higher resolution are carried out. Other possible reasons underlying such a delay in a morphogenetic process like ventral furrow formation could be defects in cell division, fate changes in the tissue or general cytoskeletal abnormalities.

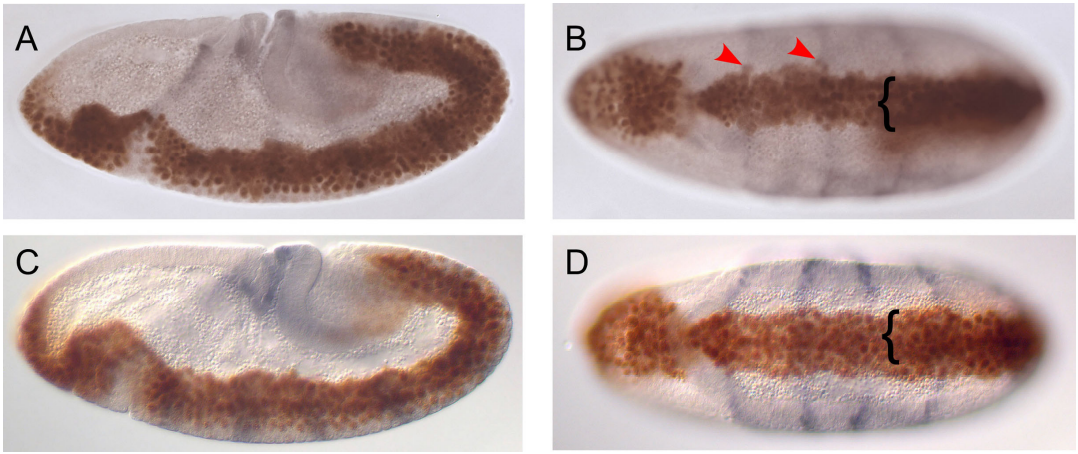

Figure 7: Whole mount Df(2L)ed-dp (A and B) and wild type (C and D) embryos stained with anti-Twi and anti-Eve antibodies showing mesoderm spreading defects. A and C - Lateral view of Df(2L)ed-dp and wild type embryos respectively. B and D - Ventral view of Df(2L)ed-dp and wild type embryos respectively. The arrowheads in B indicate some Twist positive cells away from the germ band. The width of the spread germ band is shown with the help of the brackets in B and D.

At slightly later stages, defects in spreading of the mesoderm on the underlying ectoderm is also prominent in a significant number of the embryos from a cross between Df(2L)ed-dp males and females (Figure 7B, D). In addition, several embryos with twisted or wobbly germ bands are also present in such a cross (Figure 8A-F). The degree of such germ band defects varies from mild (Figure 8A, B), to moderate (Figure 8C, D) to severe (Figure 8E, F), as compared to wild type (Figure 8G, H).

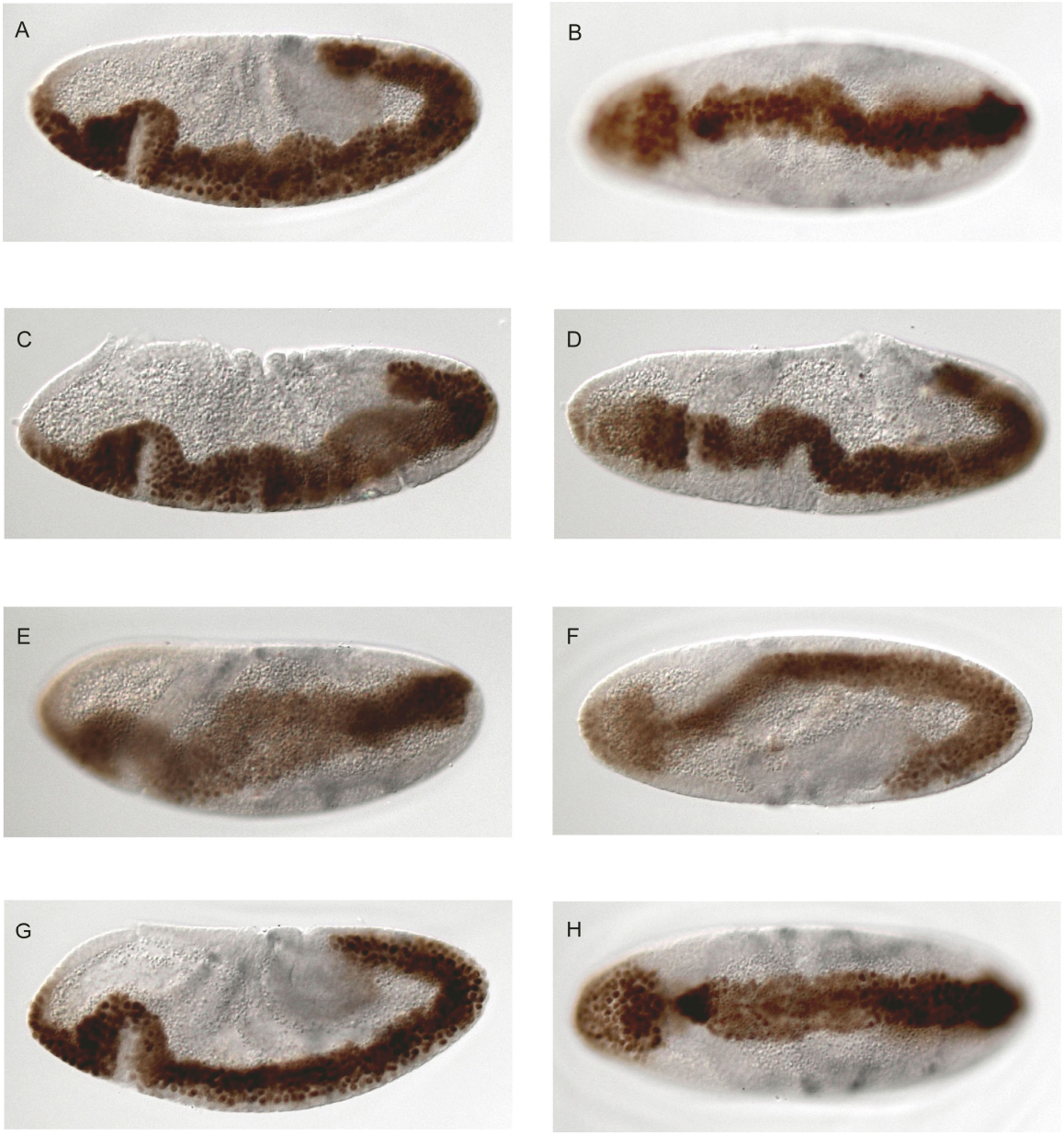

Figure 8: Whole mount Df(2L)ed-dp (A-F) and wild type (G and H) embryos stained with anti-Twi and anti-Eve antibodies showing germ band defects. A, C, E and G – Lateral view and B, D, F and H - Ventral view of embryos showing gastrulation defects in Df(2L)ed-dp (A-F) as compared to wild type embryos (G-H). The germ band defects can be mild (A, B), moderate (C, D) or severe (E, F).

3.2 Deficiencies analysed

In order to identify the gene or genes responsible for the gastrulation phenotypes discussed so far, other deficiencies which overlap partially or fully with Df(2L)ed-dp (Figure 9) were used to narrow down the genomic stretch in which these genes must lie. This can be done by looking at the gastrulation phenotypes exhibited by embryos homozygous for each of the deficiencies and identifying the deficiency stocks that show similar gastrulation defects to Df(2L)ed-dp. As the next step, the genomic stretches uncovered by these deficiencies have to be compared to that uncovered in the case of Df(2L)ed-dp. Once results from several deficiencies are available, it will be possible to identify the minimal genomic stretch harbouring the gene or genes of interest. In Figure 9, Df(2L)ed-dp and several other deficiencies that overlap partially or fully with itself are represented, with solid grey lines corresponding to the genomic region flanking the respective deficiency, dotted lines indicating genomic stretches that are unclear whether deleted or not and complete breaks representing the genomic stretch that is known to be deleted, from previous work by other groups. The dotted red lines from the top are guides to help orient to the rough break points of each deficiency, with respect to the cytogenetic map of the region. Embryos from all of these deficiencies were analysed for their gastrulation phenotype and the narrowing down of the region responsible for the phenotype was done, the results for which are summarized in Table 1. All of these classical deficiencies will be henceforth referred to as the “old deficiencies”.

However, the analysis got complicated because not all of the deficiencies represented in Figure 9 are ordinary ones, where the deficiency chromosome is kept over a balancer chromosome. This is because there is an as yet unidentified haploinsufficient locus in the cytogenetic interval 25B-D. This requires that any deletion that uncovers this haploinsufficient locus will need to have a duplication of the region, so as to maintain the deficiency as a stock. Indeed, several of the deficiency stocks have a duplication of the 24-25 region on to the X chromosome (Dp(2;1)B19), and two of the deficiency stocks have a tandem duplication on the second chromosome (Dp(2;2)B3). A detailed list of all

the deficiencies in the 24-25 cytogenetic region and their genotypes is given in the Materials and Methods section.

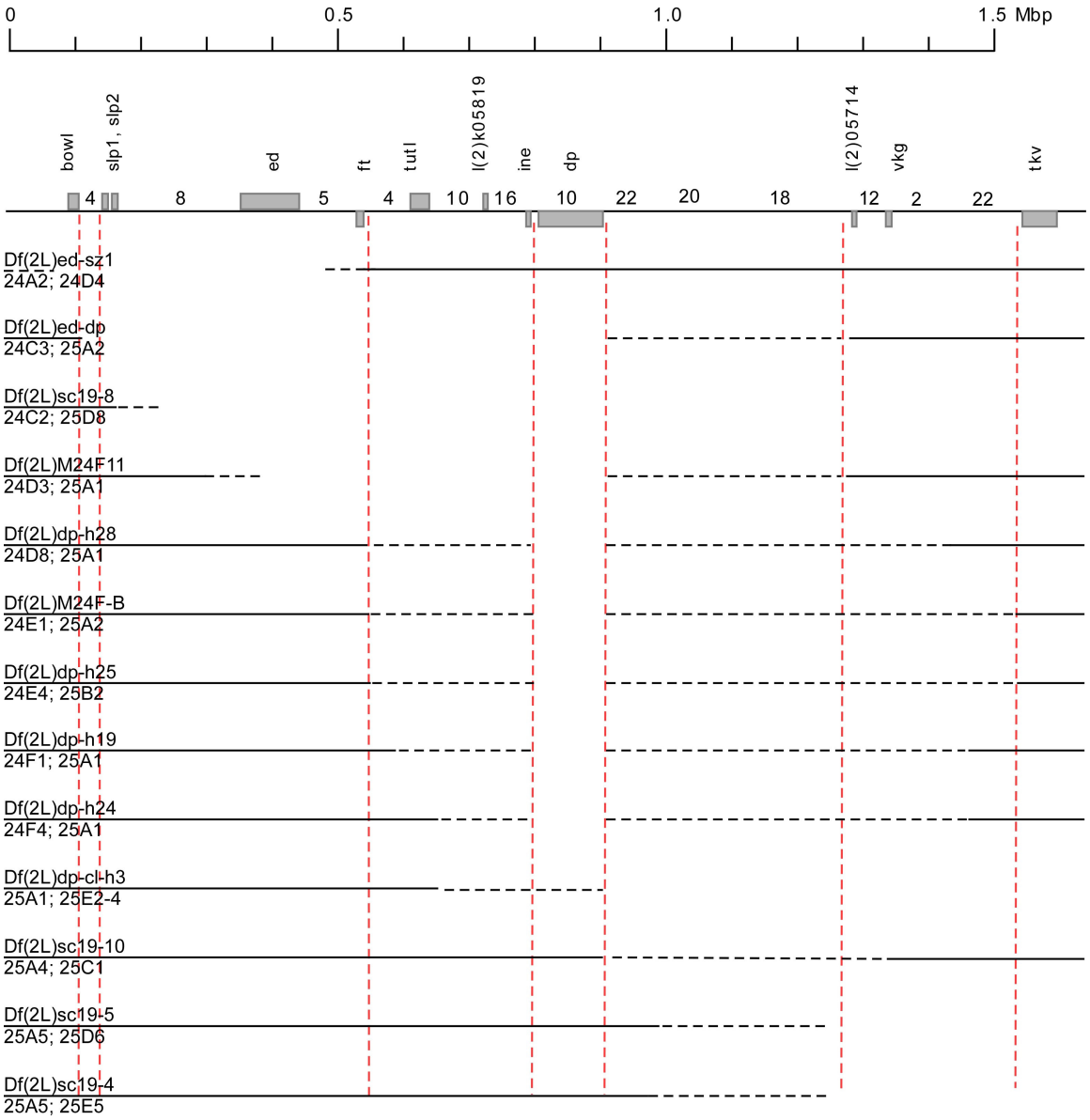

Figure 9: A simplified map of the cytogenetic region 24C-25E, representing the deficiencies of interest. The name of the deficiency is shown above and its predicted break points are shown below the representations of the respective deficiency. Dotted lines indicate regions of a deficiency that is not mapped precisely and may be deleted or not. Complete breaks are regions known to be deleted either by genetic or molecular mapping. The scale bar is shown above and the whole region represented here is 1.5Mb. A few genes within the region are also represented with their respective names and the number of genes known to be present in between any two represented genes is also shown. The vertical, dotted red lines depict the rough break points of each deficiency.

Homozygous embryos from deficiency stocks carrying the duplication on the X chromosome, Dp(2;1) B19, will not show a phenotype even if it is deleted for the gene of interest as the stock carries a normal copy of the gene on the X chromosome. In order to circumvent this problem, two methods can be made use of; either the duplication can be crossed out of the stock by crossing to wild type flies and then back crossing to the original stock, or these stocks can be crossed to a deficiency stock known to exhibit the gastrulation phenotype and tested for the phenotype as a transheterozygote. We chose the latter method as it is easier and because this method will allow any maternal effect to show up, which would otherwise be missed.

In the case of the tandem duplication, Dp(2;2)B3, the stocks can be tested as a normal deficiency because the duplication is present on the homologous arm of the deficiency chromosome and cannot affect the phenotype.

♂ \ ♀	Df(2L)ed-sz1			Df(2L)ed-dp			Df(2L)dp-h28			Df(2L)M24F-B			Df(2L)dp-h25			Df(2L)dp-h19			Df(2L)dp-h24			Df(2L)dp-cl-h3			wt		
	V	S	G	V	S	G	V	S	G	V	S	G	V	S	G	V	S	G	V	S	G	V	S	G	V	S	G
Df(2L)ed-sz1	-	-	-																								
Df(2L)sc19-8				+	+	+										+	-	-							+	-	-
Df(2L)ed-dp				+	+	+										+	-	-				+	-	-			
Df(2L)M24F-11				+	+	+										+	-	-									
Df(2L)dp-h28							+	-	-																		
Df(2L)M24F-B										+	-	-															
Df(2L)dp-h25													+	+	+												
Df(2L)dp-h19				+	-	-										+	+	+				+	-	-	+	-	-
Df(2L)dp-h24																			-	-	-						
Df(2L)dp-cl-h3																						+	-	-			
Df(2L)sc19-10																+	-	-									
Df(2L)sc19-5				+	-	-										+	-	-									
Df(2L)sc19-4				+	-	-																					
wt				+	-	-										+	-	-				+	-	-	-	-	-

Table 1: Table showing the different deficiencies and the phenotype associated with each. Males and females from the same deficiency were crossed to each other, embryos fixed and stained with anti-Twi and anti-Eve antibodies and scored for the gastrulation phenotype. Transheterozygous crosses were performed in the case of deficiency stocks carrying a duplication on the X chromosome, Dp(2;1) B19, by crossing these stocks to a deficiency known to show the phenotype. The severity of the phenotype is quite variable and in order to quantify, the phenotype was subdivided into 3 classes, marked by V (ventral furrow delay), S (mesoderm spreading defect) and G (germ band wobbly or twisted). The '+' indicates that the cross exhibits the particular phenotype, the '-' that it does not and empty columns are crosses that are not relevant.

Table 1 summarizes all the crosses performed and the phenotypes observed. The range of phenotypes exhibited by embryos derived from the different deficiencies have been classified into 3 main categories; delayed ventral furrow invagination (V), mesoderm spreading defects (S) and twisted or wobbly germ band (G). A'+' indicates that the respective cross exhibits the particular phenotype, '-' that it does not and blank columns in the table are crosses that were not performed.

3.2.1 A maternal locus contributes to the phenotype

Maternal effect genes encode gene products (RNA or protein) that are required in early development prior to zygotic transcription. A maternal effect gene is one, in which the aberrant phenotype is expressed in the offspring of mutant females (Underwood *et al.,* 1990). In other words, if the gene product is not made and contributed to the embryo by the mother for use before the zygotic transcription machinery starts functioning, the progeny exhibit characteristic defects. Sometimes, a copy of the same gene coming from the father is capable of rescuing this defect (paternal rescue). In crosses between females of either Df(2L)ed-dp or Df(2L)dp-h19 with wild type males, one of the three phenotypes scored for persists (Table 1), suggesting that at least one maternal effect locus is uncovered by both of these deficiencies. This phenotype is a delay in ventral furrow invagination; the other two phenotypes scored for were not present in such a cross in a penetrant manner. This raises two possibilities. Either it could mean that multiple loci are involved in controlling the three different phenotypes under consideration or else it could be that paternal rescue helps in rescuing the two later phenotypes and only the earliest one, delayed ventral furrow invagination, fails to be rescued and is obvious.

Surprisingly, when Df(2L)ed-dp females are crossed to Df(2L)dp-h19 males or vice versa, the progeny exhibit a similar phenotype as when either deficiency is crossed to wild type males, rather than the stronger phenotype exhibited by embryos homozygous for either deficiency. There are a few embryos that exhibit the spreading and twisted germ band phenotypes as well, although at a very low penetrance, for which reason these crosses have been scored not to exhibit these phenotypes. As embryos from both of these

deficiencies exhibit strong, penetrant phenotypes for each of the three parameters considered here, when males and females from within the same deficiency are crossed to each other, and do not do so in a transheterozygous combination, one of the two possibilities described below should hold true. The first is that, as both of the deficiencies have different breakpoints distally and proximally, each of them could have deleted genes not uncovered by the other, and in such a scenario would show the full phenotype only when crossed to itself and not in a transheterozygous combination. The second reason could be that either or both have accumulated background mutations over time, leading to gastrulation defects that do not map to the region. This is not unlikely and defects such as twisted germ band are often observed in weak stocks. In order to determine whether the latter possibility could be true, phenotypic complementation was done by looking at embryos from more transheterozygous combinations between Df(2L)ed-dp or Df(2L)dp-h19 and other deficiencies such as Df(2L)sc-19-8 or Df(2L)M24F-11 (Table 1). On comparison, it could be seen that Df(2L)ed-dp is unable to complement the three phenotypes under consideration whereas Df(2L)dp-h19 does (Table 1), indicating that indeed embryos from Df(2L)dp-h19 exhibit defects that do not map to the region. This was further confirmed by observations that Df(2L)dp-h19 failed to complement lethal alleles from outside the 24-25 region, during crosses performed for different experiments (data not shown). The weak phenotype that still persists in such transheterozygous crosses involving Df(2L)dp-h19 (Table 1) could be a dominant effect.

3.2.2 A zygotic locus contributes to the phenotype

As has been already described, at least one maternal locus contributes to the overall gastrulation defects observed in embryos from deficiency stocks such as Df(2L)ed-dp. In all crosses performed involving females having the deficiency, the maternal effect will show up and distort both the nature of the phenotype and the proportion of affected embryos, as is clear from a cross to wild type males (Table 1). This means that any phenotype which is not maternal but is zygotic (exhibited when a heterozygous male is crossed to a heterozygous female, resulting in a quarter of the progeny being homozygous mutant) will be masked by the maternal effect phenotype. In order to distinguish the

zygotic phenotype from the maternal effect, the mothers used for such cross should be wild type for the maternal locus uncovered and thereby, not show the maternal effect. This can be achieved by a genetic technique described previously (Rasmussen, 1960; Merrill *et al.,* 1988) which involved using the compound stock. In this instance, the second chromosome compound stock (C(2)v) was used as the region of interest is on the second chromosome and males carrying the deficiencies were crossed to C(2)v females.

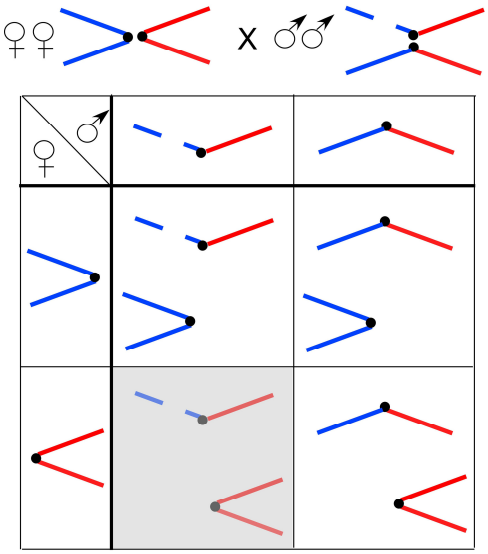

Figure 10: Schematic representation of the gametes and the zygotes formed in a cross between second chromosome compound females and a second chromosome deficiency stock. The blue lines are the second chromosome left arms and the red lines, the right arms with the black spot representing the centromere. The broken blue line indicates the deletion in the left arm of the deficiency stock. The bottom left zygote is of interest (shaded in grey), which has only the one second left arm, which is deleted for the region of interest. A zygotic gene mapping to the region uncovered by the deficiency, having an effect will show up as the embryo lacks a copy of the gene but maternal effect genes will not show its effect, as the mothers have a normal chromosomal complement.

The compound stocks have both the left arms of the chromosome attached to each other and both the right arms attached to each other at the centromere as opposed to one left arm and one right arm being attached to each other. The chromosome segregation pattern of the second chromosome compound stock is described in detail in the Introduction (Figure 3). The segregation pattern of a cross between a second chromosome compound stock female and a second chromosome left arm deficiency stock is shown in the schematic Figure 10. The blue lines are the second chromosome left arms, the red lines

the right arms and the black dots, the centromere. The break in the blue line is a representation of the chromosomal deletion in the deficiency stock left arm. The progeny of interest is the bottom left one marked in grey, wherein the zygote has only one left arm of the second chromosome, which is deleted for the region of interest. In this subset of progeny, the zygotic effects of deletion of a gene will be manifest but maternal effects will not be, as the mothers possess the complete chromosomal complement.

♀ \ ♂	Df(2L)ed-dp	Df(2L)dp-h28	Df(2L)M24F-B	Df(2L)dp-h25	Df(2L)dp-h19	Df(2L)dp-h24	wt
C(2)v	+++	+++	+++	+++	+	+	+

Table 2: Table showing the phenotype exhibited by different deficiencies and wild type males, when crossed to second chromosome compound (c(2)v) females. Deficiency and wild type males used in the crosses are represented in each column and the strength of phenotype by the '+' symbol. As is evident, wild type males give a weak phenotype (+), presumably due to loss of one copy of the *snail* gene. All the deficiencies tested exhibit either a weak phenotype similar to wild type or a strong, penetrant phenotype (+++) as shown in Figure 11.

In order to determine whether a zygotic locus is involved in the gastrulation phenotype exhibited by embryos derived from deficiencies in the 24-25 cytogenetic region, males from the deficiencies of interest, namely Df(2L)ed-dp, Df(2L)dp-h25, Df(2L)dp-h28, Df(2L)M24F-B, Df(2L)dp-h19 and Df(2L)dp-h24, as also wild type males, were crossed to the C(2)v females, and the gastrulation phenotype exhibited by embryos from each cross analysed. The results obtained from these crosses are summarized in Table 2. Each of the deficiencies and wild type males used in the cross are represented in each column in Table 2, and the second chromosome compound females in the single row. The strength of the phenotype is either weak (+) or strong (+++), with no intermediate phenotypic category. The strong phenotype represented here is stronger than the original homozygous deficiency phenotype described before (Figure 5Figure 6Figure 7Figure 8), as is clear from Figure 11, where embryos from a cross between Df(2L)dp-h25 males and C(2)v females is shown. As opposed to the embryonic homozygous deficiency phenotype, which is a delay in ventral furrow formation, in this instance, the ventral furrow does not invaginate at all or even if it does, at a later stage. The presence of this

severe, penetrant phenotype leads to the conclusion that there is indeed a zygotic locus that is required for proper ventral furrow invagination, in the 24-25 cytogenetic region. The weak phenotype depicted here, which is also exhibited by embryos when wild type males are crossed to the C(2)v females (Table 2) is presumed to be due to loss of one copy of the *snail* gene, which is known to produce a delay in ventral furrow invagination.

It is clear from Table 2 that embryos from a cross between Df(2L)ed-dp, Df(2L)dp-h25, Df(2L)dp-h28 and Df(2L)M24F-B males and C(2)v females exhibit the severe phenotype, whereas embryos from Df(2L)dp-h19, Df(2L)dp-h24 and wild type males in combination with C(2)v females exhibit the mild phenotype. In other words, the zygotic locus is not uncovered by Df(2L)dp-h19 and Df(2L)dp-h24, but is uncovered in all deficiencies that extend beyond Df(2L)dp-h19 to the left (Figure 9). This leads to the conclusion that the zygotic locus responsible for the phenotype shown in Figure 11 lies between the left break point of the deficiency Df(2L)dp-h19 and the left break point of Df(2L)dp-h25 (Figure 9).

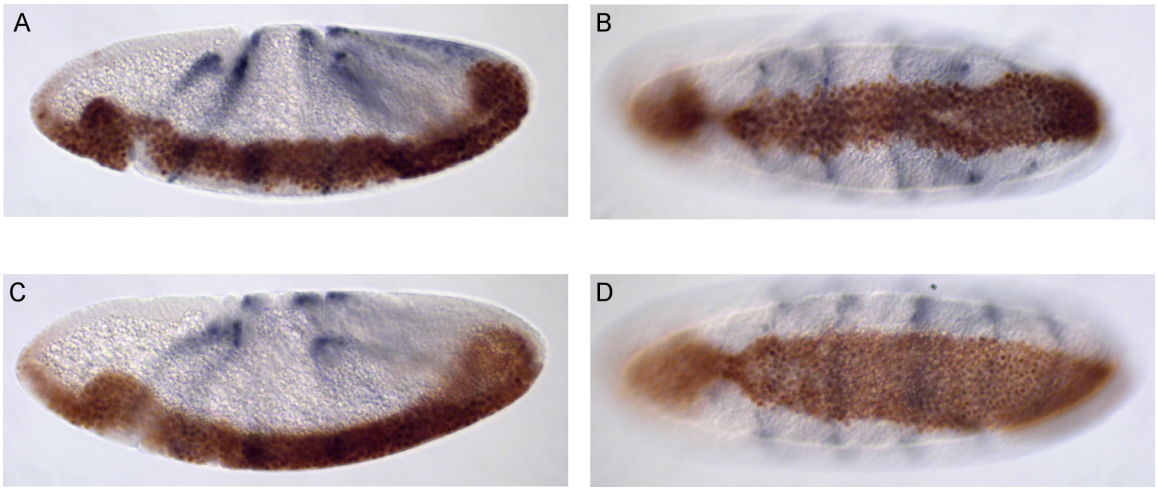

Figure 11: Whole mount embryos from a cross between second chromosome compound females c(2)v and Df(2L)dp-h25 males, stained with anti-Twi and anti-Eve antibodies. A and C are lateral views of 2 embryos and B and D, ventral views of the same embryos. The block in gastrulation is clearly visible in the lateral view (A and C) while the inability to form the ventral furrow can be visualized in the ventral view (B and D). A very rudimentary furrow can be seen in B, in the posterior half of the embryo. The twisted germ band can be seen in D.

3.3 New deficiencies

The available deficiencies that were made use of and have been described so far are large deletions whose breakpoints are not molecularly mapped, leaving the extent of the deleted genomic stretch unclear. This makes the picture complex, especially when dealing with more than one locus within the same deletion contributing to the eventual phenotype. In addition, these deficiencies are not isogenized stocks, meaning that they are not in the same genetic background; in other words, some of the deficiencies might exhibit defects in gastrulation due to mutations in unrelated loci (background mutations), accumulated over time. This called for a method to generate new deletions in the region, so as to confirm and narrow down the region responsible for the gastrulation phenotype. One obvious technique to generate deletions would have been X-ray mediated mutagenesis, which was the method used to construct most of the deficiency stocks (old deficiencies) discussed before. This method has the same drawback as the old deficiencies, in that the break points would not be precise and would require extensive genetic crosses and PCR based strategies to map.

Due to this, we opted for a modified technique for generating deletions, using special stocks which have P element insertions carrying FRT sites in them. The flanking region of each of these P element insertions have been identified by sequencing. These modified P element stocks are the Drosdel stocks (Ryder *et al.,* 2004). When two such Drosdel stocks carrying FRT sites in the appropriate orientation and proximity are crossed to each other and the required enzyme is provided, recombination occurs between the FRT sites and deletion events can be recovered between the two FRT sites, by selecting for the expression of a marker. The biggest advantage of this technique lies in the fact that the position of insertion of the P elements carrying the FRT sites is already known, and as the deletion occurs between the two FRT sites, the precise break points are already known when such deletions are made. The break points are further confirmed by complementation or PCR. Further, as all the stocks used for generating the deletions are isogenized, additional background effects playing a role can be totally ruled out.

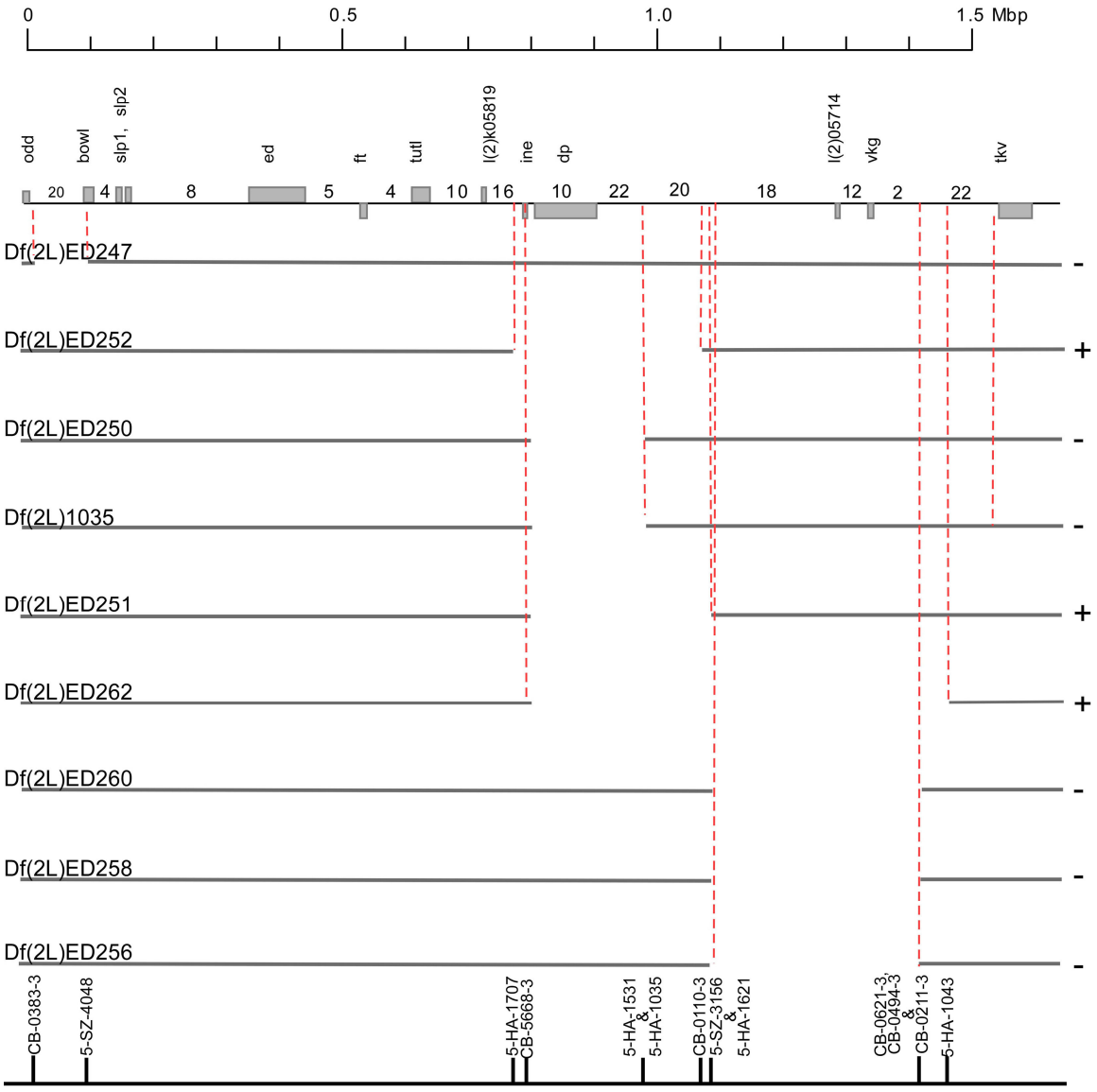

Figure 12: A simplified map of the cytogenetic region 24C-25E, depicting deficiencies made using Drosdel stocks. The solid grey lines represent the flanking genomic stretch and the gap, the actual genomic stretch deleted. The dotted red lines correspond to the proximal and distal break points of each deficiency and helps in orienting to the stretch deleted in each case. The tenth deletion could not be represented in this schematic, as it deletes a genomic stretch outside the region represented here. The name of the respective deficiency is above the line representing each deficiency. The forward and reverse elements used in each case to generate the deletion are mentioned at the bottom. The '+' on the right side indicates that embryos from the stock carrying the particular deficiency shows gastrulation defects and the '-' that they do not. The scale bar is shown above and the whole region represented is 1.5Mb.

Complete information on the stocks used for generating these new deletions are given in the Materials and Methods section and the crossing strategy used to make the deletions (Golic and Golic, 1996; Ryder *et al*, 2004) is available from the Drosdel website at http://131.111.146.35/~pseq/drosdel/ddinfo.html.

In total, ten new deficiencies were made using these stocks, out of which nine are represented in the schematic drawing in Figure 12. The names of each deficiency stock is given above the line representing each deficiency, with the solid grey line corresponding to the genomic region flanking the respective deficiency and the gap representing the actual genomic stretch deleted. The dotted red lines from the top are guides to help orient to the proximal and distal break points of each deficiency, with respect to the cytogenetic map of the region. The forward and reverse elements used to construct the deficiencies are represented at the bottom of the schematic. The tenth deficiency that was made is not represented in Figure 12 as it uncovers genomic region falling distal to the cytogenetic map represented in the figure. Several of the deficiencies uncover overlapping regions and thus provide a better coverage of the region.

3.3.1 A locus uncovered by 3 new deficiencies

The larger deficiencies in the region like Df(2L)sc-19-8 (Figure 9), uncover most of the genomic region represented in Figure 12. It is possible that such large deficiencies harbour other loci than the maternal and zygotic loci described before, which might contribute to the overall gastrulation defect exhibited by embryos derived from them. To test for such a possibility, all of the newly constructed deficiencies were analysed for gastrulation defects by collecting embryos from a cross between heterozygous males and females from the respective deficiency and looking for possible gastrulation defects. It was found that three overlapping deficiencies, Df(2L)ED252 (deletion between elements 5-HA-1707 and CB-0110-3) , Df(2L)ED251 (deletion between elements 5-SZ-3156 and CB-5668-3) and Df(2L)ED262 (deletion between elements 5-HA-1043 and CB-5668-3), all of which are marked by a '+' in Figure 12 have defects in gastrulation. Embryos were collected from a cross between heterozygous deficiency (Df(2L)ED251) females and

males and analysed and the phenotype observed is shown in Figure 13. The phenotype is similar to that exhibited by deficiencies like Df(2L)ed-dp, in that there is a delay in ventral furrow formation (Figure 13A, B) and there are instances of a lack of coordination in furrow formation (Figure 13C, D). Additional defects seen in the case of Df(2L)ed-dp, such as mesoderm spreading defects and wobbly germ band are absent in this case. This phenotype could be as a result of a dominant maternal effect locus, as a significant number of embryos from a cross between heterozygous deficiency females and males exhibit this phenotype, as also when deficiency females are crossed to wild type males.

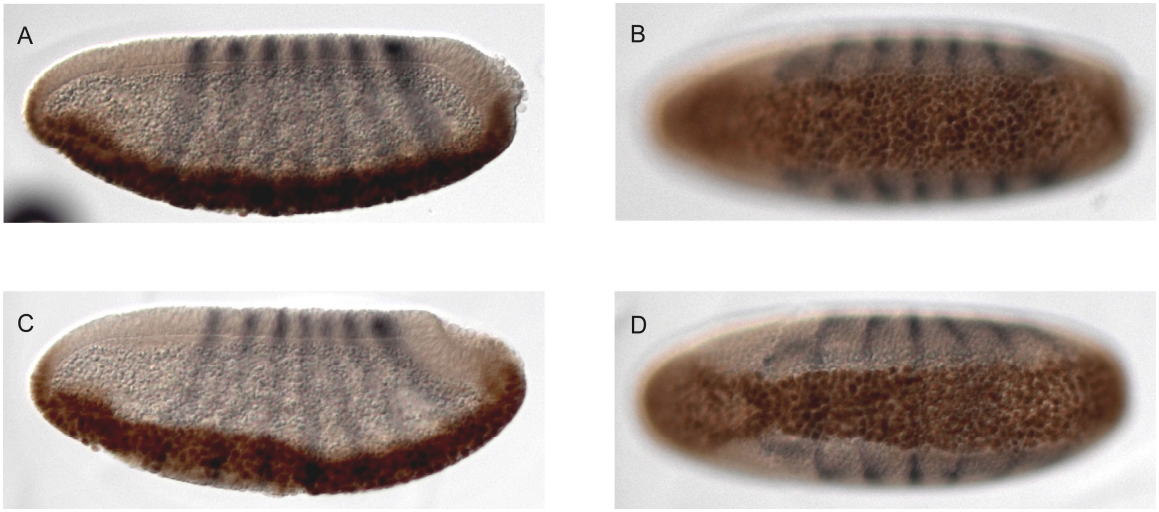

Figure 13: Whole mount preparations of embryos from a cross between Df(2L)ED251 males and females, stained with anti-Twi and anti-Eve antibodies. A and C- Lateral view and B and D- Ventral view of early (A, B) and later (C, D) stage embryos from a cross between Df(2L)ED251 males and females, exhibiting delayed ventral furrow formation.

Figure 14 helps to better orient to the region and combine several of the old and four of the newly constructed deficiencies. Embryos from all of the deficiencies marked with a '+' in Figure 14 exhibit a maternal effect gastrulation phenotype as evidenced by the persistence of the phenotype in embryos derived from a cross between deficiency females and wildtype males and those with a '-' do not exhibit this maternal gastrulation defect.

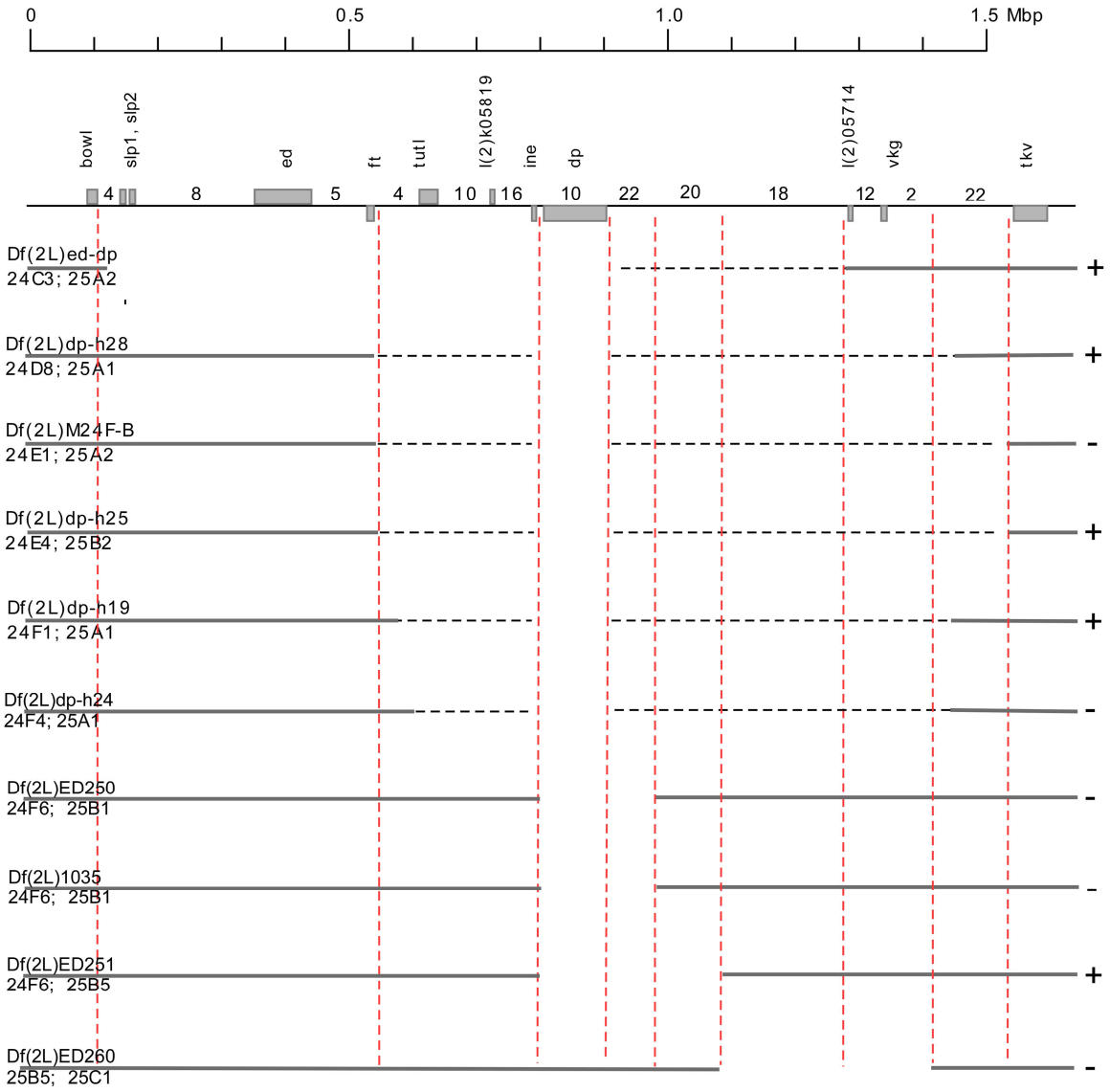

Figure 14: A simplified map of the cytogenetic region 24C-25E, representing several old deficiencies and 4 of the new deficiencies. The first 6 deficiencies are already existing ones whereas the last 4 are the newly constructed ones. As in Figure 5, the names of the deficiencies are shown above and the region deleted, below the representation of the respective deficiency. The break points are indicated by the breaks in the straight lines and the region deleted, by the gaps in the straight lines. The dotted red lines serve to orient with respect to the break points of the various deficiencies. The '+' indicates that embryos from the respective deficiency exhibits a maternal effect and the '-' that they do not. The scale bar is shown above the map and the whole region represented is 1.5Mb.

3.4 Complementation and single embryo PCR

The break points of none of the deficiencies have been mapped precisely by molecular mapping techniques, except in the case of the newly made ones, described before. Cytogenetic mapping by *in situ* hybridisation to polytene chromosomes and complementation with existing lethal alleles had been used to elucidate the break points of the older deficiencies. Cytogenetic mapping (by *in situ* hybridisation) is not high resolution whereas complementation data is incomplete for all the deficiencies of interest.

Proximal ↑ Distal ↓

♂ \ ♀	Df(2L)ed-dp	Df(2L)M24F-B	Df(2L)dp-h28	Df(2L)dp-h25	Df(2L)dp-h19	Df(2L)dp-h24
l(2)0670806708	+	+	+	+	+	+
edk01102	-	+	+	+	+	+
l(2)SH0479	-	+	+	+	+	+
ft$^{G\text{-}rv}$	-	+	+	+	+	+
tutlk14703	-	-	-	+	+	+
l(2)SH0805	-	-	-	-	+	+
dw-24E1 l(2)cg1	-	-	-	-	+	+
Tps1k08903	-	-	-	-	-	+
mRpL27[KG01128]	-	-	-	-	-	-
l(2)SH0840	-	-	-	-	-	-
dp lv1	-	-	-	-	-	-
l(2)SH1525	+	+	+	+	+	+
slf1	+	+	+	+	+	+
l(2)k10004k10004	+	+	+	+	+	+
l(2)k10217k10217	+	+	+	+	+	+
vkgk00236	+	+	+	+	+	+
l(2)k10127k10127	+	+	+	+	+	+
l(2)k11206k11206	-	+	+	+	+	+

Table 3: Results from the complementation analysis performed between lethal alleles and deficiencies. The lethal alleles used and the deficiencies to which these lethals were complemented are shown. A '+' indicates that the lethal allele can complement the corresponding deficiency and a '-' indicates that the lethal allele does not complement the deficiency.

Thus, in order to determine the break points of these deficiencies more precisely and thereby narrow down the genomic region responsible for the phenotypes described before, the old deficiencies of interest were tested for complementation with lethal alleles of genes in the region. Most of the lethal alleles used were newly identified ones, which had not been used in previous mapping experiments while a few old alleles were also used to confirm the existing data for the break points. The results from the complementation experiments are summarized in Table 3. The genotypes of the respective lethal alleles used and the deficiencies to which they were complemented are shown. Details of the lethal alleles used are given in the Materials and Methods section.

The right break point of all the deficiencies is distal to *dp* (i.e., to the right in the maps in Figures 9 and 14). Df(2L)dp-h24 is the smallest deficiency and does not uncover Tps1k08903. Df(2L)dp-h19 is the next as this deficiency along with Df(2L)dp-h24 complement the lethal alleles, *dw-24E1 l(2)cg1* and *l(2)SH0805* (Table 2). As shown before, both Df(2L)dp-h24 and Df(2L)dp-h19 do not uncover the zygotic locus responsible for the phenotype whereas Df(2L)dp-h25 does (Table 2). From Table 3, it can be seen that Df(2L)dp-h25 does not complement the lethal alleles *dw-24E1 l(2)cg1*, *l(2)SH0805* or *Tps1k08903* but complements *tutlk14703*. This indicates that the zygotic locus responsible for the phenotype lies between the genes, *Tps1* and *tutl*.

Further molecular characterization of the deficiencies was carried out by single embryo PCR in order to determine the precise break points of the deficiencies of interest. In this instance, the most important break points to be determined were the proximal breaks of Df(2L)dp-h19, which does not exhibit the phenotype when crossed to compound females and Df(2L)dp-h25, which does. In addition, the distal break points of both of these and most of the other deficiencies described before were also fine mapped by single embryo PCR. Complete mapping details for all relevant deficiencies used in the study are provided in Appendix 1. A summary of the complementation and PCR results (where available), is given in Table 4.

Proximal

Distal

Genes	Mapping method	Df(2L)ed-dp	Df(2L)M24F-B	Df(2L)dp-h28	Df(2L)dp-h25	Df(2L)dp-h19	Df(2L)dp-h24
bowl	comp	+	+	+	+	+	+
echinoid	comp	-	+	+	+	+	+
CG3714	comp	-	+	+	+	+	+
fat	comp	-	+	+	+	+	+
turtle	comp	-	-	-	+	+	+
Atet	PCR			-	+	+	
CG15429	PCR			-	-	+	
Traf1	PCR			-	-	+	
CG18013	comp	-	-	-	-	+	+
Tps1	PCR			-	-	+	+
Tps1	comp	-	-	-	-	-	+
CG3652	PCR			-	-	-	+
CG12677	PCR			-	-	-	+
CG15436	PCR	-	-	-	-	-	-
RpL27A	comp	-	-	-	-	-	-
dumpy	comp	-	-	-	-	-	-
dumpy	PCR	-	-	+	-	-	+
CG11929	PCR	-	-	+	-	-	+
CG15634	PCR	-	-	+	-	-	+
CG15631	PCR	-	-	+	-	-	+
CG3225	PCR	+	+	+	-	+	+
mRpS2	comp	+	+	+	+	+	+

Table 4: Complete results from complementation analysis and single embryo PCR, for deficiencies in the 24-25 cytogenetic region. The deficiencies analysed are given in the first row and the genes for which each of them were tested are given in the first column. The method of testing was either single embryo PCR (PCR) or complementation (comp). A '+' indicates that the gene is not uncovered and '-' that it is.

From Table 4 it is clear that the proximal break point of Df(2L)dp-h25 lies between the genes *Atet*, which is not uncovered, and *CG15429*, which is. The proximal break point of Df(2L)dp h19 lies within the gene *Tps1*, which is genetically uncovered but molecularly not (Table 4). As the phenotype has been mapped to between the proximal break points of Df(2L)dp h19 and Df(2L)dp h25, the locus responsible for the gastrulation defect observed in embryos when deficiencies in the region are crossed to compound chromosome females can be assumed to be in the genomic stretch spanning *Tps1* distally and *Atet* proximally.

Based on the mapping results shown in Table 4, it became clear that the maternal effect exhibited by embryos from the old deficiencies map proximal to *dumpy*. This is because the maternal effect is not exhibited by Df(2L)dp-h24 embryos, which is uncovered for *dumpy*, *RpL27A* and *CG15436* (Table 4). However, embryos from three of the newly made deficiencies (Df(2L)ED252, Df(2L)ED251 and Df(2L)ED262 also exhibit a maternal effect gastrulation phenotype (Figures 12,Figure 13and 14). Only one of these three deficiencies, Df(2L)ED252, uncover genomic stretches proximal to *CG15436*. Since embryos from the other two deficiencies (Df(2L)ED251 and Df(2L)ED262) also exhibit the same maternal effect, it is clear that this locus must lie distal to *dumpy* and not proximal to it. Almost all of the old deficiencies have their distal break point in or close to *dumpy* (Table 4). Embryos derived from some of the new deficiencies such as Df(2L)ED250 and Df(2L)1035, which uncover *dumpy* and genes distal to it do not exhibit a maternal effect (Figure 14). By testing embryos from several of the newly made deficiencies which uncover genomic stretches distal to *dumpy*, it was clear that the maternal effect phenotype exhibited by embryos from the three newly made deficiencies is separate from the maternal effect gastrulation defect observed in embryos from the old deficiencies (Figures 12, 14 and Table 4). The maternal effect phenotype characteristic of embryos from the newly made deficiencies mapped to a 40Kb stretch harbouring some 16 genes, distal to *dumpy*. However, the maternal effect gastrulation defects observed in embryos from the older deficiencies lie proximal to dumpy although the exact location could not be mapped. One possibility is that the same locus that harbours the gene

responsible for the zygotic gastrulation defects might be responsible for the dominant maternal defect exhibited by embryos from the old deficiencies.

3.5 Summary

The data discussed so far, shows that at least three different components contribute to the gastrulation defect which was originally observed in embryos from the deficiency Df(2L)sc-19-8 by Thomas Seher, in a deficiency screen. The first is a dominant maternal effect, exhibited by embryos derived from deficiencies such as Df(2L)ed-dp and Df(2L)dp-h25 which persists when deficiency females are crossed to wild type males, revealing that it is indeed a dominant maternal effect. Embryos from Df(2L)dp-h19 also exhibit such a phenotype but as this deficiency seems to have accumulated background mutations which contribute at least in part to the phenotype exhibited, it is unclear whether this deficiency indeed uncovers the same maternal effect locus.

The second is a zygotic effect, which is exhibited by embryos when males from deficiencies such as Df(2L)ed-dp and Df(2L)dp-h25 are crossed to the second chromosome compound (C(2)v) females and not exhibited by Df(2L)dp-h19 and Df(2L)dp-h24. The genomic stretch responsible for this phenotype has been narrowed down using ten newly constructed deficiencies and by precise mapping of the existing deficiencies. The genomic region harbouring the gene or genes responsible for this zygotic gastrulation defect lies between the proximal break points of Df(2L)dp-h19 and Df(2L)dp-h25, a region about 60 Kb in size and containing roughly 10 genes, both known and predicted.

Finally, embryos from three out of the ten newly made deficiencies exhibit a weak, dominant maternal effect phenotype. This maternal effect locus is genetically separable from the previously mentioned maternal effect locus as none of the older deficiencies uncover the genomic stretch which is responsible for this phenotype. This locus spans roughly 16 genes and a size of about 40 Kb.

The maternal and zygotic effects described before and which are exhibited by embryos from the old deficiencies such as Df(2L)ed-dp and Df(2L)dp-h25 could very well be as a

result of deletion of the same locus. Embryos from several of the older deficiency stocks which do not exhibit a strong gastrulation phenotype by themselves, such as Df(2L)M24F-B (Table 1), does exhibit the zygotic effect in combination with C(2)v (Table 2), suggesting that such deficiency stocks might have accumulated suppressor mutations over time. The phenotype exhibited by embryos from the deficiencies which are uncovered for the zygotic locus such as Df(2L)ed-dp, in combination with the C(2)v females is stronger compared to that of embryos from a cross between heterozygous deficiency males and females. This raises two possibilities. First, it could be that the zygotic locus is influenced by haploinsufficiency of the second left arm or triploidy of the second right arm or both, as the C(2)v cross results in embryos with such chromosomal combinations (Figure 10), which will be discussed further later on. It could also be that the C(2)v stock has background mutations, which enhance the deficiency phenotype.

3.6 A candidate gene responsible for the zygotic phenotype

The zygotic component responsible for the severe gastrulation phenotype exhibited by embryos from a cross between deficiency males and C(2)v females was narrowed down to between the proximal break points of Df(2L)dp-h19 and Df(2L)dp-h25. In order to identify this candidate, the genomic stretch between the aforementioned breakpoints was scanned. The distal boundary of this stretch is the gene *Tps1* and the proximal, *Atet* (Table 4). This region is magnified and shown as a snapshot from Flybase in Figure 15. The red arrows mark the boundaries of the region harbouring the zygotic locus in Figure 15, which spans about 50Kb and some ten genes. Two methods were employed to identify the possible zygotic component responsible for the gastrulation defects. The first was to look for possible P element insertions or other mutants in this region of interest and test whether embryos derived from a cross between any of these mutations and C(2)v females exhibited the severe phenotype as observed with deficiencies in the region. The second was to look for genes within this genomic stretch with suggestive mRNA expression patterns, either based on published data or from the BDGP mRNA *in situ* expression pattern resource (http://www.fruitfly.org/index.html).

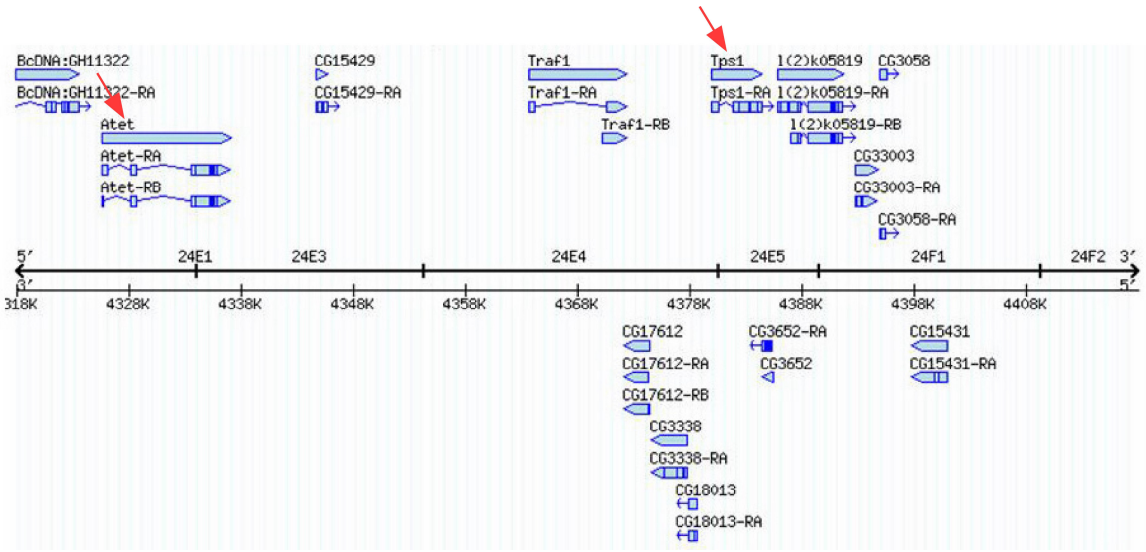

Figure 15: A snap shot from Flybase of the 24E-F region, depicting the genomic stretch harbouring the zygotic locus of interest. The zygotic locus must lie between *Atet* on the proximal side and *Tps1* distally, both of which are marked by arrows. The genes between are also represented and there are stretches not coding for known or predicted genes. The entire genomic region depicted here is 100Kb as shown by the scale bar in the middle, with the region between the two arrows being about 55Kb. The direction of the arrowhead representing each gene corresponds to the direction of transcription.

With regard to the first method, there were two lethal P element insertions (in *Tps1* and *CG18013*-Table 3) and a collection of stocks generated by EMS mutagenesis, henceforth referred to as EMS alleles (Szidonya and Reuter, 1988), which could be used for the purpose. All of these stocks and details of the genes they affect are listed in Table 5. Males from both the P element insertion carrying stocks were tested for the possible zygotic phenotype by crossing to C(2)v females. Embryos from neither of them reproduced the zygotic phenotype (Table 5). Unless these two P element insertions are not null alleles, this would mean that neither *Tps1* nor *CG18013* are responsible for the zygotic phenotype. As both the P element insertions result in lethality and fail to complement deficiencies in the region (Table 3), it seems likely that they are null or strong loss of function alleles. Embryos from the EMS alleles were also tested for possible gastrulation defects. Details of the EMS alleles used are available in the

Materials and Methods section. It was found that embryos from none of the EMS alleles crossed to C(2)v females could reproduce the enhanced zygotic phenotype either (Table 5), indicating that none of the EMS alleles uncover the zygotic locus involved in gastrulation.

Alleles used	Mutagen	Genes predicted to be affected	Genes found to be affected	Phenotype when crossed to C(2)v females	Phenotype when crossed to itself
Tps1k08903	P element	*Tps1*	*Tps1*	-	-
l(2)SH0805	P element	*CG18013*	*CG18013*	-	-
b11(jf4)	EMS	*tutl*	*tutl*	-	-
a18(jf5)	EMS	*Tps1*	*Tps1*	-	-
a19(jf5)	EMS	*Tps1*	*Tps1*	-	-
b2(jf5)	EMS	*Tps1*	*Tps1*	-	-
h10(jf5)	EMS	*Tps1*	*Tps1*	-	-
sz31(jf5)	EMS	*Tps1*	*Tps1*, *dumpy*	-	+
sz3(jf6)	EMS	*l(2)24Fa*	not done	-	-

Table 5: Details of all the alleles, both P element and EMS, that were used to identify the zygotic locus responsible for the gastrulation phenotype. The first column represents the alleles that were available for the region of interest and were made use of; the second column shows the mutagen used to generate the particular allele; the third shows the genes that are affected by the mutation based on published data; the fourth column represents the results from complementation experiments done to confirm the published data – only one allele, *sz31*(*jf5*) behaves in a different manner compared to previous reports and is lethal for the *dumpy* gene as well as *Tps1*; the sz3(*jf6*) allele could not be complemented over the *l(2)24Fa* allele as this allele is not available anymore; the fifth column shows whether embryos from any of the mutants exhibit a gastrulation phenotype when crossed to C(2)v females (none do, marked by -) and the last column shows whether embryos from any of the mutant alleles exhibit gastrulation defects by themselves – only embryos from the sz31(jf5) allele exhibit gastrulation defects by itself (marked with +).

Embryos from one of the EMS alleles, *sz31*(*jf5*) reported to be an allele of *Tps1* (Szidonya and Reuter, 1988), exhibit gastrulation defects wherein all embryos derived from a cross between males and females of the stock exhibit delayed ventral furrow invagination (data not shown). This allele does not complement another gene in the region, *dumpy* (Table 5) suggesting that the stock has additional mutations other than in the *Tps1* gene. Further, as embryos from other loss of function alleles of *Tps1* do not exhibit gastrulation defects, it is clear that mutations in *Tps1* are not responsible for the

defects exhibited by embryos from the *sz31*(*jf5*) stock. When this stock is crossed to the C(2)v stock, no enhanced zygotic gastrulation defects are observed (Table 5). This shows that the gastrulation phenotype exhibited by embryos from the *sz31*(*jf5*) stock is maternal in nature, although whether the phenotype maps to the 24-25 region which is being investigated is not clear.

The second strategy was to check for the embryonic mRNA expression pattern of genes in the region by *in situ* hybridization. One of the genes in the genomic stretch, *Traf1* (TNF Receptor Associated Factor 1), was expressed in the mesoderm during gastrulation stages. Further, the available mRNA expression data for other genes in the genomic stretch of interest such as *Atet*, *CG17612*, *CG18013* and *Tps1* (BDGP gene expression database) suggested that they might not play a role in gastrulation. This made *Traf1* the most likely candidate gene responsible for the zygotic gastrulation phenotype among the genes in the genomic interval of interest. The mRNA expression pattern of *Traf1* was available from the BDGP mRNA resource as well as from an earlier publication (Preiss *et al.,* 2001). In order to verify and analyse this in more detail, *in situ* hybridization using an anti sense *Traf1* mRNA probe was carried out, the results from which are shown in Figure 16. The *Traf1* mRNA is supplied maternally (Preiss *et al.,* 2001; Figure 16A and B) to the early embryo. By early cellularization, the mRNA is localized to a broad ventral domain and in seven stripes from the anterior of the embryo to the posterior, with the first and last stripes being most prominent (Figure 16C, D). This expression pattern persists through cellularization (Figure 16E and F). By early gastrulation, the ventral domain of expression is restricted to the cells that invaginate during ventral furrow formation (Figure 16G-J). The seven stripes of expression persist through these stages and are lost by mid-gastrulation. Later on, the mRNA can be detected in the mesoderm and the neuro-ectoderm (Figure 16K, L). The ectodermal expression resembles that of typical proneural genes (BDGP mRNA resource). Because the embryonic *Traf1* mRNA expression was in the ventral domain where mesoderm invagination occurs, *Traf1* was considered a potential candidate gene which might be responsible for the zygotic gastrulation defects mapped to the genomic stretch described before.

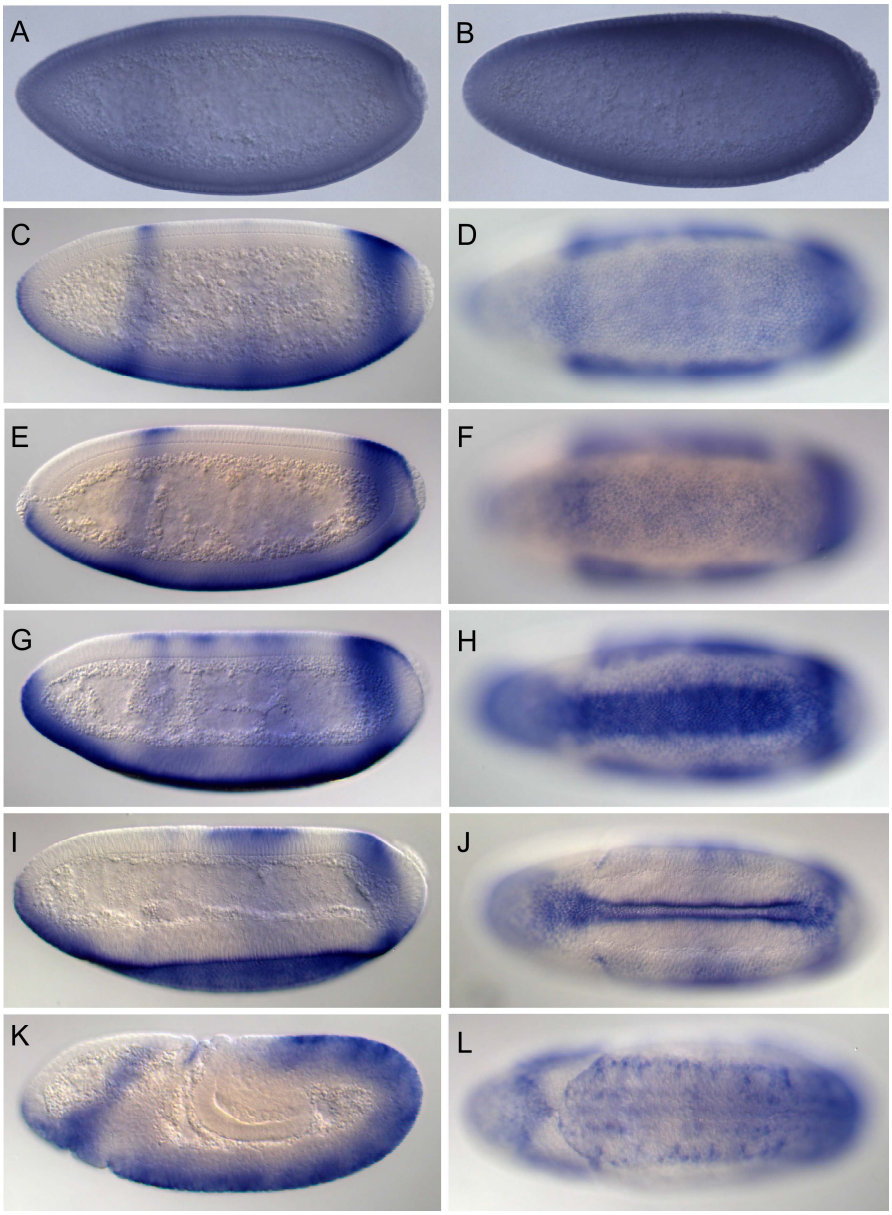

Figure 16: Anti *Traf1* mRNA *in situ* hybridization on wild type embryos. A, B, C, E, G, I and K (Lateral view) and D, F, H, J and L (Ventral view) of embryos hybridized with an anti-*Traf1* mRNA probe. The *Traf1* transcript is maternally provided to early embryos as shown in A and B. By early cellularization, the *Traf1* transcript is localized to the ventral side of the embryo in a broad domain, as also in seven stripes from the anterior to the posterior of the embryo, with the first and last stripes most prominent (C and D). The pattern persists through late cellularization (E and F) and by early gastrulation stages, prior to and during ventral furrow formation, is present only in the mid-ventral cells that invaginate to give rise to the mesoderm (G-J). The stripes of expression persist during these stages. The transcript can be detected later on in the mesoderm, as also in the ectoderm (K and L).

3.6.1 Twist but not Snail is required for the ventral *Traf1* expression

As described in the Introduction, the logic of the deficiency screen by Thomas Seher was to identify new targets of *twi*, because mutations in the known *twi* targets do not reproduce the *twist* loss of function phenotype. This suggested that there might be additional *twi* targets yet to be identified, which are involved in gastrulation. Almost all the known ventrally expressed genes are targets of Dorsal or Twist and several are repressed ventrally by Snail (reviewed by Stathopoulos and Levine, 2002A). A few ventrally expressed genes, such as *Zfh1* and *DFR1* require Snail, directly or indirectly, for their ventral expression (Casal and Leptin, 1996; Shishido *et al.,* 1993). Although the early *Traf1* mRNA expression is maternal (Figure 16A and B), the ventral domain of expression should depend on Dorsal, Twist or Snail. In order to test this, *Traf1* mRNA *in situ* hybridization was carried out on embryos mutant for *snail* and *twist* (Figures 17 and 18). The ventral domain of *Traf1* mRNA expression is intact in both early and late embryos homozygous mutant for *snail* (Figure 17), whereas in homozygous *twist* mutant embryos (Figure 18), this ventral *Traf1* mRNA expression is lost. This proves that indeed Traf1 is a downstream target of Twist. It is possible that Dorsal also has a role in *Traf1* mRNA expression, as several high affinity Dorsal binding sites upstream of the *Traf1* coding region are predicted by programmes that identify transcription factor binding sites (data not shown). This could not be tested because Twist and Snail are also Dorsal targets and therefore, mutations affecting *dorsal* would affect Twist and thereby Traf1. One possible solution to this is an artificial system wherein embryos lacking Twist but having an ectopic anteroposterior Dorsal gradient is used to check for activation of *Traf1* in a Dorsal dependent manner (Stathopoulos and Levine, 2002B).

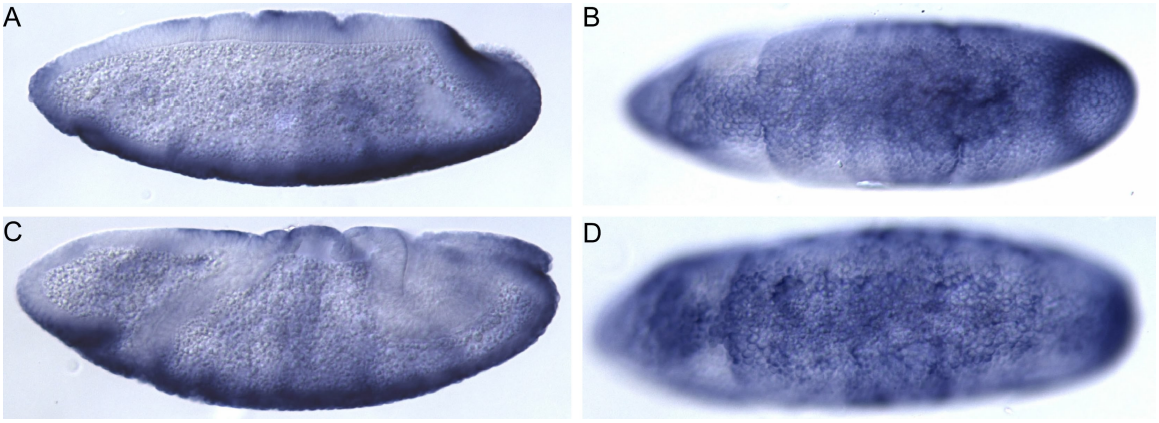

Figure 17: Embryos mutant for *snail* hybridized with an RNA probe against *Traf1*. A and C- Lateral view and B and D- Ventral view of *snail* mutant embryos, hybridized with an anti-*Traf1* RNA probe. The early (A) and late (C) mRNA expression of *Traf1* in the ventral domain is intact in the *snail* mutant embryos. The absence of ventral furrow or mesoderm invagination and the presence of the typical shallow folds indicate that the embryos are homozygous mutant for *snail*.

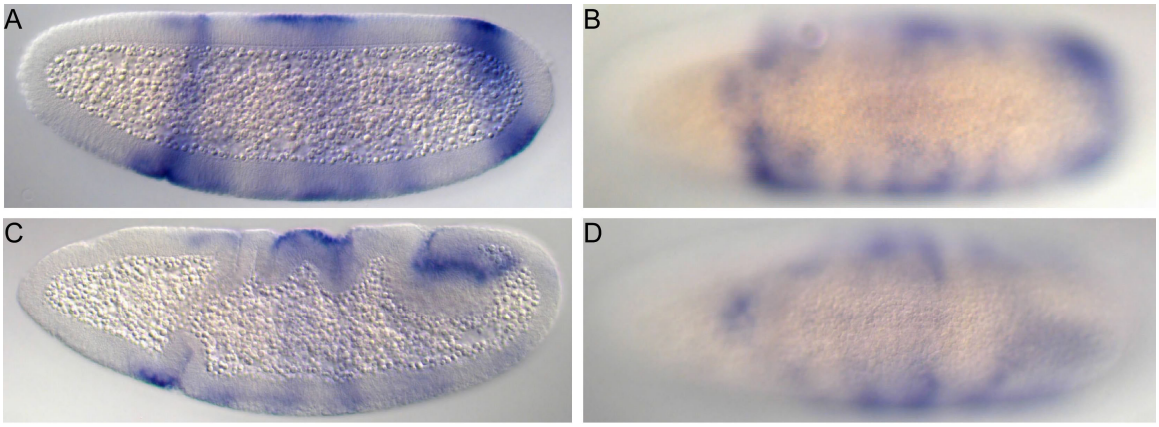

Figure 18: Embryos mutant for *twist* hybridized with an RNA probe against *Traf1*. A and C- Lateral view and B and D- Ventral view of *twist* mutant embryos, hybridized with an anti-*Traf1* RNA probe. The early (A) and late (C) mRNA expression of *Traf1* in the ventral domain is lost in the *twist* mutant embryos, although the seven stripes of expression is not affected (B and D). The absence of ventral furrow or mesoderm invagination indicates that the embryos are homozygous mutant for *twist*.

3.6.2 Organization of the *Traf1* gene and available mutants

If loss of *Traf1* is responsible for the zygotic gastrulation defects exhibited by embryos from deficiencies that uncover the genomic stretch including, proximal and distal to *Traf1*, embryos derived from a *Traf1* mutant stock should be able to reproduce these

gastrulation defects. This required the generation of *Traf1* mutant fly stocks. For this purpose, the genomic region in close proximity to *Traf1* was scanned (Flybase) for available mutant stocks, which will be discussed below. In order to familiarize with the locus, the organization of the *Traf1* gene is shown in the schematic in Figure 19. The entire genomic stretch shown in Figure 19 is about 10 Kb. The *Traf1* gene is composed of two exons, labelled 1 and 2 in Figure 19, separated by an intron of about 6.4 Kb. Two transcripts are made, Traf1-RA and Traf1-RB, which differ in their 5' region (Flybase). Traf1-RA uses the first exon and 5'UTR whereas Traf1-RB transcribes just the second exon, with a separate 5' UTR from the intron (Figure 19). Both the transcripts share the second exon and 3' UTR. The second exon codes for seven zinc finger motifs marked by the black vertical lines in Figure 19 and a characteristic TRAF domain at the C-terminus, shown in red.

An EP element, EP578 (Rorth, 1996; Tseng and Hariharan, 2002), is inserted about 50 bps upstream of the translation start site, within the 5' UTR of Traf1-RA (Kuranaga *et al.,* 2002), depicted in Figure 19. The EP578 insertion does not lead to lethality in homozygous condition. It has been shown that flies homozygous for this insertion transcribe reduced levels of the *Traf1* mRNA (Kuranaga *et al.,* 2002) showing that it is a hypomorphic allele of *Traf1*. Therefore, embryos from this stock were collected and observed for gastrulation defects. It was found that a weak delay in ventral furrow invagination occurred in several embryos from such a cross, although this phenotype was not more than 30-40% penetrant. Another important observation was that flies carrying this EP insertion on the second chromosome have a floating third chromosome balancer. Although several attempts were made to cross out this balancer from the stock, these proved unsuccessful, as the stock became sterile and extinct when the third chromosome balancer was lost. This suggests that this third chromosome balancer has suppressor mutations, which enable the stock to remain fertile. It could be due to two possibilities that the ventral furrow invagination defect exhibited by embryos from this stock is weak. First, as described above, the third chromosome balancer might have suppressor mutations that influence not only the fertility but also the gastrulation phenotype. Second,

the P element insertion is not a null mutation for *Traf1*, as some mRNA for *Traf1* can be detected by RT-PCR from this stock (Kuranaga *et al.,* 2002; Cha *et al.,* 2003). Thus, EP578 is a hypomorphic allele for Traf1, which exhibits weak gastrulation defects suggesting that indeed Traf1 might be the gene which when mutated causes the zygotic gastrulation defects.

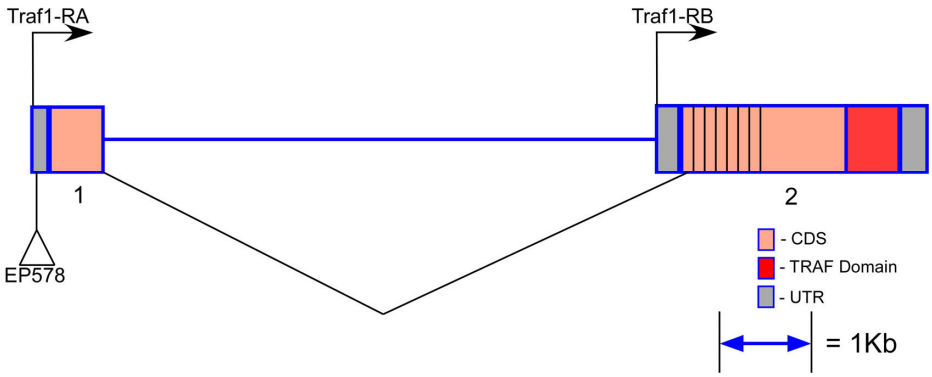

Figure 19: Schematic representation of the *Traf1* genomic region and the organization of the *Traf1* gene. The Traf1 gene spans about 10 Kb, comprising of two exons (labelled 1 and 2 in the figure) and one intron (blue line connecting the two exons). Two transcripts are made Traf1-RA and Traf1-RB represented above each of the transcription start arrows. These two transcripts differ from each other only in the 5' region, with Traf1-RA using exon 1 and Traf1-RB using the intron. A P element stock, EP578, has the P insertion about 50 bps upstream of the translation start site, within the 5' UTR of the Traf1-RA transcript, shown in the schematic. The intron is about 6.4 Kb in size. The second exon codes for seven zinc finger motifs, marked by the black vertical lines and a characteristic TRAF domain, shown in red. The UTR's are represented by the grey parts of the boxes representing the exons.

Another EP insertion, P{EPgy2}EY09771, reported to map to the same genomic locus as EP578 was identified in a screen by BDGP (Bellen *et al.,* 2004). I found that this stock had multiple P element insertions in addition to the one reported in *Traf1*. In order to clean up the stock, the EP insertion bearing chromosome was allowed to recombine. However, it turned out that the second chromosome had no P element insertion, contrary to the BDGP report (data not shown).

Attempts to generate imprecise excision alleles of the original EP insertion, EP578, to generate null alleles of *Traf1* proved unsuccessful even after screening about two thousand chromosomes. Several lines were obtained after imprecise excisions that were lethal but in all cases, the lethality mapped to a different locus than the *Traf1* genomic

region, as evident from complementation analysis. X-ray mediated mutagenesis on the EP578 stock also yielded the same result. However, a loss of function allele of *Traf1* generated by imprecise excision of the EP578 insertion was reported (Cha *et al.,* 2003). This allele was reported to have the entire first exon and part of the intron deleted (about 2.8 Kb), to have no detectable *Traf1* mRNA by RT-PCR and to be homozygous lethal (Cha *et al.,* 2003). This allele of *Traf1* was named Traf1^{ex1} (Cha *et al.,* 2003). I analysed Traf1^{ex1} homozygous embryos for possible gastrulation defects. Except for a weak delay in ventral furrow invagination also seen in the case of the EP578 stock, there were no obvious gastrulation defects (data not shown). In order to test whether indeed *Traf1* is the zygotic component responsible for the gastrulation defect, the Traf1^{ex1} males were crossed to C(2)v females and embryos analysed, as was done for deficiencies in the region. Embryos from such a cross did exhibit the severe gastrulation defects as was the case with deficiencies such as Df(2L)ed-dp (Figure 11), but in a less penetrant manner. Whereas embryos from deficiency males crossed to C(2)v females yielded approximately a quarter of the embryos with severe gastrulation defects, when Traf1^{ex1} males were crossed to C(2)v females, approximately 10% of embryos exhibited the severe gastrulation defects. This reduction in penetrance could be due to two reasons. As discussed above for the EP578 stock, it could be because of the presence of suppressor mutations in the Traf1^{ex1} stock. Another possibility is that this stock is not a null mutation, contrary to the published data (Cha *et al.,* 2003). This will be dealt with in more detail below.

Further, the *Drosophila* genome harbours two more *Traf* genes, *Traf2* and *Traf3* on the X chromosome (Grech *et al.,* 2000). Out of these two genes, a mutant allele exists for *Traf2*. Moreover, Traf2 has been reported to be essential in the Toll signalling cascade in *Drosophila* (Cha *et al.,* 2003). In order to rule out any functional redundancy between *Traf1* and *Traf2*, embryos double mutant for both of these genes were also analysed. However, no enhancement of the *Traf1* gastrulation effects could be observed, agreeing with the original report that *Traf1* and *Traf2* function independent of each other (Cha *et al.,* 2003).

3.7 The zygotic phenotype and the modified genetic background

The zygotic phenotype exhibited by embryos when deficiency males are crossed to C(2)v females (Figure 11), is more severe than the phenotype exhibited by embryos from a cross between deficiency males and females (Figure 5). This suggests that the C(2)v genetic background has a role in the enhancement of the phenotype. In the former case, the embryos that exhibit the enhanced phenotype lack one copy of the entire left arm of the second chromosome and have an extra copy of the right arm of the second chromosome (Figure 10; grey cloumn). This suggests that the loss of one copy of the second left chromosome (haploinsufficiency), or the addition of one copy of the second right chromosome (triploidy), or both of these together might be responsible for the enhancement of the phenotype. In order to understand whether any of these possibilities were correct, two strategies were adopted. The first was to look for obvious candidate genes on the left or right arm of the second chromosome, known to be involved in gastrulation and reproducing the haploinsufficient or triploid situation for such genes in the background of deficiencies for the 24-25 region and analysing for an enhancement of the gastrulation defect. In other words, look for obvious interactors of the zygotic locus, which enhance the gastrulation phenotype. The second strategy was to make use of translocation stocks so as to reproduce as similar a situation to haploinsufficiency or triploidy of the second chromosome as possible, in the background of deficiencies of the 24-25 region, in order to be able to identify whether it is haploinsufficiency of the second left arm or triploidy of the second right arm that is responsible for the enhancement of the zygotic gastrulation phenotype.

The first strategy was to look for obvious candidate genes which are on the second left arm or right arm and which might be responsible for the enhancement of the zygotic phenotype, by interacting genetically with the zygotic locus. The criteria used for identifying such candidate genes were that they should be known to be involved in gastrulation, be zygotic and be affected in this modified genetic background (become haploinsufficient or triploid). One obvious candidate was the *snail* gene, as it is on the

second left arm and is thus haploinsufficient in the modified genetic background. Moreover, loss of function *snail* mutations have a dominant gastrulation effect and *Traf1* is expressed independent of *snail* (Figure 17). In order to test whether indeed haploinsufficiency of *snail* is the cause of the enhanced phenotype, the exact genetic situation has to be mimicked as when deficiencies that remove *Traf1* are crossed to C(2)v females, but in this instance, haploinsufficiency is restricted to the *snail* gene. In order to achieve this, double mutants between Df(2L)ed-dp and *snail*, as also between $Traf1^{ex1}$ and *snail* were made by recombination and males from these stocks were crossed to Df(2L)ed-dp or $Traf1^{ex1}$ females respectively.

Figure 20 is a schematic representation of the possible chromosomal combinations of the progeny from such a cross. The combination of interest is the top right one (marked in grey), wherein both copies of the genomic region deleted in the case of Df(2L)ed-dp are missing, as is one copy of the *sna* gene. This is an identical situation as far as the *snail* gene is concerned, as is the situation when deficiency males are crossed to C(2)v females. Any strong enhancement of the zygotic gastrulation phenotype caused by haploinsufficiency of *sna* should be apparent in this situation. However, the gastrulation phenotype was much less severe than in crosses of deficiency males to C(2)v females. The experiments were also repeated with recombinants between $Traf1^{ex1}$ and *snail*, with the same result. This means that *sna*, by itself, is not the factor enhancing the zygotic gastrulation phenotype in embryos when deficiencies such as Df(2L)ed-dp males are crossed to C(2)v females. It could not be ruled out that *sna* might have a subtle effect in enhancing the zygotic effect, which might not be obvious in this situation. It could also be that *sna* is one among many factors that are affected in this situation and contributes to the eventual severe gastrulation defect in an additive manner.

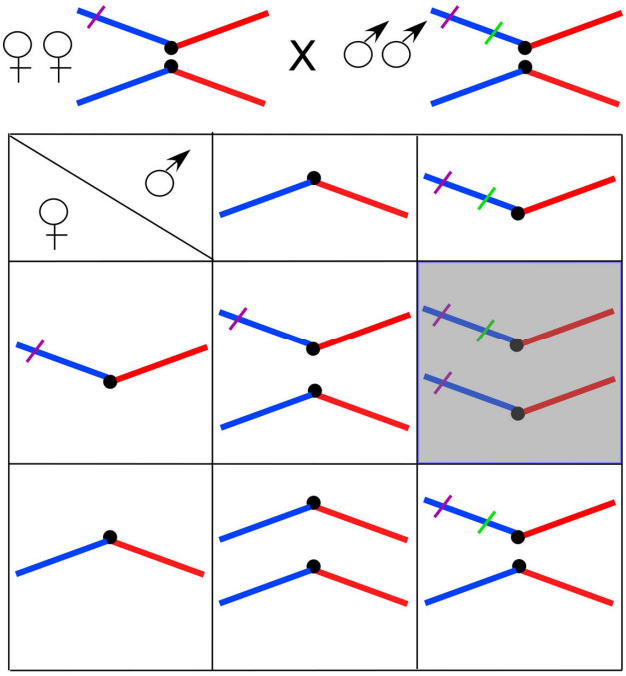

Figure 20: Schematic showing the chromosome segregation pattern in a cross between Df(2L)ed-dp, *snail* recombinant males and Df(2L)ed-dp females. Strategy to reproduce the haploinsufficient genetic situation as when Df(2L)ed-dp males are crossed to C(2)v females, but only affecting the *snail* locus. The left arm of the second chromosome is shown in blue, the right arm in red and the black dot connecting them, the centromere. The deficient region in the case of the Df(2L)ed-dp chromosome is represented by the purple transverse line (distal to the centromere) and the deficient region in the case of the *snail* mutant chromosome is represented by the green transverse line (proximal to the centromere). These two chromosomes have been recombined together so as to have the chromosome deficient for both Df(2L)ed-dp as well as *snail* and is represented here as the chromosome having the purple as well as the green transverse lines. Males from a fly stock carrying such a recombined second chromosome, when back crossed to Df(2L)ed-dp females yield progeny with the four chromosomal combinations represented in the figure. The subset of progeny marked in grey (top right box) is the one of interest, wherein the *snail* gene is present only in one copy while the genomic region uncovered by Df(2L)ed-dp is missing on both chromosomes. The same cross was repeated for recombinants between Traf1^{ex1} and *snail* as well.

Another interesting candidate was the *twi* gene, which is on the right arm of the second chromosome, which means that if it is indeed *twi* that enhances the zygotic gastrulation phenotype, it would be triploidy of *twi*, as the second right arm is triploid in the modified genetic context in which the zygotic phenotype is enhanced (Figure 10). This was also tested by making recombinants between Df(2L)ed-dp or Traf1^{ex1} and *twi* mutants. Males from such recombinant stocks were crossed to C(2)v females. If it is indeed triploidy of the *twi* gene that is the cause of the enhanced zygotic gastrulation phenotype, it should be

suppressed now, as the *twi* gene is present only in two functional copies as opposed to three in the original cross. However, there was no obvious suppression of the gastrulation defect in this case, indicating that triploidy of *twi* was also not directly responsible for the enhancement of the zygotic gastrulation phenotype.

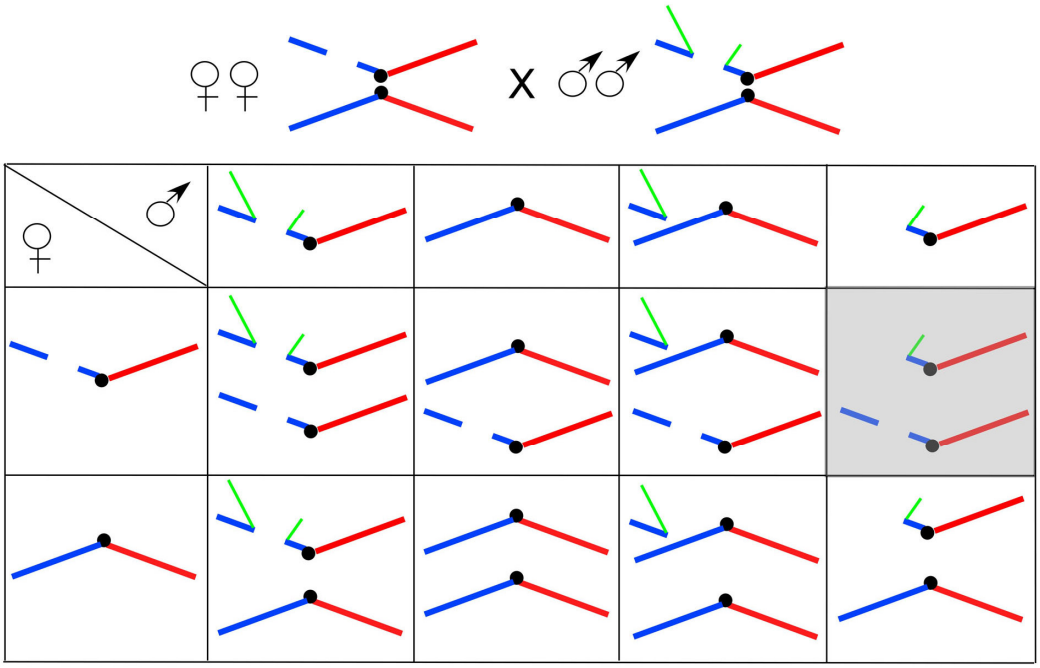

Figure 21: Schematic showing the chromosome segregation pattern in a cross between second chromosome translocation stock males and Df(2L)ed-dp females. The translocation stock chromosome segregation pattern has been discussed in the Introduction. The blue lines represent the left arm of the second chromosome and the red lines, the right arm, with the black dots, the centromere. In the case of deficiency stocks, the left arm has a break, indicating the chromosomal deletion. In the case of the translocation, the two green lines separating the break indicate the translocation. One eighth of embryos from such a cross lack the translocated part of the second left chromosome including the region uncovered by the deficiency and the homologous chromosome is the deficiency chromosome (top right column marked in grey). Any enhancement of the zygotic phenotype by haploinsufficiency of loci uncovered by the translocation should be obvious in one eighth of the progeny from such a cross.

As neither *snail* nor *twist* were directly responsible for the enhancement of the zygotic gastrulation phenotype, a second strategy was adopted to test whether haploinsufficiency of the second left arm or triploidy of the second right arm was responsible for the enhancement of the zygotic gastrulation phenotype. In order to test the effect of haploinsufficiency, fly stocks that carry translocations of varying lengths of the second left arm on to the X chromosome were utilized. Males from such translocation stocks

were crossed to deficiencies such as Df(2L)ed-dp and embryos from such a cross analysed for gastrulation defects. Details of all the translocation stocks used are given in the Materials and Methods section. One example of how chromosomal segregation occurs in such a cross is shown in the schematic Figure 21. One eighth of the progeny is haploinsufficient for the loci uncovered by the translocation and lack the region deleted in the deficiency stock (panel marked in grey in Figure 21). Several overlapping translocations reaching the proximal part of the chromosome, close to the centromere and thus covering nearly all of the chromosome arm were used in this manner and it was found that none of them could reproduce the enhanced zygotic gastrulation phenotype as was the case when deficiency stock males were crossed to C(2)v females. The stretch that was uncovered in this manner was till about the cytoband 39 (Flybase). The 39-40 region could not be ruled out as no translocations could be obtained for this stretch. The maternal effect gene *concertina* (*cta*), known to be essential for gastrulation is in this stretch and although *cta* is thought to have no zygotic effect, such a possibility could not be ruled out by the use of the available translocations.

For triploidy of the right arm, stocks carrying translocations of varying lengths of the right arm of the second chromosome were used. Details of the stocks used for this purpose are given in the Materials and Methods section. In this instance, the flies carrying the translocation were crossed to flies carrying the deficiency and male flies carrying both the translocation and the deficiency were collected and back crossed to females from the deficiency stock. This would yield one sixteenth of the progeny bearing the translocation (triploid for the translocated stretch) as well as homozygous mutant for the region uncovered by the deficiency. There was no apparent enhancement of the zygotic gastrulation defect by any of the translocations tested. The cytogenetic region from about cytoband 43 till the distal tip of the right arm could be ruled out in this manner. The proximal part of the second right arm could not be accessed by any available translocations (cytoband41-43) and this stretch could not be ruled out to be harbouring the locus responsible for the enhancement of the zygotic gastrulation defect. Also, very few stocks could be used in this instance that were fertile in combination with the

deficiency chromosome (males carrying a combination of translocation and deficiency), in order to be back crossed to the deficiency stock females. Thus, triploidy of most part of the right arm of the second chromosome as a possible cause for the enhancement of the zygotic gastrulation phenotype could be ruled out.

The results from these experiments indicate that barring the heterochromatic regions of the left and right arms proximal to the centromere (about cytoband 39-43) of the second chromosome, neither haploinsufficiency of the left arm nor triploidy of the right arm of the second chromosome are responsible for the enhancement of the zygotic gastrulation phenotype, seen in embryos when males from deficiencies in the 24-25 region are crossed to C(2)v females. This raises several possibilities which might play a role in the enhancement of the phenotype. First, it might be that both of these events (haploinsufficiency of the left arm of the second chromosome and triploidy of the right arm of the second chromosome) together is required for the enhancement. Reproducing such a genetic situation other than with the C(2)v stock is very difficult with the existing genetic tools. Second, the regions not accessed by the translocation stocks might harbour the locus responsible for the enhancement. This can be only tested by recombining existing mutations for all such loci on to the Df(2L)ed-dp or analogous deficiency chromosomes and verifying whether the enhancement of the zygotic phenotype occurs. Recombining several such loci is quite cumbersome as also impossible in several cases (tandem duplications are known to be very difficult to recombine; (personal communication from Gubb, D)). Third, the C(2)v stock used might have second site mutations, which enhance the gastrulation defect observed. In other words, it might be that the enhancement of the gastrulation phenotype observed might not be a zygotic effect but a maternal effect that is observed as a result of background mutations in the C(2)v stock. Such loci are already known, which can enhance the effect of a mutation at a different locus. One precedent for this is the *wimp* mutation, which is a change of function mutation in the second largest subunit of RNA polymerase (Parkhurst and Ish-Horowicz, 1991 and Rosenberg and Parkhurst, 2002). This possibility is described further below. Fourth, the C(2)v stock might have mutations in the very same locus as the one

under investigation, which is responsible for the gastrulation defects in the 24-25 cytogenetic interval. These mutations might not cause an obvious phenotype in embryos of the C(2)v stock itself as the mutations might be hypomorphic or might function so as to reduce the maternal contribution of the concerned gene. However, when females from this stock (which have a reduced dose of the postulated gene product responsible for the phenotype) are crossed to deficiencies in the region which are deleted for the same gene, the severity of the phenotype is enhanced; i.e., fully paternally rescued by the hypomorphic copy but not by the deficiency.

The third possibility described above could be tested in a simple manner. If mutations in the C(2)v stock which result in reducing the maternal dose of a gene product is responsible for the enhanced gastrulation defects observed in embryos from a cross between deficiency males and C(2)v females, one should be able to verify this by performing the cross in the opposite manner. In other words, if deficiency females are crossed to C(2)v males, any maternal effect arising from the C(2)v stock would be abolished, although the maternal effect from the deficiency will influence the result. Further, the C(2)v stock males are known to produce four types of gametes as opposed to two types by C(2)v females (details in Introduction), which would mean that much larger numbers of embryos will have to be scored for a conclusive result. Nevertheless, such a cross between C(2)v males and deficiency females was performed and preliminary results indicate that the enhancement of the zygotic phenotype is less prominent as compared to the original cross. This has to be further verified by testing larger numbers of embryos. If proven, this would suggest the presence of mutations in the C(2)v stock, which are responsible for the enhancement of the observed phenotype. Moreover, the enhancement observed would be a maternal effect rather than a zygotic effect, as originally understood.

3.8 Characterization of the Traf1^{ex1} mutant

The embryos derived from the Traf1^{ex1} P element excision stock (Cha *et al.,* 2003) males, when crossed to C(2)v females did reproduce the gastrulation defects exhibited by embryos when deficiencies in the region such as Df(2L)ed-dp males were crossed to

C(2)v females. However, the penetrance of the phenotype in the former cross was about one in ten embryos, whereas in the latter it was about one in four. Although this indicated that *Traf1* might be the gene responsible for the zygotic gastrulation phenotype, the lesser penetrance of the phenotype in the case of Traf1^{ex1} stock suggested that this stock might not be a null mutant or this stock has second site suppressor mutations that act to reduce the severity of the observed gastrulation defects. Another possibility is that there are additional genes uncovered in Df(2L)ed-dp that contribute to the eventual gastrulation defects in an additive manner.

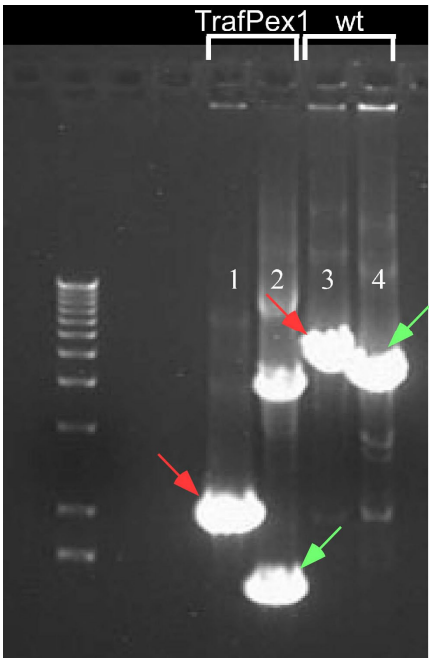

Figure 22: Agarose gel stained with ethidium bromide, showing PCR products generated from genomic DNA derived from the Traf1^{ex1} stock and wild type flies, using two pairs of primers flanking the genomic region predicted to be uncovered in Traf1^{ex1}. Lanes 1 and 2 show the PCR products derived using Traf1^{ex1} genomic DNA and lanes 3 and 4, using wild type genomic DNA. Lanes 1 and 3 (red arrows) have PCR products amplified using the same pair of primers (Forward-LEP1F; Reverse-Traf5RR) and lanes 2 and 4 (green arrows) have PCR products amplified using the same primer pairs (Forward-LEP2F; Reverse-Traf5RR). Comparing the size of the PCR products in lanes 1 and 3, there is a size difference of 2.8 Kb, as is also the case when the PCR product in lane 2 is compared to that in lane 4.

In order to test these possibilities, complementation experiments were performed, wherein males from the Traf1^{ex1} stock were crossed to females from several of the

deficiencies in the 24-25 region, such as Df(2L)ed-dp, Df(2L)dp-h28, Df(2L)dp-h25, Df(2L)M24F-B, Df(2L)dp-h19, Df(2L)dp-h24 etc. As Traf1^{ex1} was reported to be a lethal mutation in the *Traf1* gene (Cha *et al.,* 2003) and because several of the aforementioned deficiencies uncover the *Traf1* gene, Traf1^{ex1} should not be able to complement such deficiencies. Surprisingly, it was found that in such complementation experiments, the Traf1^{ex1} stock is able to complement all of the deficiencies in the 24-25 cytogenetic region. This proved that the lethality exhibited by the Traf1^{ex1} stock did not map to the *Traf1* gene but elsewhere on the second chromosome. In other words, the Traf1^{ex1} stock was carrying one or more lethal mutations that did not map to the 24-25 cytogenetic region. This unexpected finding required that the Traf1^{ex1} stock be retested as to whether it carries a partial deletion of the *Traf1* gene, as originally reported (Cha *et al.,* 2003). For this purpose, primers were designed flanking the region supposed to be uncovered in the Traf1^{ex1} allele so as to amplify the genomic region across the deleted stretch by PCR. Compared to wild type genomic DNA, when such a PCR is performed on genomic DNA derived from the Traf1^{ex1} stock, it was found that the PCR product was about 2.8 Kb less in size, confirming that indeed the Traf1^{ex1} stock has a deletion in the *Traf1* gene (Figure 22).

A schematic representing the genomic stretch deleted in the Traf1^{ex1} stock is shown in Figure 23. The rectangular boxes represent the exons and the blue line connecting them, the intron. The neighbouring genomic region is represented by the black lines. The EP insertion and the transcripts are also marked in Figure 23A. The dotted line in Figure 23B represents the genomic region uncovered in Traf1^{ex1}, as compared to the EP578 stock in Figure 23A. It can be seen that the entire first exon and part of the intron is removed in the case of the Traf1^{ex1} mutation. The genomic region harbouring the second exon is unaffected by the excision.

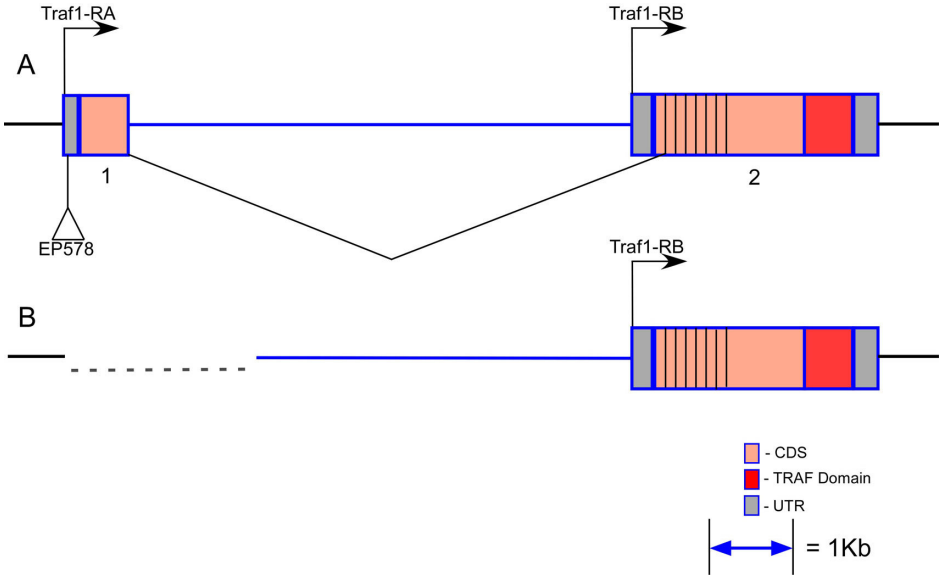

Figure 23: Schematic comparing the *Traf1* genomic stretch in the EP578 and the Traf1^{ex1} stocks. The *Traf1* genomic region in the EP578 stock (A), as compared to the imprecise excision allele derived from EP578, Traf1^{ex1} (B). The coloured rectangular boxes are the two exons of the *Traf1* gene, the blue line the intron and the black lines the bordering genomic stretch. The genomic region uncovered in Traf1^{ex1} is marked by the grey dotted line in B. The deletion is 2.8 Kb in size, uncovering the promoter region upstream of the first exon, the first exon and part of the intron. The genomic region harbouring the second exon is not affected.

The next step was to recombine away the lethal mutation from the Traf1^{ex1} stock. This was done by bringing the Traf1^{ex1} mutation over a wild type chromosome and allowing it to freely recombine. Recombinant chromosome bearing flies were selected such that they were uncovered for the *Traf1* locus as in the Traf1^{ex1} stock (by PCR) but did not carry the lethal mutation that mapped elsewhere than the *Traf1* locus. Several such stocks were made and it was found that in each case, the Traf1^{ex1} mutation bearing flies were homozygous viable. However, such homozygous Traf1^{ex1} males were sterile even when crossed to wild type females which necessitated the presence of a balancer chromosome in the stock. Homozygous females from these stocks were viable and fertile. Embryos derived from heterozygous males from such cleaned up stocks crossed to C(2)v females reproduced the enhanced zygotic phenotype, albeit with the same low penetrance as Traf1^{ex1}(about 10% penetrance as opposed to about 25% observed in the case of

deficiencies), suggesing that the excision of *Traf1* was indeed responsible for the enhanced phenotype.

One of the most likely reasons that might have caused the reduction in penetrance of the observed phenotype is that the Traf1^{ex1} excision is not a null mutation of the *Traf1* gene. Whereas larger deficiencies in the region uncover the entire genomic stretch harbouring the *Traf1* gene, Traf1^{ex1} uncovers the promoter region upstream of the first exon, the first exon and part of the intron (Figure 23). However, the possibility of a second promoter within the intron and transcribing the second exon alone could not be ruled out. Because the Traf1^{ex1} excision does not affect the larger part of the coding sequence encoded by the second exon or the immediate upstream region, it might be that a second promoter function is not affected. In order to test this possibility, the entire genomic region harbouring the *Traf1* gene and about 500 bps upstream and downstream were analysed using the genomatix gene2promoter software, which predicts promoter regions. It was indeed found that a possible second promoter exists close to the second exon (data not shown). Further evidence pointing in this direction was the reported presence of an EST sequence, encoding just the second exon and a separate 5' UTR mapping to the intronic sequence (personal communication, Medzhitov, R).

In order to test whether the second promoter was still active, RT-PCR was performed on cDNA derived from a stock carrying the Traf1^{ex1} chromosome over the Df(2L)ed-dp chromosome, referred to below as the mutant stock. Because Df(2L)ed-dp is a deletion of the entire *Traf1* genomic region, no *Traf1* product should be contributed by this chromosome and therefore any *Traf1* product, if detected in the mutant stock should be exclusively from the Traf1^{ex1} chromosome. The primers used in this experiment were from the second exon (details in Materials and Methods). Indeed a PCR product was detectable in flies of the mutant stock (Figure 24 Lane2) proving that Traf1^{ex1} is not a null mutant for *Traf1*. Compared to wild type (Figure 24 Lane4), the PCR product derived from the mutant stock was slightly weaker (Figure 24 Lane2), which might be because one chromosome is a complete deletion for the *Traf1* locus in the mutant combination, as opposed to wild type. This might also be because the second promoter is weaker.

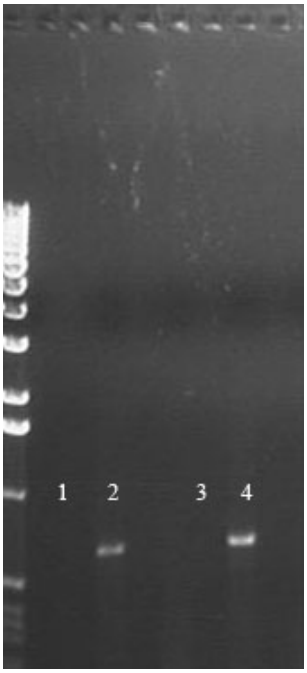

Figure 24: RT-PCR showing that Traf1^{ex1} is not a null mutant for *Traf1*. Lanes 1 and 2 are RT-PCR products derived from flies carrying the Traf1^{ex1} chromosome over Df(2L)ed-dp chromosome, whereas lanes 3 and 4 are products derived from wild type flies. The primers used in all cases were from the second exon (Forward-Traf804XhoIF, Reverse-TrafBamH1mutR). Lanes 1 and 3 are the no RT controls where as expected, no products are detectable. Lanes 2 and 4 are the actual samples and compared to the wild type product (lane 4), a slightly weaker product can be detected in the case of the mutant chromosome combination (lane 2). This shows that Traf1^{ex1} is not a null mutant for *Traf1*.

Furthermore, when embryos derived from a cross between heterozygous Traf1^{ex1} males and homozygous Traf1^{ex1} females were hybridized with an anti-*Traf1* mRNA probe synthesized from the second exon, clear *Traf1* expression was observed in all the embryos (data not shown). If indeed Traf1^{ex1} was a null allele for the *Traf1* gene, half of the embryos from such a cross should lack the *Traf1* transcript and therefore not give a *Traf1* specific mRNA expression pattern. As all the embryos gave a *Traf1* specific mRNA expression, this was further confirmation that Traf1^{ex1} is not a null allele for the *Traf1* gene.

3.9 Summary

The genomic stretch harbouring the zygotic locus responsible for the gastrulation phenotype was analysed in detail and one potential candidate gene was identified. This gene was *Traf1* and the mRNA expression pattern of *Traf1* was the suggestive feature which made *Traf1* a likely candidate gene responsible for the zygotic gastrulation defects. The ventral domain of *Traf1* mRNA expression was Twist dependent but not Snail dependent. The *Traf1* gene is encoded by two exons, separated by an intron. Two transcripts of *Traf1* are transcribed, differing with respect to the 5' end; Traf1-RA utilizes the first exon whereas Traf1-RB does not and has a distinct 5' end transcribed from the intron, although both transcripts share the second exon.

A P element insertion within the 5' UTR of the *Traf1* gene, EP578, was an available allele of *Traf1* and was reported to be a hypomorphic allele. A lethal, null allele of *Traf1*, $Traf1^{ex1}$ was reported by Cha *et al.,* 2003, which was a deletion of the promoter region, first exon and part of the intron of *Traf1*. Embryos derived from a cross between $Traf1^{ex1}$ males and C(2)v females reproduced the zygotic gastrulation phenotype as described in the case of larger deficiencies, suggesting that *Traf1* is the zygotic gene responsible for the gastrulation defects observed. However, the penetrance of the phenotype decreased significantly in the case of $Traf1^{ex1}$ compared to deficiencies. This led to further investigations, which revealed that $Traf1^{ex1}$ is not a null allele of *Traf1* and that the lethality exhibited by this stock does not map to the *Traf1* locus.

The reasons behind the enhancement of the zygotic gastrulation phenotype, when deficiencies in the 24-25 cytogenetic region or $Traf1^{ex1}$ were crossed to C(2)v females, as opposed to crosses within the deficiency were also investigated. One hypothesis was that haploinsufficiency of the left arm of the second chromosome or triploidy of the right arm of the second chromosome, in a deficiency homozygous background resulted in the enhanced zygotic phenotype. This was tested using translocation stocks and it was found that neither the left arm nor the right arm, barring the region proximal to the centromere (cytoband 39-43) which could not be tested, are responsible for the enhancement. This effectively ruled out genes such as *twist* (right arm) and *snail* (left arm) which are genes

essential for gastrulation as possible interacting loci. Moreover, this led to the idea that either the interacting locus could not be accessed and is in the heterochromatic region close to the centromere, or a combination of haploinsufficiency of the left arm and triploidy of the right arm simultaneously is required for the enhancement of the zygotic gastrulation phenotype. Neither of these possibilities could be tested with the available genetic tools. Another possibility is that the C(2)v stock has background mutations which causes the enhancement of the zygotic gastrulation defect. Preliminary results supported the latter explanation.

3.10 Overexpression of Traf1 in the mesoderm and associated effects

Because *Traf1* is a potential candidate responsible for the zygotic gastrulation defects described before, overexpression experiments of Traf1 using the UAS-GAL4 system were also carried out to study possible effects on gastrulation as well as other processes which will be discussed below. The P element insertion upstream of the *Traf1* locus, EP578, is a modified P element, carrying UAS repeats which allows modular misexpression studies using tissue specific GAL4 driver lines (Rorth, 1996). In addition to the EP578 insertion, an UAS-DTraf1 construct carrying stock was also reported (Kuranaga *et al.,* 2002) and used in the overexpression experiments.

In order to investigate whether overexpression of Traf1 early in the mesoderm causes defects in ventral furrow invagination, males from the EP578 stock were crossed to females from the twist-Gal4 (Greig and Akam, 1993) stock and the embryos analysed. However, no apparent defects were observed (data not shown). When the same experiment was repeated with the stock carrying the UAS-DTraf1 construct, ventral furrow formation was abolished in about 60-70% of the embryos (Figure 25). These experiments were further validated using another driver line, maternal GAL4 (unpublished data, St. Johnston, D) with similar results. Such differences have been observed between EP insertion stocks and UAS stocks, upon overexpression (personal communication, Seher, T). This is possibly because the EP insertion is not as efficient in

transcribing the downstream gene as the UAS construct, depending on the location of the respective insertions in the genome.

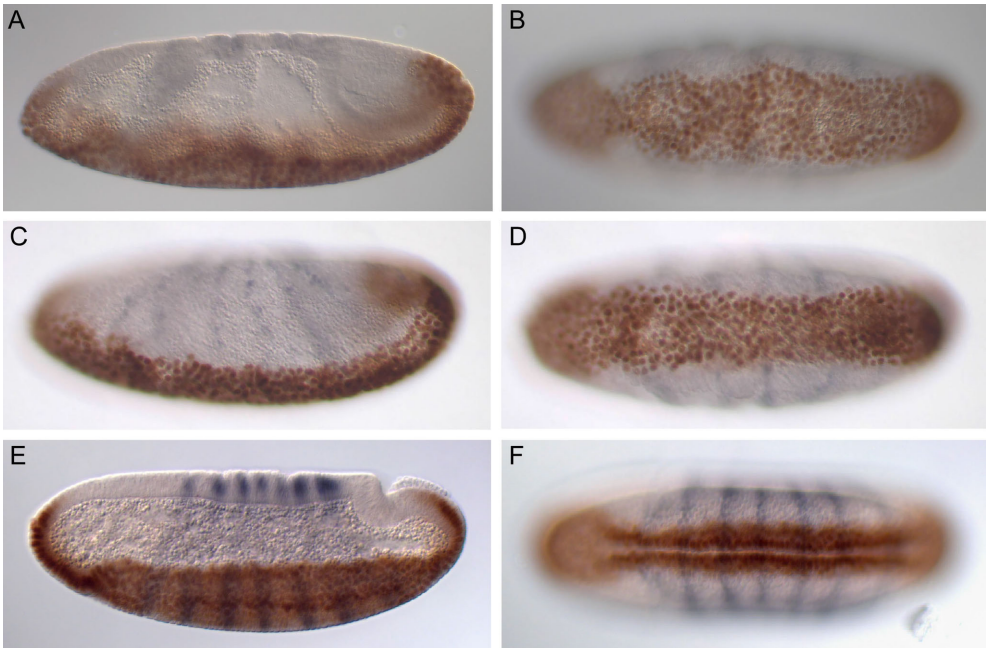

Figure 25: Embryos from a cross between twistGal4 females and UAS-DTraf1 males and wild type embryos, stained with anti-Twist and anti-Eve antibodies. Lateral view (A, C and E) and ventral view (B, D and F) of two representative embryos from a cross between twistGal4 females and UAS-DTraf1 males (A, B and C, D) as compared to wild type embryos (E, F) stained with anti-Twist and anti-Eve antibodies. The wild type embryos are younger compared to the two Traf1 overexpressing embryos. However, compared to the wild type where the ventral furrow has formed (F), no furrow is formed in the Traf1 overexpressing embryos (B and D).

The likely reasons responsible for the ventral furrow defect when Traf1 is overexpressed in the mesoderm are defects in cell shape changes, cell division or cell fate. In order to test whether mesodermal cell fate is affected upon Traf1 overexpression in the mesoderm, the expression of genes required to maintain mesodermal cell fate were tested in such embryos. One such gene is *twist* and as already shown, the Twist expression pattern is normal in the Traf1 overexpression situation (Figure 25). Expression of *snail*, another key regulator of mesodermal identity was also found to be normal (Figure 26A and B). A third gene tested was *singleminded* (*sim*), which is expressed in a single row of cells flanking the mesodermal germ layer on either side, called the mesectoderm (Nambu *et*

al., 1990). In mutants such as *snail* where the mesodermal identity is lost, the expression of *sim* broadens into the mesoderm due to the lack of repression of *sim* expression by *snail* (Kasai *et al.,* 1992). Again, it was found that *sim* expression was not abnormal compared to wild type, in the case of the Traf1 overexpressing embryos (Figure 26; C, D, E and F). These results suggest that cell fate changes are not the underlying cause behind the ventral furrow defects observed when Traf1 is overexpressed in the mesoderm. Aberrations in cell division as a possible cause of the gastrulation defects could also be ruled out by careful observation of the Traf1 overexpressing embryos, which underwent normal cell division as compared to mutants for genes such as *tribbles* or *fruhstart* known to be required to regulate cell division during gastrulation (Grosshans and Wieschaus, 2000; Mata *et al.,* 2000; Seher and Leptin, 2000).

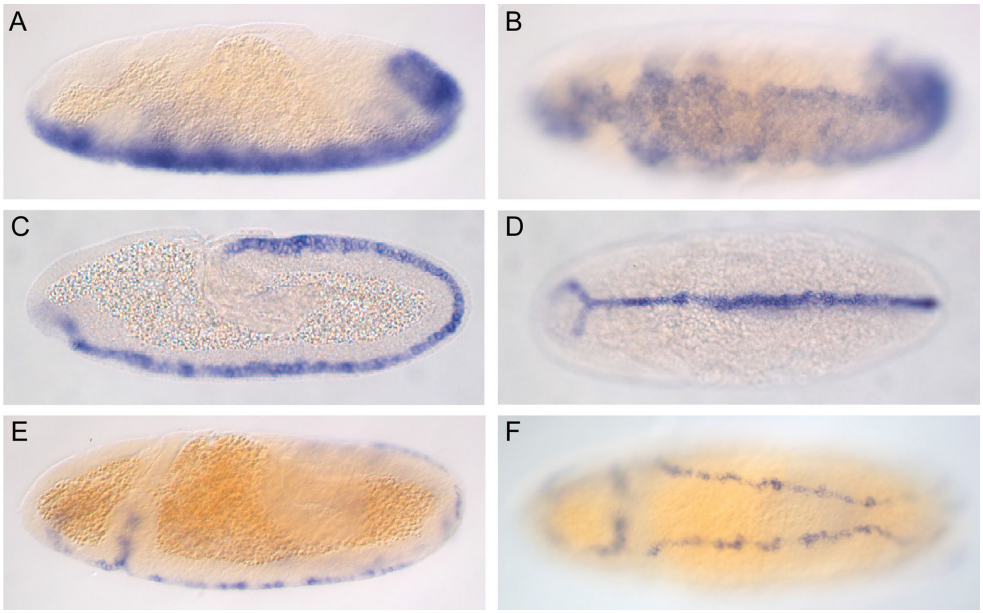

Figure 26: Mesodermal cell fate changes are not apparent in embryos overexpressing Traf1. Embryos overexpressing Traf1 under the control of the twistGal4 (A, B, E and F) and wild type embryos (C and D), hybridized with anti-*snail* (A and B) or anti-*sim* (C, D, E and F) RNA probes respectively. A, C, E are lateral view and B, D, F ventral view of embryos. The *snail* mRNA expression pattern is not affected significantly in the Traf1 overexpressing embryos (A and B). *sim* mRNA is expressed in the mesectoderm bordering the mesoderm and the two stripes of cells expressing *sim* come together once the ventral furrow has invaginated in wild type embryos (C and D). Derepression of *sim* is not observed in Traf1 overexpressing embryos, although the two stripes of *sim* expression fail to come together due to the failure in ventral furrow invagination (E and F).

In order to confirm that indeed overexpression of Traf1 early in the mesoderm is responsible for the observed ventral furrow invagination defects, transgenic fly stocks expressing Traf1 under the control of the *twist* proximal element (2xPE) were generated (Jiang and Levine, 1993). In such stocks, the *Traf1* gene is constitutively expressed in the Twist domain. Further, the activation is spatially and temporally regulated in the same way as *twist*, where activation happens at peak levels of Dorsal due to the low Dorsal binding affinity of the PE sequence (Jiang and Levine, 1993). When embryos from several such PE-Traf1 stocks were examined, it was found that they exhibit gastrulation defects, at an estimated penetrance level of about 40-50%. An example of the observed defects from one representative stock is shown in Figure 27, where the early defects observed are delayed ventral furrow invagination (Figure 27A, B) and later on, no ventral furrow forms (Figure 27E, F) or the ventral furrow is discontinuous (Figure 27C, D). If overexpression of Traf1 in the early mesoderm is detrimental to embryos, it would be conceivable that generating such PE-Traf1 stocks would result in selection against insertions that are in transcriptionally highly active regions of the genome. This might be the reason behind the reduced penetrance of the observed phenotype. Further, several such PE-Traf1 stocks had variegated expression of the marker gene used to select for the presence of the transgene, suggesting that the transgene was unstable.

In summary, overexpression of Traf1 in the mesoderm leads to gastrulation defects. These defects are not caused by cell fate changes or defects in cell division. This indicates that the observed defects are a result of the effect of Traf1 on some other process or event such as cytoskeletal rearrangement, adhesion or another signalling mechanism than the ones ruled out. Further studies, especially using cell biological markers would help in addressing this question.

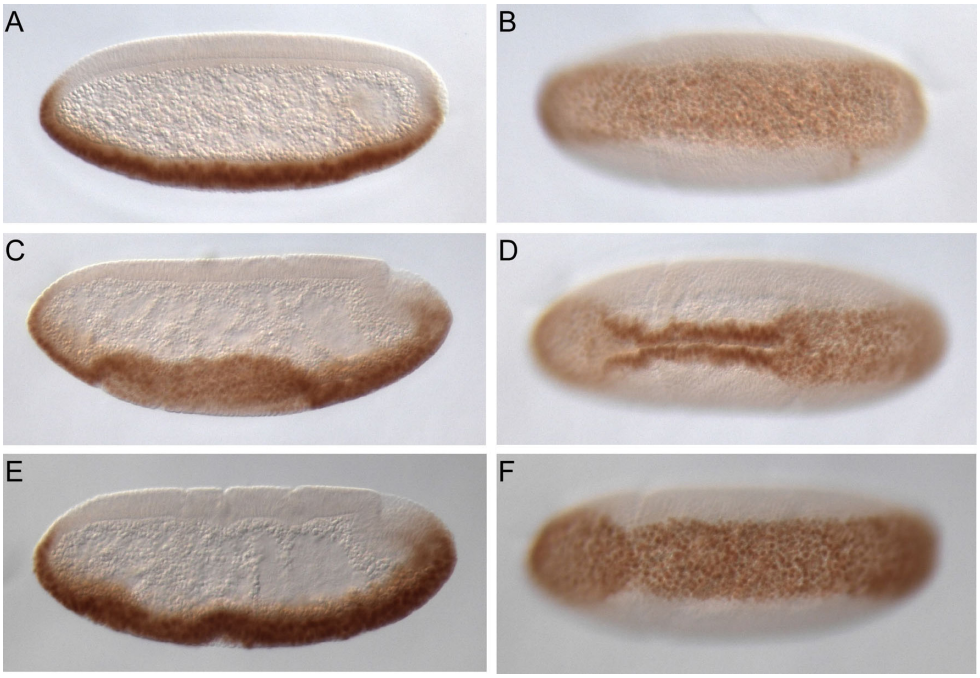

Figure 27: Embryos that are expressing a constitutively active *Traf1* construct (PE-Traf1) in the mesoderm. Lateral view (A, C and E) and ventral view (B, D and F) of representative embryos from flies carrying the PE-Traf1 construct stained with an anti-Twist antibody. At early stages, a delay in invagination is obvious (A, B). At later stages, absence of the ventral furrow (E, F) or mal-formed and discontinuous furrow is observed (C, D). The penetrance of these defects were estimated to be about 40-50%.

3.11 Overexpression of the *Drosophila* JNK pathway causes defects in gastrulation

Several independent studies have previously demonstrated that Traf1 functions in the JNK signalling cascade (Cha *et al.,* 2003; Kuranaga *et al.,* 2002; Liu *et al.,* 1999). The JNK signalling cascade has been shown to be essential for several morphogenetic processes in *Drosophila* such as dorsal closure, thorax closure, wound healing (reviewed by Kockel *et al*., 2001; Martin and Parkhurst, 2004; Xia and Karin, 2004), as well as in other organisms (reviewed by Davis, 2000; Martin and Parkhurst, 2004). This raised the possibility that the phenotype observed when Traf1 is overexpressed in the mesoderm might be due to its effect on the JNK pathway. In order to test this, fly stocks carrying overexpression (UAS) constructs of several members of the JNK pathway were

overexpressed in the early embryonic mesoderm and the embryos analysed (Table 6). The JNK pathway members analysed include Misshapen (Msn), Hemipterous (Hep), Basket (Bsk) and Puckered (Puc), in addition to the TNF ligand and receptor, Eiger (Egr) and Wengen (Wgn) as shown in Table 6. Gene products of all of the JNK pathway members mentioned here are either contributed maternally (Msn, Hep, Bsk, Puc) or actively transcribed in the early embryo (Egr, Wgn). It was found that with the exception of *puckered*, a phosphatase which negatively regulates the JNK pathway (Martin-Blanco *et al.,* 1998) and *wengen* (Kanda *et al*., 2002; Kauppila *et al*., 2003), all the other members of the JNK pathway tested yield embryos which have defects in gastrulation. One representative example of the defects observed upon such overexpression, in this instance with the UAS-*hemipterous* construct, is shown in Figure 28. The results from these experiments are tabulated in Table 6. Details of the stocks used in these overexpression experiments are given in the Materials and Methods section.

Genes Tested	Function in the pathway	Phenotype
Eiger	TNF Ligand	+
Wengen	TNF Receptor	-
Traf1	Adaptor molecule	+
Misshapen	MAPKKK	+
Hemipterous	MAPKK	+
Basket	MAPK	+
Puckered	Phosphatase	-

Table 6: Results from the overexpression of JNK pathway members in the early embryonic mesoderm. The first column shows the genes in the JNK pathway that were tested, the second the predicted or known function of the respective gene in the JNK pathway and the final column, whether defects in gastrulation were observed upon overexpression or not. '+' indicates that defects were observed with at least 40-50% penetrance and '-', that they were not.

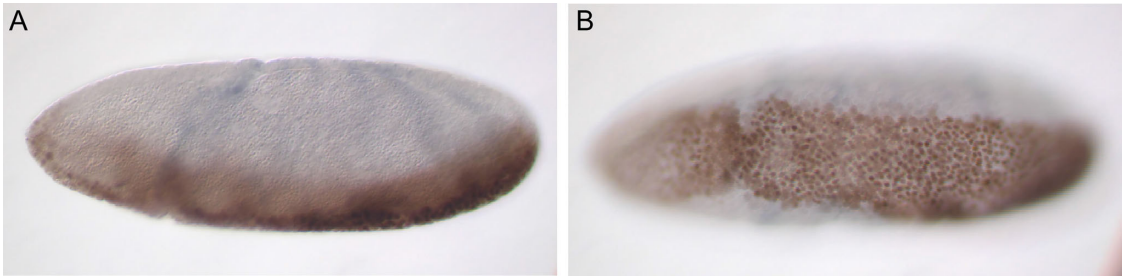

Figure 28: Overexpression of Hemipterous, the JNK Kinase in the mesoderm causes gastrulation defects. Lateral view (A) and ventral view (B) of an embryo stained with anti-Twist and anti-Eve antibodies in which Hemipterous was overexpressed using the twist-Gal4 driver. Ventral furrow formation is abolished with a penetrance of about 40-50%. Similar phenotypes are observed when various components of the JNK signaling cascade are overexpressed in the mesoderm, details of which are given in Table 6.

One likely reason why Puckered (Puc) overexpression does not cause gastrulation defects is because it is a negative regulator of the pathway (Martin-Blanco *et al.,* 1998). This might mean that activation of the JNK pathway is not required for the observed gastrulation phenotype. However, it has been shown that Puc is required to regulate the JNK pathway at least in dorsal closure and too little or too much activity leads to defects in dorsal closure. Thus, it could also be that the particular *puc* insertion used in this instance is not activated enough so as to cause a significant reduction in the activity of the JNK pathway. This can be verified by repeating the experiment with other UAS-*puc* insertions. In the case of *wengen* (*wgn*) which encodes the TNF receptor, the UAS construct used was not an activated one. It might be that ligand mediated activation of the receptor is a pre-requisite for downstream cascade activation. In accordance with this explanation, it was found that overexpression of the UAS-*wgn* construct in the eye or the wing had no effect, in contrast to observations with other members of the JNK pathway, including the TNF ligand (data not shown).

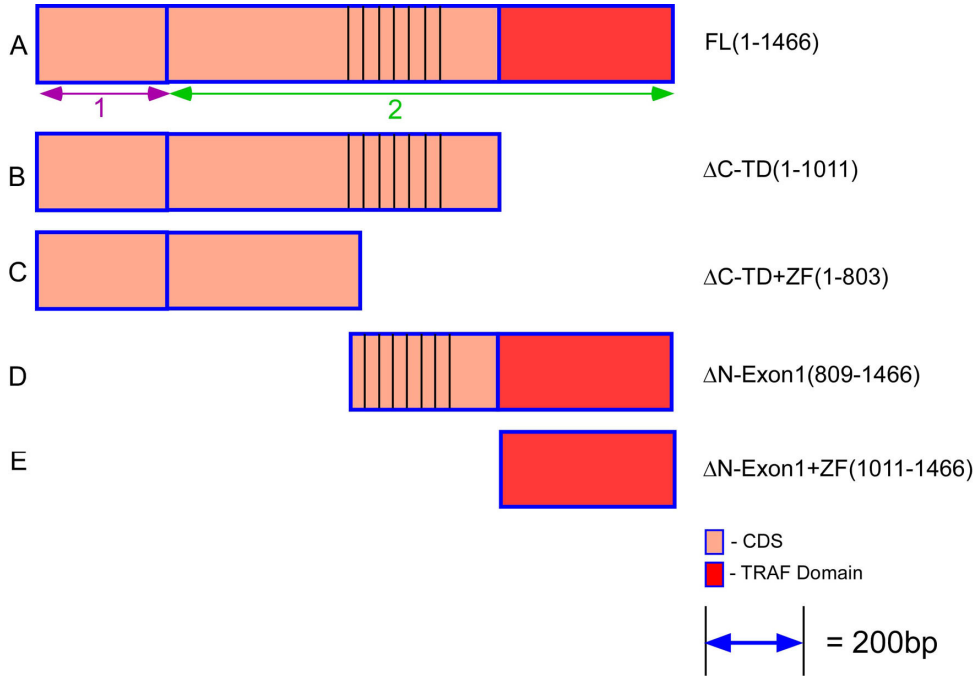

Figure 29: Schematic representing the different UAS-Traf1 constructs made and tested in flies. Each of the constructs shown here except A, are C or N terminal truncations of the Traf1 coding sequence. This is mentioned for each construct on the right hand side, whether it is a C or N terminal truncation, what domains are deleted and the base pairs that are not deleted. A is the full length construct made up of exons 1 and 2 and is 1466 bps in size, coding for seven zinc finger domains (ZF) and the Traf domain (TD). B and C are C terminal truncations, with B lacking the Traf domain (bp1011-1466) and C lacking both the Traf domain and the zinc fingers (bp803-1466). D and E are N terminal truncations with D lacking the entire first exon and part of the second exon upto the zinc fingers (bp1-809) and E lacking the entire CDS except for the Traf domain (bp1-1011). Each of these constructs were cloned into the PUAST vector, transgenic lines made and tested for the Traf1 overexpression phenotype.

It has been reported for *Traf1* that the characteristic Traf domain is both essential and sufficient for activation of the JNK pathway in cultured cells, mediated by its binding to the JNK pathway MAP4Kinase, Misshapen (Liu *et al.,* 1999). If indeed as described above, the JNK pathway is essential for causing the gastrulation defects when Traf1 is overexpressed in the mesoderm, then truncation constructs of *Traf1* that lack the Traf domain should not cause gastrulation defects. On the other hand, constructs coding for only the Traf domain should be able to phenocopy the phenotype exhibited by the full length Traf protein. In order to test this, four *Traf1* truncation constructs were cloned in the PUAST vector, transgenic lines established and overexpression experiments performed with flies carrying each of these constructs. Further details regarding these

constructs are given in the Materials and Methods section. The schematic Figure 29 shows the four constructs that were made, in comparison to the full length *Traf1* construct. The full length *Traf1* construct is shown in A; B represents the construct lacking the C terminal Traf domain; C shows the construct lacking the Traf domain as well as the zinc finger motifs; D, the construct having an N terminal truncation which removes the first exon and part of the second exon and E is the N terminal truncation construct that lacks the first exon and part of the second exon including the zinc finger motifs leaving just the Traf domain intact.

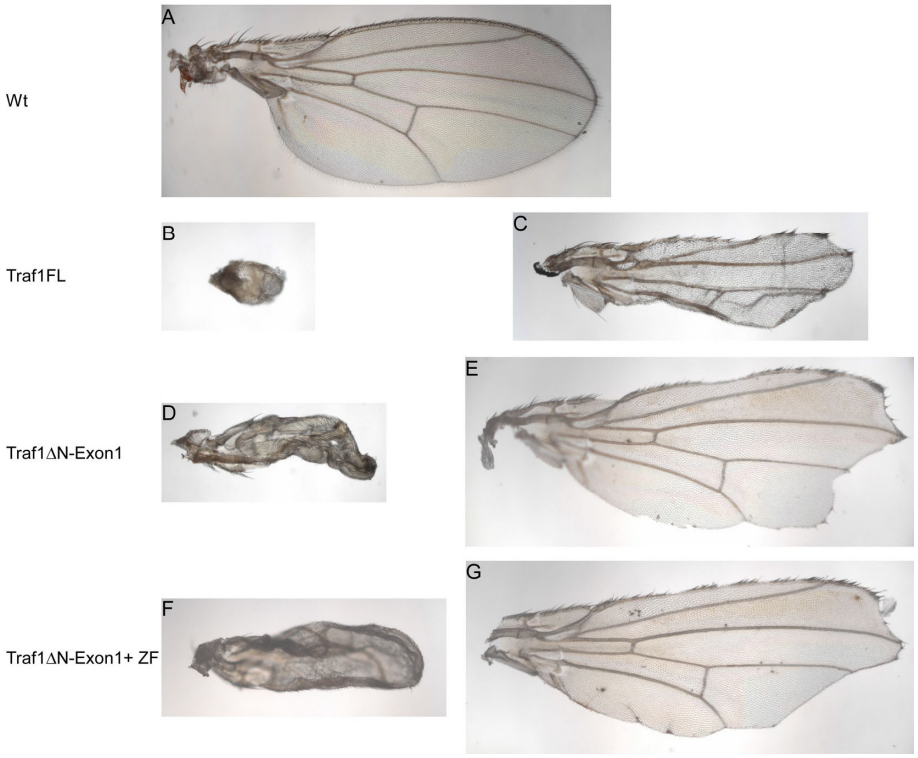

Figure 30: Results from misexpression of the various *Traf1* constructs in the *Drosophila* wing. The respective genotype is shown on the left**.** A wild type wing is shown in A. When full length *Traf1* is misexpressed in the wing using the sd-Gal4 driver, almost the entire wing is lost, save a rudimentary structure (B). This phenotype is variable, depending on the strength of the insertion used and weaker insertions give rise to weaker phenotypes as in C, where the wing is still highly rudimentary or even weaker effects (data not shown). Similar strong defects are observed with the construct lacking the N terminal first exon (D); weaker effects are also observed in this case (E). The construct lacking the entire sequence except the Traf domain also gives similar effects according to the strength of the insertion used (F and G) although in this instance the weaker phenotypes are more penetrant than the stronger ones. The other two constructs lacking the C terminal Traf domain do not show any defects on misexpression. These results are tabulated in Table 7.

In order to test whether the *Traf1* truncation constructs described above are functional, they were tested by misexpression in another system, the adult wing. This is because it has been reported that the JNK pathway is essential for wing morphogenesis by inducing apoptosis as well as by facilitating tissue spreading/fusion (Adachi-Yamada *et al.,* 1999; Adachi-Yamada and O'Connor, 2002, Agnes *et al.,* 1999; Lee *et al.,* 2003; Pastor-Pareja *et al.,* 2004; Ryoo *et al.,* 2004). It has been reported that overexpression of the TNF ligand Eiger, severely compromises wing development and a rudimentary structure results (Igaki *et al*., 2002; Moreno *et al.,* 2002). Similar effects are also observed on the eye, upon overexpression (Cha *et al.,* 2003; Geuking *et al.,* 2005; Igaki *et al*., 2002; Moreno *et al.,* 2002). Moreover, these phenotypes can be rescued by reducing the activity of the JNK pathway, either by heterozygosity of downstream JNK effector molecules such as *basket* or *hemipterous* or by co-overexpressing the negative regulator of the pathway, Puckered (Igaki *et al.,* 2002; Moreno *et al.,* 2002; Cha *et al.,* 2003). Thus, the wing would serve as a good model system to test the Traf1 constructs as well as the constructs for genes functioning in the JNK pathway.

When the full length Traf1 construct was misexpressed in the wing using a Scalloped-Gal4 driver, defects in morphogenesis of the wing were observed (Figure 30B, C). The highly expressed insertions led to almost complete ablation of the wing (Figure 30B), as observed in the case of misexpression of the TNF ligand, Eiger (Igaki *et al.,* 2002; Moreno *et al.,* 2002; data not shown), compared to the wild type wing (Figure 30A) whereas weaker phenotypes were also observed with weaker insertions (Figure 30C). C terminal truncation constructs of *Traf1* which lack the Traf domain (Figure 29B and C) upon misexpression gave rise to normal, wild type wings (data not shown). Further, N terminal truncation constructs which do not delete the Traf domain (Figure 29D and E) were able to reproduce the phenotypes exhibited by the full length construct, upon misexpression (Figure 30D-G) except that the N terminal truncation construct that leaves the Traf domain alone intact, upon misexpression exhibits the weaker effects (Figure 30G) at a higher frequency than the stronger ones (Figure 30F). This indicated that expressing the Traf domain alone leads to instability of the protein, which results in a

weaker effect. It could also be that the Traf domain alone is not sufficient to mediate the observed effects in the wing. Another possible explanation is that localization of the protein is defective in the construct carrying the intact Traf domain alone, as discussed below. Nevertheless, these experiments suggested that almost all the *Traf1* truncation constructs are functional. Moreover, it also proved that the Traf domain is necessary for JNK signal activation, as already reported (Liu *et al*., 1999). Complete results from these misexpression experiments are tabulated in Table 7.

Once it was clear that the Traf1 constructs are functional, they were tested by overexpression in the mesoderm as described before. It was found that constructs lacking the Traf domain (Figure 29B and C) do not reproduce the gastrulation defects characteristic of the full length *Traf1* construct. Further, constructs having an intact Traf domain (Figure 29D and E) were able to reproduce the gastrulation defects in the early embryo upon overexpression. However, the penetrance of the phenotype exhibited by the construct coding for the Traf domain alone upon overexpression was found to be lower than the full length construct or the construct coding for the Traf domain and the zinc finger motifs. As already mentioned, one reason for this might be that the truncation causes a loss of stability of the protein resulting in reduced severity of the phenotype. It could also be that the Traf domain alone is not sufficient to reproduce the defects. Another possibility is that the zinc finger motifs are essential for the normal cytoplasmic localization of Traf1, where Traf1 is proposed to function. There is evidence in this regard from experiments on mammalian Traf4, the homologue of *Drosophila* Traf1, where loss of the zinc finger motifs caused nuclear localization of the protein (Glauner *et al*., 2002). Further studies using tagged constructs are required to determine whether this holds true for flies as well. The results from all of these experiments indicate that the JNK pathway activation is the most likely cause leading to the observed gastrulation defects when Traf1 or other members of the JNK pathway are overexpressed in the mesoderm of the early *Drosophila* embryo.

3.12 The JNK pathway and wing morphogenesis

In a similar set of experiments, JNK pathway members were also misexpressed in the wing in order to understand whether related phenotypes as observed for Traf1 misexpression are observed. Furthermore, other molecules such as Rho1, RhoGEF2, which are required for cell shape changes during gastrulation, dorsal closure etc and which are known to function in a cooperative manner to the JNK pathway in certain contexts such as planar cell polarity signalling (Strutt *et al.,* 1997), dorsal closure (Bloor and Kiehart, 2002) etc could also be tested in the wing. This might give an indication regarding the mechanism by which the gastrulation defects exhibited by embryos where the JNK pathway is overexpressed in the mesoderm occurs.

The results from these experiments are shown in Figure 31. The genotype of the stock or the member of the pathway that was misexpressed in the particular instance is shown on the left side of each panel. As shown before, expression of the full length Traf1 construct results in a range of phenotypes with the most severe cases exhibiting complete wing ablation (Figure 31B) as also weaker defects (Figure 31C and D). Similar results are obtained when Egr is misexpressed in the wing (Igaki *et al.,* 2002; Moreno *et al.,* 2002; data not shown). However, overexpression of Wgn resulted in normal wings, possibly because the construct used was not an activated one (data not shown). When the JNK kinase Hep is misexpressed, complete ablation of the wing is observed (Figure 31E and F) as also some flies having malformed and crumpled wings which are reduced in size as well (Figure 31G). These phenotypes bear a strong resemblance to the ones exhibited when Traf1 or Egr are misexpressed. Misexpression of a constitutively active form of Hep led to pupal lethality as was also the case with a strong Eiger insertion. Other members of the JNK pathway that were tested include *msn*, *bsk* and *puc*. Msn and Bsk misexpression yielded weaker effects similar to the one shown in Figure 31D, whereas Puc misexpression did not result in noticeable defects. However, only one insertion each was used to test these three JNK pathway members and conclusive proof regarding the role of these molecules requires further experiments testing more insertions.

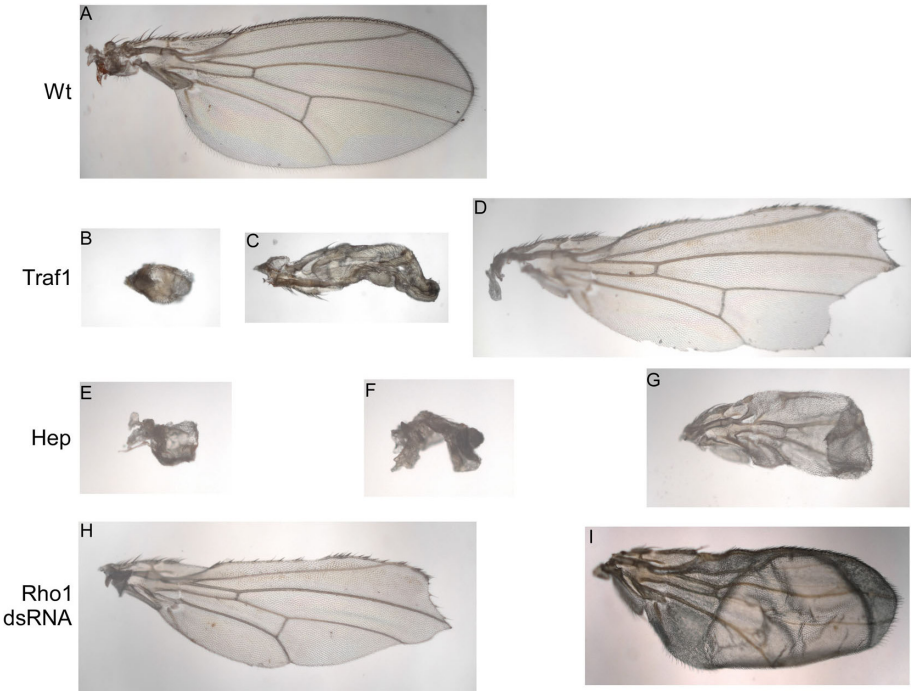

Figure 31: Defects observed when various members of the JNK pathway are misexpressed or when Rho1 is depleted in the wing, as compared to wild type wing. The genotype or the construct which is misexpressed in each instance is represented on the left side of each panel. A wild type wing is shown in A. The range of wing defects when a Traf1 full length construct is misexpressed in the wing is shown in B, C and D. When Hep, a member of the JNK pathway is misexpressed in the wing, similar rudimentary structures result (E, F and G). However, when Rho1 levels are depleted using a Rho1 dsRNA construct, similar defects as exhibited by weaker Traf1 insertions are shown, wherein part of the wing and the margin hairs are lost (H). Stronger effects can also be observed in such cases which are shown in I, such that the entire wing is reduced in size and wrinkled, as is the case with the stronger insertions of *Traf1* or *hep*. These results are tabulated in Table 7.

In addition to the JNK pathway members, dsRNA constructs of *Rho1* were also tested for their effect on the wing. This was due to two reasons. First, Rho1 is known to be required in several processes where JNK signalling is also involved, such as dorsal closure and planar polarity signalling. This suggests that both of these pathways interact at some level raising such possibilities in gastrulation as well, where Rho1 is known to be required for cell shape changes (Barrett *et al.,* 1997; Hacker and Perrimon, 1998). Second, the guanine nucleotide exchange factor for Rho1, RhoGEF2 has been shown to be required for proper wing morphogenesis (Nikolaidou and Barrett, 2004) indicating that Rho1 might also have a similar role. Interestingly, weak effects of depletion of Rho1 (Figure

31H) reproduced the phenotype exhibited upon weak misexpression of the JNK pathway (Figure 31D). Stronger effects of depletion of Rho1 (Figure 31I) resulted in crumpled, twisted wings, resembling somewhat the stronger effects of JNK misexpression (Figure 31C and G). Although preliminary, these results might indicate a potential connection between JNK signalling and *Rho1* in wing morphogenesis. Further studies involving epistatic as well as cell biological analysis are required to substantiate these findings.

Constructs tested	Mesoderm	Wing		
		W	M	S
UAS-Eiger	+	-	+	+
UAS-Traf1FL	+	+	+	+
UAS-Traf1ΔC-TD	-	-	-	-
UAS-Traf1ΔC-TD+ZF	-	-	-	-
UAS-Traf1 ΔN-Exon1	+	+	+	+
UAS-Traf1ΔN-Exon1+ZF	+	+	+	-
UAS-Wengen	-	-	-	-
UAS-Misshapen	+	+	-	-
UAS-Basket	+	+	-	-
UAS-Hemipterous	+	-	+	+
UAS-Puckered	-	-	-	-
UAS-dsRNARho1	**nd**	+	+	-

Table 7: Summary of results from overexpression of the Traf1 constructs as well as JNK pathway members in the mesoderm as well as the wing. The first column represents the different constructs used in the overexpression experiments, the second whether there is any effect on the mesoderm and the third, whether there is any effect on the wing upon misexpression. The third column is subdivided further into 3 sub columns in order to specify the range of phenotypes and penetrance exhibited by each construct. W refers to weak effects upon misexpression, M medium effects and S severe effects (Figure 29 B-D). These results are obtained from the stronger insertions from the available set of transgenic lines. It can be seen that a clear correlation exists between the severity of the phenotype in the wing and the ability to induce gastrulation defects upon overexpression. The UAS-dsRNARho1 construct was not tested for gastrulation defects although it is known from previous studies that depletion of Rho1 leads to gastrulation defects.

3.13 Summary

Overexpression of Traf1 in the mesoderm gives rise to gastrulation defects which are not due to cell fate changes or abnormalities in cell division. This indicates that the observed defects are a result of the effect of Traf1 on some other process such as cytoskeletal rearrangement or cell-adhesion. From previous reports, it is known that Traf1 activates the JNK signalling cascade. Thus, the overexpression phenotype exhibited by Traf1 might be due to activation of the JNK signalling cascade. In order to test this, members of the JNK pathway were overexpressed in the mesoderm. It was found that overexpression of several members of the JNK pathway also led to similar gastrulation defects. This was further tested using truncation constructs of *Traf1*. The Traf domain of Traf1 was reported to be essential for activation of JNK signalling. Misexpression experiments in the *Drosophila* wing indicated that this is indeed the case, although the construct coding for the Traf domain alone did not exhibit the phenotype with high penetrance. In the mesoderm, it was found that constructs lacking the Traf domain do not exhibit gastrulation defects upon overexpression whereas constructs having an intact Traf domain alone reproduce the gastrulation defects. However, as in the wing, the construct coding for the Traf domain alone when overexpressed in the mesoderm exhibited gastrulation defects with lesser penetrance. Further studies are required to test whether this reduction in penetrance is due to loss of stability of the protein or due to a JNK independent effect of Traf1.

4. Discussion

4.1 Several loci essential for gastrulation map to the 24-25 region

It is evident from this study that at least three loci involved in gastrulation map to the 24-25 cytogenetic region. These include two maternal effect loci and one zygotic locus which will be discussed in greater detail below.

4.1.1 The maternal loci

A maternal effect gene is one whose main activity takes place during the formation of the egg in the mother before fertilization (Gurdon, 2005). From this study, two maternal loci involved in gastrulation were identified.

The first maternal locus was found to be uncovered by several of the old deficiencies such as Df(2L)ed-dp, as evident from the results shown in Table 1. This locus will be referred to as the maternal effect locus at 24F (*mat24F*) henceforth. This locus has proven difficult to map and could only be narrowed down to a short genomic stretch. In a previous study, a maternal effect locus involved in gastrulation was predicted to be uncovered by the deficiency Df(2L)ed dp (Hoang and Wieschaus, 1999), named *accordion* and was reported to be mapping to the 24F1 region (Flybase). However, this locus could not be identified in subsequent analyses (personal communication, Dawes-Hoang, R). Further, embryos from an EMS allele for the gene *Tps1* mapping to the region where the maternal effect locus has been narrowed down to (24E-F), *sz31*(*jf5*), also exhibits gastrulation defects (Table 5). However, *Tps1* has no discernable role in gastrulation as embryos from several other *Tps1* loss of function alleles exhibit normal gastrulation (Table 5). It is clear that *sz31*(*jf5*) has additional mutations in at least one other gene in the region than *Tps1*, *dumpy* (Table 5). This suggests that *sz31*(*jf5*) might have some genetic rearrangement in the genomic stretch in proximity to *Tps1*, possibly uncovering the mat24F locus uncovered in deficiencies such as Df(2L)ed-dp, if indeed the gastrulation defects exhibited by *sz31*(*jf5*) map to the 24-25 region. One possibility to test this would be by sequencing the entire region flanking the *Tps1* gene although it

might be difficult to pick out point mutations in this manner. Otherwise, available genetic techniques are inadequate to map this locus.

Embryos from certain deficiencies in the 24-25 region such as Df(2L)M24F-B and Df(2L)dp-h28 exhibit a weaker maternal effect phenotype compared to that from deficiencies such as Df(2L)ed-dp (Table 1), although all of them uncover the predicted genomic stretch where *mat24F* locus maps. This observation further complicated the study. However, a possible explanation for such effects would be the accumulation of suppressor mutations that suppress the full extent of the phenotype in some of the deficiency stocks.

The second maternal effect locus is genetically separable from *mat24F* and is not uncovered by any of the old deficiencies. This locus was identified during the course of the detailed mapping of the region, for which purpose ten new deficiencies were generated with precisely mapped break points. It was found that three of the newly constructed deficiencies which uncovered genomic stretches distal to that of the old deficiencies, exhibited a maternal gastrulation defect. Further studies on the genomic stretch uncovered by these three new deficiencies are required in order to pinpoint and characterize this locus. One deficiency stock, Df(2L)sc-19-8, which has a duplication on to the X chromosome, is predicted to uncover both the maternal loci although embryos from this stock could not be tested due to reduced fertility of the stock.

4.1.2 The zygotic locus

At least one zygotic locus involved in gastrulation is also uncovered by several of the old deficiencies (Table 2). This is evident from the gastrulation defects exhibited by embryos from a cross between males from such deficiencies and C(2)v females (Figure 11). Embryos derived from such a cross exhibit even more severe gastrulation defects compared to embryos derived from a cross between deficiency males and females (Compare Figures 5 and 11). This is unexpected because the zygotic effect should be fully manifest in embryos derived from a cross between deficiency males and females. The increased severity observed in embryos from the C(2)v background suggested that

the C(2)v background (haploinsufficiency of left arm or triploidy of right arm) contributes to the enhancement of the zygotic phenotype. However, this turned out not to be the case for at least 90% of the second left arm and 85% of the second right arm. The involvement of the remainder of both of these chromosomal arms in proximity to the centromere could not be ruled out using available genetic tools. The maternal effect gene *concertina* (*cta*), known to be involved in cell shape changes in gastrulation, maps to this stretch and although *cta* is thought to have no zygotic effect, such a possibility cannot be ruled out. Further, preliminary evidence from analysing embryos from experiments where the C(2)v cross was performed in the opposite manner (deficiency females to C(2)v males) suggests that the reason behind the enhancement of the zygotic phenotype might be background mutations in the C(2)v stock. If true, this suggests that the zygotic effect might be enhanced by background mutations that cause an enhancement by reducing maternal transcript levels. This might mean that the so called zygotic locus and the first maternal effect locus are the same. Reduction in maternal transcript levels could be either due to second site mutations which reduce global maternal transcript levels or due to mutations in the same locus as the one uncovered in deficiencies so as to reduce its own maternal transcript levels. These possibilities have to be tested further by using other C(2)v stocks as also by experiments designed to reduce the maternal contribution. One way to reduce the maternal contribution to the embryo is by bringing the deficiencies in a modified genetic background and analysing the embryos. One example for such a background is the *wimp* mutation, which is a change of function mutation in the second largest subunit of RNA polymerase (Parkhurst and Ish-Horowicz, 1991; Rosenberg and Parkhurst, 2002), which enhances the severity of the phenotype caused by mutations in several loci by reducing the maternal transcript levels of the concerned gene. The *wimp* mutation can reduce but not eliminate the maternal contribution of the *dSir2* RNA, causing patterning defects (Rosenberg and Parkhurst, 2002). Thus, provided the *wimp* locus is capable of reducing the maternal transcript levels of the gene being studied here, by analysing embryos derived from deficiencies in the 24-25 region in a *wimp*

background, one would be able to ascertain whether maternal effects contribute to the observed enhancement of the phenotype.

Such experiments might reveal the reason behind the enhancement of the zygotic phenotype. If indeed it turns out that mutations in the same locus as the one uncovered by deficiencies cause the enhancement in the C(2)v background, it might be possible to identify and map the nature of the mutation by sequencing. However, if second site mutations in the C(2)v stock turn out to be the cause, pinpointing the exact interacting locus responsible for the enhancement might be impossible because the C(2)v stock is not amenable to normal genetic studies such as generating mutations or mapping them.

4.2 *Traf1*, a candidate gene involved in gastrulation

The zygotic locus responsible for the gastrulation defects was narrowed down and fine mapped to the *Traf1* gene. The mRNA expression pattern of *Traf1* (Figure 12) was the suggestive feature which indicated that it might have a role in gastrulation. Further, the other predicted genes in the region were not expressed in the mesoderm during gastrulation although some of them were maternally contributed (BDGP expression pattern database). It was also found that Twist and not Snail regulates the ventral domain of *Traf1* expression (Figure 18). However, subtle effects mediated by Dorsal or Snail could not be ruled out to be required for *Traf1* expression. The presence of several consensus Dorsal binding sites upstream of the *Traf1* gene suggested a role for Dorsal in regulating *Traf1*. Dorsal is required for *twist* activation and therefore, mutations affecting *dorsal* would affect *twist* and have an effect on *Traf1*. One possible solution to test the role of *dorsal* is an artificial system wherein embryos lacking Twist but having an ectopic anteroposterior Dorsal gradient can be generated to check for activation of *Traf1* in a Dorsal dependent manner (Stathopoulos and Levine, 2002B).

Further evidence regarding the role of *Traf1* in gastrulation was the phenotype exhibited by embryos from a hypomorphic P element insertion allele of *Traf1*, EP578, which exhibited a delay in gastrulation. However, efforts by me to generate a null mutation by imprecise excision of the P element proved futile. Another group reported an imprecise

excision allele, Traf1^{ex1}. Embryos obtained from this stock also exhibited the weak ventral furrow invagination defect as with the EP 578 stock. Moreover, embryos derived from a cross between Traf1^{ex1} males and C(2)v females reproduced the enhanced gastrulation phenotype as was the case with embryos from a cross between deficiencies in the region and C(2)v females, albeit at a lesser frequency. Further investigations revealed that Traf1^{ex1} was not a null allele for *Traf1*, as originally reported, which may explain the reduced penetrance of the phenotype in the C(2)v background. This was because the Traf1^{ex1} allele deleted the first exon and promoter without affecting the second exon. It was found that the second exon was being transcribed in this stock from a different promoter. Further studies involving promoter fusions to reporter genes and transcript specific probes are required to understand whether the two promoters regulate *Traf1* expression in different developmental contexts.

Available reports on *Traf1* function also supported the idea that it is important in morphogenesis. Several independent studies demonstrated that *Traf1* functions in the JNK signalling cascade (Cha *et al.,* 2003; Kuranaga *et al.,* 2002; Liu *et al.,* 1999; Moreno *et al.,* 2002) which has been implicated in diverse morphogenetic processes, both in invertebrates and vertebrates (reviewed by Davis, 2000; Martin and Parkhurst, 2004). In mice mutant for *Traf4*, the closest orthologue of *Drosophila Traf1*, neural tube closure, tracheal morphogenesis and axial skeleton development were severely impaired (Shiels *et al.,* 2000; Regnier *et al.,* 2002).

The Traf family of proteins diverged during evolution and whereas *Drosophila* have three Traf genes, higher vertebrates have six (Grech *et al.,* 2000). However, comparing the C terminal Traf domains of all the Traf proteins, it was clear that *Drosophila* Traf1 was more closely related to vertebrate Traf4 than to the other *Drosophila* Traf molecules (reviewed by Chung *et al.,* 2002). This conservation is also maintained in functionality in that *Drosophila* Traf1 and vertebrate Traf4 function in the JNK signalling cascade (Cha *et al.,* 2003; Abell and Johnson, 2005; Xu *et al.,* 2002) whereas *Drosophila* Traf2 and its vertebrate orthologue Traf6 function in the Dorsal/NF-κB signalling cascade (Cha *et al.,* 2003; Shen *et al.,* 2001; Leo *et al*., 1999; reviewed by Chung *et al.,* 2002). Some early

reports suggested that *Drosophila Traf1* might also play a role in the activation of Dorsal by interacting with the Pelle kinase which mediates Toll signalling in *Drosophila*, based on evidence from yeast two hybrid experiments and binding assays (Zapata *et al.,* 2000). These findings indicated that *Traf1* might influence gastrulation due to its effect on Dorsal. However, subsequent studies demonstrated that this was not the case (Cha *et al.,* 2003). No enhancement of the gastrulation phenotype was observed in *Traf1*, *Traf2* double mutant embryos indicating that if *Traf1* is responsible for the defects, *Traf2* does not contribute to it. One possibility that has not been tested is whether Traf1 exerts a feedback effect on Dorsal, as has been reported recently for Wnt D (Ganguly *et al.,* 2005; Gordon *et al.,* 2005).

If *Traf1* is responsible for the gastrulation defects exhibited by embryos derived from deficiencies in the 24-25 region, it might be due to the effect of Traf1 on processes such as cytoskeletal rearrangement or cell adhesion. This is because of the role that JNK signalling is known to play in cell movement, actin cytoskeleton remodelling and epithelial morphogenesis (reviewed by Xia and Karin, 2004).

In order to gain conclusive evidence regarding the role of *Traf1* in gastrulation, a null mutant allele is required. However, strategies such as imprecise excision and X-ray mutagenesis have failed to generate loss of function alleles. It is surprising that the only deletions available for the *Traf1* locus are relatively large, X-ray generated deficiencies such as Df(2L)ed-dp, made several years ago (Szidonya and Reuter, 1988). None of the large scale and high resolution new deletion screens including the Drosdel project (Ryder *et al*., 2004) and the Exelixis project (Thibault *et al.,* 2004) have been able to uncover the *Traf1* locus suggesting that generating deletions in this region is difficult and might require different strategies. One possibility in this regard is targeted gene knock out, which has progressed tremendously in recent years (Rong and Golic, 2000; Gong and Golic, 2003; Gong and Golic, 2004; Xie and Golic, 2004). Another possibility is generating dsRNA for *Traf1 in vitro* and microinjecting it into blastoderm stage embryos in order to achieve gene knockdown (reviewed by Carthew, 2001).

Rescue experiments using a *Traf1* UAS construct early in the embryo is another method to prove the role of Traf1 in gastrulation. However, such experiments are difficult to perform in the early embryo, because of a lack of early acting driver lines. This difficulty has been circumvented by generating the 2xPE Traf1 construct, which allows Traf1 expression in the Twist domain (Jiang and Levine, 1993). However, the phenotype exhibited by embryos derived from deficiencies in the 24-25 region is subtle, necessitating detailed analysis involving scoring large numbers of embryos to confirm results from any rescue experiments. In this regard, an easier option is to perform a rescue experiment of the enhanced phenotype observed in embryos derived from a cross between deficiency males and C(2)v females. As discussed in the next section, embryos expressing a 2xPETraf1 construct exhibit a dominant gastrulation defect as well. This would complicate the rescue analysis as well. However, the dominant effect exhibited is dependent on the level at which *Traf1* is expressed, varying from insertion to insertion. Thus, some of the weakly expressed transgenic lines which exhibit the dominant effect at highly reduced rates have been chosen for the rescue experiments.

4.3 A possible role for JNK and TNF signalling in gastrulation

One clear indication that *Traf1* is involved in gastrulation came from the observation that overexpression of Traf1 in the early embryo causes a block in ventral furrow formation. This observation was confirmed by using different Gal4 driver lines to drive Traf1 expression in the early embryo as also by observing embryos from flies expressing a 2xPE Traf1 transgene, which expresses Traf1 in the Twist domain, both of which resulted in defective gastrulation. In order to narrow down and thus identify the minimal coding sequence required to elicit this dominant effect, truncation constructs of *Traf1* were made. These constrcts were first tested in the adult wing. All of the constructs harbouring the Traf domain showed a dominant effect in the wing upon misexpression and were thus functional, although the construct having the Traf domain alone did not exhibit the high level of penetrance as the other constructs. This might be due to instability of this protein or due to a lack of functional domains such as the zinc finger repeats, which might be

required for proper localization of the protein as reported for Traf4 (Glauner *et al*., 2002). It could also suggest that the Traf domain is not sufficient by itself to mediate the observed effects. These possibilities have to be tested using tagged versions of all the constructs in future experiments. Constructs lacking the Traf domain did not exhibit the dominant effect on the wing, suggesting that either they lacked the essential domain or that they were non-functional. Further studies are required to distinguish between these possibilities.

After testing the truncation constructs on the wing, they were overexpressed in the mesoderm. Results from these experiments suggested that the C terminal Traf domain is indispensable for the dominant gastrulation effect (Table 6). Previous studies have shown that this domain is both necessary and sufficient for JNK signal activation in *Drosophila* cell lines, which is predicted to occur through Traf1 binding to the JNK pathway MAP4Kinase molecule, Misshapen (Liu *et al*., 1999). Interestingly, this seems to be a conserved function in vertebrates as well, where it has been reported that Traf4 binds the MAP4Kinase, MEKK4 and activates JNK signalling (Abell and Johnson, 2005; Xu *et al*., 2002). However, Traf4 by itself could only weakly activate JNK signalling (Abell and Johnson, 2005; Xu *et al*., 2002). Furthermore, overexpression of different members of the *Drosophila* JNK signalling cascade in the mesoderm led to gastrulation defects as well (Table 6). However, neither the negative regulator of the pathway, *puc* nor the TNF receptor *wgn* exhibited these defects. In the case of *wgn*, this might be because the construct used was not an activated one. However, the results from *puc* might point towards a JNK independent effect of the observed gastrulation defects although the results have to be verified using other insertions for *puc*. Nevertheless, these results indicate that members of the JNK cascade are important in gastrulation and that the effects that Traf1 has on gastrulation might be mediated through JNK signalling.

Previous studies have led to reports that Misshapen (Msn), the JNK pathway member immediately downstream of Traf1 might be involved in gastrulation (Su *et al*., 2000; Xue *et al*., 2001). The expression of Msn in the early mesoderm suggested that it might be involved in gastrulation (Su *et al*., 1998; Treisman *et al*., 1997). However, the

involvement of *msn* in gastrulation could not be conclusively proven because of the germline requirement of Msn and associated inability to generate germ line clones that completely lack maternal and zygotic Msn (Treissman *et al*., 1997). Nevertheless, overexpression experiments using a dominant negative construct of Msn which lacked the kinase domain resulted in embryos with defective ventral patterning, further strengthening the possibility that *msn* plays a role in gastrulation (Su *et al*., 2000). Interestingly, results from the vertebrate homologue of Msn, MEKK4 indicate that mice lacking this gene have severe mesodermal patterning defects and somitogenesis defects (Xue *et al*., 2001), as well as neural tube development defects (Chi *et al*., 2005). However, it was also reported that the mesodermal defects associated with loss of MEKK4 are JNK independent, raising the possibility that MEKK4 and upstream activators can function in an as yet unidentified, JNK independent manner as well (Xue *et al*., 2001).

With the exception of *msn*, there are no other published reports regarding downstream molecules in the JNK cascade in *Drosophila* having any effect on gastrulation. Moreover, embryos mutant for *hep*, the JNK kinase, do not exhibit gastrulation defects (personal communication, Wilson, R). However, this does not rule out the possibility that Traf1 or Msn utilize other downstream JNK kinases than Hep to activate JNK signalling. There are previous reports that suggest the presence of additional JNKkinases than Hep (Chen *et al*., 2002). It could also be that, as in vertebrates, the observed defects are a direct consequence of loss of function of the concerned molecule, in this instance *msn* or *Traf1*, rather than its effect on activation of JNK signalling (Xue *et al*., 2001).

Another interesting development in the recent years was the identification of a TNF receptor and ligand in *Drosophila*. The TNF pathway is essential for cell death and is known to be closely associated with the JNK signalling cascade in vertebrates (reviewed by Varfolomeev and Ashkenazi, 2004; Weston and Davis, 2002). In accordance with these reports, the TNF ligand Eiger (Egr) and the receptor Wengen (Wgn) have been shown to be required for JNK signal activation (Igaki *et al*., 2002; Kanda *et al*., 2002; Kauppila *et al*., 2003; Moreno *et al*., 2002). Interestingly, the early embryonic mRNA

expression pattern of both of these molecules is mutually exclusive. Whereas *egr* is expressed on the dorsal side of the embryo under the control of Dorsal, *wgn* is expressed on the ventral side, suggesting that both of these molecules might be important in early embryonic patterning (Stathopoulos *et al*., 2002C; Kauppila *et al*., 2003). Available evidence from vertebrate model systems suggest that Traf molecules function as adaptors in the signalling complex associated with the intracellular part of the TNF receptor (reviewed by Bradley and Pober, 2001; Wajant *et al*., 2001). Upon ligand binding and receptor activation by trimerization, this signalling complex is recruited and downstream signalling activated, which feeds into activation of signalling cascades such as JNK or NF-κB (reviewed by Baud and Karin, 2001). However, Traf4 has been implicated in very few such reports (reviewed by Zapata, 2003). Although detailed studies have not been conducted on the fly TNF homologues, some biochemical evidence exists that Egr binds Wgn and leads to JNK activation (Kanda *et al*., 2002). However, other reports suggest that they do not bind to each other (Kauppila *et al*., 2003). Nevertheless, genetic experiments have clearly shown that *egr* mediated JNK activation can be suppressed by loss of *wgn* function in flies (Kanda *et al*., 2002; Kauppila *et al*., 2003). Whether downstream effects of this activation is mediated through Traf1 is an as yet unanswered question, although it has been shown that developmental defects caused by Egr misexpression in the adult *Drosophila* eye can be partly rescued by reducing the dose of *Traf1* (Moreno *et al*., 2002). Further experiments in this regard are required to verify these results and understand the link between the TNF and JNK pathways in *Drosophila*.

4.4 Signalling upstream and downstream of Traf1

As discussed above, the TNF receptor Wgn might be required for Traf1 activation by recruiting a signalling complex, possibly upon activation by the ligand Egr, in its role as a JNK effector (Kanda *et al*., 2002). In this regard, it is interesting that the early embryonic mRNA expression patterns of *egr* and *wgn* are mutually exclusive (Kauppila *et al*., 2003; data not shown). There are reports which suggest that Egr has to be proteolytically cleaved to form a soluble, mature form so as to increase the range over which it can be

active (Kauppila *et al*., 2003). In mammals, this cleavage is accomplished by the TNF-alpha converting enzyme (TACE), a *cis*-acting membrane associated metalloprotease (Blobel, 1997). Interestingly, a gene with homology to TACE is present in the *Drosophila* genome as well and it remains to be seen whether it regulates the processing of Eiger (Kauppila *et al*., 2003). Further studies are required to substantiate these findings. Although reports suggest that Traf1 does not interact with the Toll/Interleukin pathway based on genetic evidence (Cha *et al*., 2003), it cannot be ruled out entirely whether it can bind and activate signals from other receptors of the Toll family. Further, it is unclear what causes downstream signal activation once Traf molecules are recruited to the receptor. Available evidence from vertebrate models indicate that oligomerization and interaction with other members of the recruited signalling complex results in downstream signal activation (Dempsey *et al*., 2003).

I have shown that Twist regulates the mRNA expression of *Traf1* in the mesoderm (Figure 18). The presence of consensus Dorsal binding sites upstream of the *Traf1* coding sequence suggests that Dorsal might also play a role in transcriptional activation of *Traf1*. Further, a precedent for this exists in vertebrates where it has been shown that the Dorsal homologue NF-κB can bind to and activate transcription of Traf molecules such as *Traf1* (Munzert *et al*., 2002; Wang *et al*., 1998). The expression of Traf1 in ectodermal stripes which are not lost in *twist* mutants (Figure 18) suggests that an additional mechanism is possibly involved in transcriptional regulation of *Traf1*.

There is evidence that *thread* (*Diap1*), the fly homologue of an inhibitor of apoptosis (IAP) family member, is required to degrade Traf1 by ubiquitination, in order to prevent JNK activation (Kuranaga *et al*., 2002; Ryoo *et al*., 2004). Available evidence from vertebrate models also suggests that the IAPs (Inhibitor of Apoptosis Proteins) function closely with the TNF pathway and cooperatively with the Traf family of proteins (Wang *et al*., 1998). Taken together, these data imply that Traf1 is under complex transcriptional and post-translational control.

Although it is plausible that almost all of the effects observed with regard to Traf1 overexpression might be due to its ability to bind Msn and activate JNK signalling,

questions exist regarding a JNK independent effect as well (Xue *et al*., 2001). The latter possibility is particularly interesting due to its novelty and requires extensive investigation. On the other hand, if the observed effects are JNK dependent, it would be interesting to identify which effectors are involved. For example, canonical JNK signalling leads to activation of the Jun and Fos transcription factors which heterodimerize to form the AP1 transcriptional complex, thought to mediate activation of downstream target genes (reviewed by Xia and Karin, 2004). However, in the planar polarity pathway, Rho1 has been reported to be necessary to activate JNK signalling (Strutt *et al*., 1997). Interestingly, the JNK signalling cascade is also reported to interact with the Wingless cascade in planar polarity signalling, during processes like dorsal closure (Kaltschmidt *et al*., 2002; reviewed by Mlodzik, 2002). Further studies are required to investigate the exact manner in which *Traf1* functions and which particular downstream targets it activates in specific developmental contexts such as gastrulation, dorsal closure or wing morphogenesis. The question becomes even more complicated to address because of the redundant nature of the MAPKinase signalling pathways, where individual MAPKinases are used in more than one cascade (reviewed by Yang *et al*., 2003) depending on the situation.

Utilizing the available details of Traf1 signalling known in flies and taking into account the precedents established from work on vertebrates, a simplified model has been proposed to outline the regulation of Traf1 (Figure 32). The extracellular, intracellular and nuclear compartments are represented with the different molecules involved in the signalling pathways discussed depicted with different colours and their respective names. At the transcriptional level, *Traf1* is activated by Twist and possibly Dorsal. Recruitment of Traf1 to a signalling complex requires trimerization and activation of the TNF receptor Wgn, by ligand (Egr) binding. Traf1 then recruits and activates the Ste20 MAP4Kinase Msn, which leads to activation of JNK signalling. There is strong evidence from vertebrates that a JNK independent role for Msn and Traf1 during development exists. The effects of activation of the JNK dependent or independent pathways would be cytoskeletal rearrangement, transcriptional activation of target genes, cell adhesion

changes, effects on polarity and so on. Traf1 is also regulated posttranslationally by DIAP1 or Thread, which facilitates degradation of Traf1 by ubiquitination.

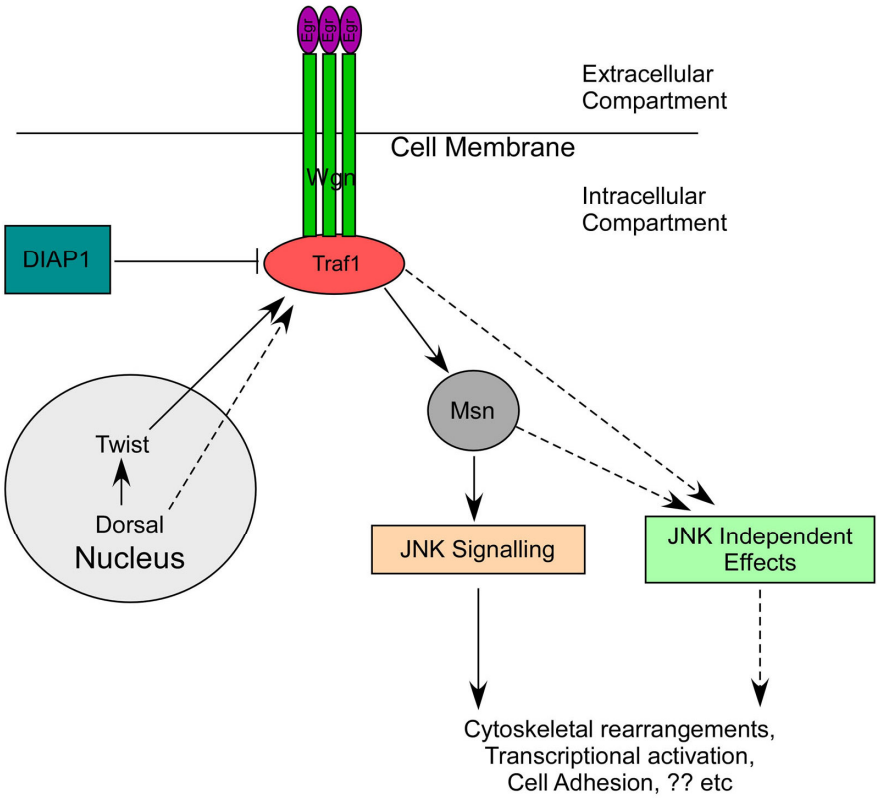

Figure 32: A simplified model showing the different components involved in the regulation of *Drosophila Traf1* and signalling downstream of Traf1. The nucleus, intracellular and extracellular compartments of a cell are shown. The arrows represent regulation at the transcriptional or post translational levels, with the broken arrows representing effects that are not yet verified in flies but have a precedent in vertebrates. Upon ligand (Egr) binding to the transmembrane TNF receptor (Wgn), trimerization of the receptor occurs, facilitating the recruitment of a signalling complex to the intracellular part of the receptor. Only Traf1 is shown in this instance to be recruited, mainly because the identities of other molecules recruited is not known in flies. Traf1 then binds the Ste20 MAP4Kinase Msn and activates the JNK signalling cascade. The effects studied here during wing development and gastrulation could be mediated via JNK signalling or via an as yet unidentified JNK independent Msn dependent or independent pathway. The predicted effects of activation of the different possible pathways are also represented. It is also known that DIAP1 or Thread, an inhibitor of apoptosis protein ubiquitinates Traf1 to target it for degradation. Further, transcriptional regulation of Traf1 is mediated by Twist and possibly Dorsal. The model has utilized data from other sources as well as our own observations.

4.5 Conclusions

The study presented here was aimed at mapping, identifying and characterizing the locus/loci involved in gastrulation, in the cytogenetic interval 24-25. Detailed genetic analysis of the region led to the conclusion that at least two genetically separable maternal loci and one zygotic locus contribute to the observed gastrulation defects. Preliminary evidence suggests that the zygotic locus and one of the maternal loci might be one and the same although detailed analysis is required to confirm this. All of the loci were narrowed down to short genomic stretches of 15-20 Kb each and further studies are required to pinpoint the genes responsible for the maternal effects.

Traf1 was identified as the most likely candidate gene responsible for the zygotic effect observed although analysis of a null mutant is essential to verify this. Detailed analysis of *Traf1* was carried out to understand the signalling cascade involving Traf1 and its role in gastrulation. This led to the finding that the defects observed with respect to Traf1 might be mediated through the JNK signalling cascade or through a novel, JNK independent mechanism. Future investigations in this regard, mainly experiments to understand the cellular processes affected in Traf1 null or overexpressing situations are required to distinguish between these possibilities and thus, to understand the role of Traf1 in *Drosophila* morphogenesis.

5. Bibliography

Abell, A. N. and Johnson, G. L. (2005). MEKK4 is an effector of the embryonic TRAF4 for JNK activation. *J Biol Chem* **280**, 35793-6.

Adachi-Yamada, T., Fujimura-Kamada, K., Nishida, Y. and Matsumoto, K. (1999). Distortion of proximodistal information causes JNK-dependent apoptosis in Drosophila wing. *Nature* **400**, 166-9.

Adachi-Yamada, T. and O'Connor, M. B. (2002). Morphogenetic apoptosis: a mechanism for correcting discontinuities in morphogen gradients. *Dev Biol* **251**, 74-90.

Agnes, F., Suzanne, M. and Noselli, S. (1999). The Drosophila JNK pathway controls the morphogenesis of imaginal discs during metamorphosis. *Development* **126**, 5453-62.

Ashburner, M. (1989). Drosophila - A laboratory handbook.: Cold Spring Harbor Laboratory Press.

Barrett, K., Leptin, M. and Settleman, J. (1997). The Rho GTPase and a putative RhoGEF mediate a signaling pathway for the cell shape changes in Drosophila gastrulation. *Cell* **91**, 905-15.

Baud, V. and Karin, M. (2001). Signal transduction by tumor necrosis factor and its relatives. *Trends Cell Biol* **11**, 372-7.

Bayer, C. A., Halsell, S. R., Fristrom, J. W., Kiehart, D. P. and von Kalm, L. (2003). Genetic interactions between the RhoA and Stubble-stubbloid loci suggest a role for a type II transmembrane serine protease in intracellular signaling during Drosophila imaginal disc morphogenesis. *Genetics* **165**, 1417-32.

Beiman, M., Shilo, B. Z. and Volk, T. (1996). Heartless, a Drosophila FGF receptor homolog, is essential for cell migration and establishment of several mesodermal lineages. *Genes Dev* **10**, 2993-3002.

Bellen, H. J., Levis, R. W., Liao, G., He, Y., Carlson, J. W., Tsang, G., Evans-Holm, M., Hiesinger, P. R., Schulze, K. L., Rubin, G. M. et al. (2004). The BDGP gene disruption project: single transposon insertions associated with 40% of Drosophila genes. *Genetics* **167**, 761-81.

Billuart, P., Winter, C. G., Maresh, A., Zhao, X. and Luo, L. (2001). Regulating axon branch stability: the role of p190 RhoGAP in repressing a retraction signaling pathway. *Cell* **107**, 195-207.

Blobel, C. P. (1997). Metalloprotease-disintegrins: links to cell adhesion and cleavage of TNF alpha and Notch. *Cell* **90**, 589-92.

Bloor, J. W. and Kiehart, D. P. (2002). Drosophila RhoA regulates the cytoskeleton and cell-cell adhesion in the developing epidermis. *Development* **129**, 3173-83.

Bradley, J. R. and Pober, J. S. (2001). Tumor necrosis factor receptor-associated factors (TRAFs). *Oncogene* **20**, 6482-91.

Brand, A. H. and Perrimon, N. (1993). Targeted gene expression as a means of altering cell fates and generating dominant phenotypes. *Development* **118**, 401-15.

Bryant, P. J., Huettner, B., Held, L. I., Jr., Ryerse, J. and Szidonya, J. (1988). Mutations at the fat locus interfere with cell proliferation control and epithelial morphogenesis in Drosophila. *Dev Biol* **129**, 541-54.

Campos-Ortega, J. A. and Hartenstein, V. (1985). The Embryonic Development of Drosophila melanogaster: Springer, Berlin.

Carthew, R. W. (2001). Gene silencing by double-stranded RNA. *Curr Opin Cell Biol* **13**, 244-8.

Casal, J. and Leptin, M. (1996). Identification of novel genes in Drosophila reveals the complex regulation of early gene activity in the mesoderm. *Proc Natl Acad Sci U S A* **93**, 10327-32.

Cha, G. H., Cho, K. S., Lee, J. H., Kim, M., Kim, E., Park, J., Lee, S. B. and Chung, J. (2003). Discrete functions of TRAF1 and TRAF2 in Drosophila melanogaster mediated by c-Jun N-terminal kinase and NF-kappaB-dependent signaling pathways. *Mol Cell Biol* **23**, 7982-91.

Chen, W., White, M. A. and Cobb, M. H. (2002). Stimulus-specific requirements for MAP3 kinases in activating the JNK pathway. *J Biol Chem* **277**, 49105-10.

Chi, H., Sarkisian, M. R., Rakic, P. and Flavell, R. A. (2005). Loss of mitogen-activated protein kinase kinase kinase 4 (MEKK4) results in enhanced apoptosis and defective neural tube development. *Proc Natl Acad Sci U S A* **102**, 3846-51.

Chung, J. Y., Park, Y. C., Ye, H. and Wu, H. (2002). All TRAFs are not created equal: common and distinct molecular mechanisms of TRAF-mediated signal transduction. *J Cell Sci* **115**, 679-88.

Costa, M., Wilson, E. T. and Wieschaus, E. (1994). A putative cell signal encoded by the folded gastrulation gene coordinates cell shape changes during Drosophila gastrulation. *Cell* **76**, 1075-89.

Curry. (1941). The mutant dwarf-24F 2-13.5+/- which is included in two overlapping deficiencies. *D. I. S.* **14**, 49-50.

Davis, R. J. (2000). Signal transduction by the JNK group of MAP kinases. *Cell* **103**, 239-52.

Dawes-Hoang, R. E., Parmar, K. M., Christiansen, A. E., Phelps, C. B., Brand, A. H. and Wieschaus, E. F. (2005). folded gastrulation, cell shape change and the control of myosin localization. *Development* **132**, 4165-78.

Dempsey, P. W., Doyle, S. E., He, J. Q. and Cheng, G. (2003). The signaling adaptors and pathways activated by TNF superfamily. *Cytokine Growth Factor Rev* **14**, 193-209.

Frasch, M. and Levine, M. (1987). Complementary patterns of even-skipped and fushi tarazu expression involve their differential regulation by a common set of segmentation genes in Drosophila. *Genes Dev* **1**, 981-95.

Gallo, K. A. and Johnson, G. L. (2002). Mixed-lineage kinase control of JNK and p38 MAPK pathways. *Nat Rev Mol Cell Biol* **3**, 663-72.

Ganguly, A., Jiang, J. and Ip, Y. T. (2005). Drosophila WntD is a target and an inhibitor of the Dorsal/Twist/Snail network in the gastrulating embryo. *Development* **132**, 3419-29.

Geuking, P., Narasimamurthy, R. and Basler, K. (2005). A Genetic Screen Targeting the TNF/Eiger Signaling Pathway: Identification of Drosophila TAB2 as a Functionally Conserved Component. *Genetics*.

Glauner, H., Siegmund, D., Motejadded, H., Scheurich, P., Henkler, F., Janssen, O. and Wajant, H. (2002). Intracellular localization and transcriptional regulation of tumor necrosis factor (TNF) receptor-associated factor 4 (TRAF4). *Eur J Biochem* **269**, 4819-29.

Golic, K. G. and Golic, M. M. (1996). Engineering the Drosophila genome: chromosome rearrangements by design. *Genetics* **144**, 1693-711.

Gong, W. J. and Golic, K. G. (2003). Ends-out, or replacement, gene targeting in Drosophila. *Proc Natl Acad Sci U S A* **100**, 2556-61.

Gong, W. J. and Golic, K. G. (2004). Genomic deletions of the Drosophila melanogaster Hsp70 genes. *Genetics* **168**, 1467-76.

Gordon, M. D., Dionne, M. S., Schneider, D. S. and Nusse, R. (2005). WntD is a feedback inhibitor of Dorsal/NF-kappaB in Drosophila development and immunity. *Nature* **437**, 746-9.

Grace, D. (1980). Genetic analysis of the dumpy complex locus in Drosophila melanogaster: complementation, fine structure and function. *Genetics* **94**, 647-62.

Grau, Y., C. Carteret, and P. Simpson. (1984). Muatations and chromosomal rearrangements affecting the expression of *snail*, a gene involved in embryonic patterning in *Drosophila melanogaster*. *Genetics* **108**, 347-360.

Grech, A., Quinn, R., Srinivasan, D., Badoux, X. and Brink, R. (2000). Complete structural characterisation of the mammalian and Drosophila TRAF genes: implications for TRAF evolution and the role of RING finger splice variants. *Mol Immunol* **37**, 721-34.

Greig, S. and Akam, M. (1993). Homeotic genes autonomously specify one aspect of pattern in the Drosophila mesoderm. *Nature* **362**, 630-2.

Grosshans, J., Muller, H. A. and Wieschaus, E. (2003). Control of cleavage cycles in Drosophila embryos by fruhstart. *Dev Cell* **5**, 285-94.

Grosshans, J. and Wieschaus, E. (2000). A genetic link between morphogenesis and cell division during formation of the ventral furrow in Drosophila. *Cell* **101**, 523-31.

Gurdon, J. B. (2005). Sinistral Snails and Gentlemen Scientists. *Cell* **123**, 751-753.

Hacker, U. and Perrimon, N. (1998). DRhoGEF2 encodes a member of the Dbl family of oncogenes and controls cell shape changes during gastrulation in Drosophila. *Genes Dev* **12**, 274-84.

Hampoelz, B., Hoeller, O., Bowman, S. K., Dunican, D. and Knoblich, J. A. (2005). Drosophila Ric-8 is essential for plasma-membrane localization of heterotrimeric G proteins. *Nat Cell Biol*.

Hipfner, D. R., Keller, N. and Cohen, S. M. (2004). Slik Sterile-20 kinase regulates Moesin activity to promote epithelial integrity during tissue growth. *Genes Dev* **18**, 2243-8.

Hoang, R. and Wieschaus, E. (1999). The control of cell shape changes during ventral furrow formation. *A. Dros. Res. Conf.,* **40**, 314A.

Hunter, C. and Wieschaus, E. (2000). Regulated expression of nullo is required for the formation of distinct apical and basal adherens junctions in the Drosophila blastoderm. *J Cell Biol* **150**, 391-401.

Igaki, T., Kanda, H., Yamamoto-Goto, Y., Kanuka, H., Kuranaga, E., Aigaki, T. and Miura, M. (2002). Eiger, a TNF superfamily ligand that triggers the Drosophila JNK pathway. *Embo J* **21**, 3009-18.

Ip, Y. T., Maggert, K. and Levine, M. (1994). Uncoupling gastrulation and mesoderm differentiation in the Drosophila embryo. *Embo J* **13**, 5826-34.

Jiang, J. and Levine, M. (1993). Binding affinities and cooperative interactions with bHLH activators delimit threshold responses to the dorsal gradient morphogen. *Cell* **72**, 741-52.

Kaltschmidt, J. A., Lawrence, N., Morel, V., Balayo, T., Fernandez, B. G., Pelissier, A., Jacinto, A. and Martinez Arias, A. (2002). Planar polarity and actin dynamics in the epidermis of Drosophila. *Nat Cell Biol* **4**, 937-44.

Kam, Z., Minden, J. S., Agard, D. A., Sedat, J. W. and Leptin, M. (1991). Drosophila gastrulation: analysis of cell shape changes in living embryos by three-dimensional fluorescence microscopy. *Development* **112**, 365-70.

Kanda, H., Igaki, T., Kanuka, H., Yagi, T. and Miura, M. (2002). Wengen, a member of the Drosophila tumor necrosis factor receptor superfamily, is required for Eiger signaling. *J Biol Chem* **277**, 28372-5.

Kasai, Y., Nambu, J. R., Lieberman, P. M. and Crews, S. T. (1992). Dorsal-ventral patterning in Drosophila: DNA binding of snail protein to the single-minded gene. *Proc Natl Acad Sci U S A* **89**, 3414-8.

Kauppila, S., Maaty, W. S., Chen, P., Tomar, R. S., Eby, M. T., Chapo, J., Chew, S., Rathore, N., Zachariah, S., Sinha, S. K. et al. (2003). Eiger and its receptor, Wengen, comprise a TNF-like system in Drosophila. *Oncogene* **22**, 4860-7.

Kockel, L., Homsy, J. G. and Bohmann, D. (2001). Drosophila AP-1: lessons from an invertebrate. *Oncogene* **20**, 2347-64.

Kosman, D., Ip, Y. T., Levine, M. and Arora, K. (1991). Establishment of the mesoderm-neuroectoderm boundary in the Drosophila embryo. *Science* **254**, 118-22.

Kuranaga, E., Kanuka, H., Igaki, T., Sawamoto, K., Ichijo, H., Okano, H. and Miura, M. (2002). Reaper-mediated inhibition of DIAP1-induced DTRAF1 degradation results in activation of JNK in Drosophila. *Nat Cell Biol* **4**, 705-10.

Lecuit, T. (2004). Junctions and vesicular trafficking during Drosophila cellularization. *J Cell Sci* **117**, 3427-33.

Lee, S. B., Cho, K. S., Kim, E. and Chung, J. (2003). blistery encodes Drosophila tensin protein and interacts with integrin and the JNK signaling pathway during wing development. *Development* **130**, 4001-10.

Leo, E., Welsh, K., Matsuzawa, S., Zapata, J. M., Kitada, S., Mitchell, R. S., Ely, K. R. and Reed, J. C. (1999). Differential requirements for tumor necrosis factor receptor-associated factor family proteins in CD40-mediated induction of NF-kappaB and Jun N-terminal kinase activation. *J Biol Chem* **274**, 22414-22.

Leptin, M. (1991). twist and snail as positive and negative regulators during Drosophila mesoderm development. *Genes Dev* **5**, 1568-76.

Leptin, M. (1999). Gastrulation in Drosophila: the logic and the cellular mechanisms. *Embo J* **18**, 3187-92.

Leptin, M. (2005). Gastrulation movements: the logic and the nuts and bolts. *Dev Cell* **8**, 305-20.

Leptin, M. and Grunewald, B. (1990). Cell shape changes during gastrulation in Drosophila. *Development* **110**, 73-84.

Lindsley, D. L. and Zimm, G. G. (1992). The genome of *Drosophila melanogaster*.

Liu, H., Su, Y. C., Becker, E., Treisman, J. and Skolnik, E. Y. (1999). A Drosophila TNF-receptor-associated factor (TRAF) binds the ste20 kinase Misshapen and activates Jun kinase. *Curr Biol* **9**, 101-4.

Magie, C. R., Meyer, M. R., Gorsuch, M. S. and Parkhurst, S. M. (1999). Mutations in the Rho1 small GTPase disrupt morphogenesis and segmentation during early Drosophila development. *Development* **126**, 5353-64.

Martin-Blanco, E., Gampel, A., Ring, J., Virdee, K., Kirov, N., Tolkovsky, A. M. and Martinez-Arias, A. (1998). puckered encodes a phosphatase that mediates a feedback loop regulating JNK activity during dorsal closure in Drosophila. *Genes Dev* **12**, 557-70.

Martin, P. and Parkhurst, S. M. (2004). Parallels between tissue repair and embryo morphogenesis. *Development* **131**, 3021-34.

Mata, J., Curado, S., Ephrussi, A. and Rorth, P. (2000). Tribbles coordinates mitosis and morphogenesis in Drosophila by regulating string/CDC25 proteolysis. *Cell* **101**, 511-22.

Merrill, P. T., Sweeton, D. and Wieschaus, E. (1988). Requirements for autosomal gene activity during precellular stages of Drosophila melanogaster. *Development* **104**, 495-509.

Miller, K. G., Field, C. M. and Alberts, B. M. (1989). Actin-binding proteins from Drosophila embryos: a complex network of interacting proteins detected by F-actin affinity chromatography. *J Cell Biol* **109**, 2963-75.

Mlodzik, M. (2002). Planar cell polarization: do the same mechanisms regulate Drosophila tissue polarity and vertebrate gastrulation? *Trends Genet* **18**, 564-71.

Moreno, E., Yan, M. and Basler, K. (2002). Evolution of TNF signaling mechanisms: JNK-dependent apoptosis triggered by Eiger, the Drosophila homolog of the TNF superfamily. *Curr Biol* **12**, 1263-8.

Morize, P., Christiansen, A. E., Costa, M., Parks, S. and Wieschaus, E. (1998). Hyperactivation of the folded gastrulation pathway induces specific cell shape changes. *Development* **125**, 589-97.

Moussian, B. and Roth, S. (2005). Dorsoventral axis formation in the Drosophila embryo--shaping and transducing a morphogen gradient. *Curr Biol* **15**, R887-99.

Muller, H., Samanta, R. and Wieschaus, E. (1999). Wingless signaling in the Drosophila embryo: zygotic requirements and the role of the frizzled genes. *Development* **126**, 577-86.

Munzert, G., Kirchner, D., Stobbe, H., Bergmann, L., Schmid, R. M., Dohner, H. and Heimpel, H. (2002). Tumor necrosis factor receptor-associated factor 1 gene overexpression in B-cell chronic lymphocytic leukemia: analysis of NF-kappa B/Rel-regulated inhibitors of apoptosis. *Blood* **100**, 3749-56.

Nabel-Rosen, H., Toledano-Katchalski, H., Volohonsky, G. and Volk, T. (2005). Cell divisions in the drosophila embryonic mesoderm are repressed via posttranscriptional regulation of string/cdc25 by HOW. *Curr Biol* **15**, 295-302.

Nambu, J. R., Franks, R. G., Hu, S. and Crews, S. T. (1990). The single-minded gene of Drosophila is required for the expression of genes important for the development of CNS midline cells. *Cell* **63**, 63-75.

Nibu, Y., Zhang, H., Bajor, E., Barolo, S., Small, S. and Levine, M. (1998). dCtBP mediates transcriptional repression by Knirps, Kruppel and Snail in the Drosophila embryo. *Embo J* **17**, 7009-20.

Nikolaidou, K. K. and Barrett, K. (2004). A Rho GTPase signaling pathway is used reiteratively in epithelial folding and potentially selects the outcome of Rho activation. *Curr Biol* **14**, 1822-6.

Nusslein-Volhard, C., E. Wieschaus, and H. Kluding. (1984). Mutations affecting the pattern of the larval cuticle in *Drosophila melanogaster*. I. Zygotic loci on the second chromosome. *Wilhelm Roux's Arch. Dev. Biol* **193**, 267-282.

Nusslein-Volhard, C., Lohs-Schardin, M., Sander, K. and Cremer, C. (1980). A dorso-ventral shift of embryonic primordia in a new maternal-effect mutant of Drosophila. *Nature* **283**, 474-6.

Nusslein-Volhard, C. and Wieschaus, E. (1980). Mutations affecting segment number and polarity in Drosophila. *Nature* **287**, 795-801.

Oda, H. and Tsukita, S. (2001). Real-time imaging of cell-cell adherens junctions reveals that Drosophila mesoderm invagination begins with two phases of apical constriction of cells. *J Cell Sci* **114**, 493-501.

Odell, G. M., Oster, G., Alberch, P. and Burnside, B. (1981). The mechanical basis of morphogenesis. I. Epithelial folding and invagination. *Dev Biol* **85**, 446-62.

Oh, S. W., Kingsley, T., Shin, H. H., Zheng, Z., Chen, H. W., Chen, X., Wang, H., Ruan, P., Moody, M. and Hou, S. X. (2003). A P-element insertion screen identified mutations in 455 novel essential genes in Drosophila. *Genetics* **163**, 195-201.

Paricio, N., Feiguin, F., Boutros, M., Eaton, S. and Mlodzik, M. (1999). The Drosophila STE20-like kinase misshapen is required downstream of the Frizzled receptor in planar polarity signaling. *Embo J* **18**, 4669-78.

Parkhurst, S. M. and Ish-Horowicz, D. (1991). wimp, a dominant maternal-effect mutation, reduces transcription of a specific subset of segmentation genes in Drosophila. *Genes Dev* **5**, 341-57.

Parks, S. and Wieschaus, E. (1991). The Drosophila gastrulation gene concertina encodes a G alpha-like protein. *Cell* **64**, 447-58.

Pastor-Pareja, J. C., Grawe, F., Martin-Blanco, E. and Garcia-Bellido, A. (2004). Invasive cell behavior during Drosophila imaginal disc eversion is mediated by the JNK signaling cascade. *Dev Cell* **7**, 387-99.

Preiss, A., Johannes, B., Nagel, A. C., Maier, D., Peters, N. and Wajant, H. (2001). Dynamic expression of Drosophila TRAF1 during embryogenesis and larval development. *Mech Dev* **100**, 109-13.

Rasmussen, I. (1960). Attached 2R:2L0. *Dros. Information Serv*, 53.

Regnier, C. H., Masson, R., Kedinger, V., Textoris, J., Stoll, I., Chenard, M. P., Dierich, A., Tomasetto, C. and Rio, M. C. (2002). Impaired neural tube closure, axial skeleton malformations, and tracheal ring disruption in TRAF4-deficient mice. *Proc Natl Acad Sci U S A* **99**, 5585-90.

Reuter, R. and Casal, J. (1994). Gastrulation in Drosophila. *Sem Dev Biol* **5**, 111-119.

Reuter, R. and Leptin, M. (1994). Interacting functions of snail, twist and huckebein during the early development of germ layers in Drosophila. *Development* **120**, 1137-50.

Rong, Y. S. and Golic, K. G. (2000). Gene targeting by homologous recombination in Drosophila. *Science* **288**, 2013-8.

Rorth, P. (1996). A modular misexpression screen in Drosophila detecting tissue-specific phenotypes. *Proc Natl Acad Sci U S A* **93**, 12418-22.

Rosenberg, M. I. and Parkhurst, S. M. (2002). Drosophila Sir2 is required for heterochromatic silencing and by euchromatic Hairy/E(Spl) bHLH repressors in segmentation and sex determination. *Cell* **109**, 447-58.

Roth, S., Stein, D. and Nusslein-Volhard, C. (1989). A gradient of nuclear localization of the dorsal protein determines dorsoventral pattern in the Drosophila embryo. *Cell* **59**, 1189-202.

Rubin, G. M. and Spradling, A. C. (1982). Genetic transformation of Drosophila with transposable element vectors. *Science* **218**, 348-53.

Ryder, E., Blows, F., Ashburner, M., Bautista-Llacer, R., Coulson, D., Drummond, J., Webster, J., Gubb, D., Gunton, N., Johnson, G. et al. (2004). The DrosDel collection: a set of P-element insertions for generating custom chromosomal aberrations in Drosophila melanogaster. *Genetics* **167**, 797-813.

Ryoo, H. D., Gorenc, T. and Steller, H. (2004). Apoptotic cells can induce compensatory cell proliferation through the JNK and the Wingless signaling pathways. *Dev Cell* **7**, 491-501.

Sambrook, J., Fritsch, E. F. and Maniatis, T. (1989). Molecular Cloning A Laboratory Manual.

Seher, T. C. and Leptin, M. (2000). Tribbles, a cell-cycle brake that coordinates proliferation and morphogenesis during Drosophila gastrulation. *Curr Biol* **10**, 623-9.

Shen, B., Liu, H., Skolnik, E. Y. and Manley, J. L. (2001). Physical and functional interactions between Drosophila TRAF2 and Pelle kinase contribute to Dorsal activation. *Proc Natl Acad Sci U S A* **98**, 8596-601.

Shiels, H., Li, X., Schumacker, P. T., Maltepe, E., Padrid, P. A., Sperling, A., Thompson, C. B. and Lindsten, T. (2000). TRAF4 deficiency leads to tracheal malformation with resulting alterations in air flow to the lungs. *Am J Pathol* **157**, 679-88.

Shishido, E., Higashijima, S., Emori, Y. and Saigo, K. (1993). Two FGF-receptor homologues of Drosophila: one is expressed in mesodermal primordium in early embryos. *Development* **117**, 751-61.

Simpson, P. (1983). Maternal-zygotic gene interactions during formation of the dorsoventral pattern in *Drosophila* embryos. *Genetics* **105**, 615-632.

Sonnenblick, B. P. (1950). The early embryology of Drosophila melanogaster. *Demerec, M. (editor). Biology of Drosophila*, 62-167.

Speck, O., Hughes, S. C., Noren, N. K., Kulikauskas, R. M. and Fehon, R. G. (2003). Moesin functions antagonistically to the Rho pathway to maintain epithelial integrity. *Nature* **421**, 83-7.

Spradling, A. C. and Rubin, G. M. (1982). Transposition of cloned P elements into Drosophila germ line chromosomes. *Science* **218**, 341-7.

Stathopoulos, A. and Levine, M. (2002A). Dorsal gradient networks in the Drosophila embryo. *Dev Biol* **246**, 57-67.

Stathopoulos, A. and Levine, M. (2002B). Linear signaling in the Toll-Dorsal pathway of Drosophila: activated Pelle kinase specifies all threshold outputs of gene expression while the bHLH protein Twist specifies a subset. *Development* **129**, 3411-9.

Stathopoulos, A., Van Drenth, M., Erives, A., Markstein, M. and Levine, M. (2002C). Whole-genome analysis of dorsal-ventral patterning in the Drosophila embryo. *Cell* **111**, 687-701.

Stern, C. D. (2004). Gastrulation: from cells to embryo. Cold Spring Harbor, N.Y.: Cold Spring Harbor Laboratory Press.

Strutt, D. I., Weber, U. and Mlodzik, M. (1997). The role of RhoA in tissue polarity and Frizzled signalling. *Nature* **387**, 292-5.

Su, Y. C., Maurel-Zaffran, C., Treisman, J. E. and Skolnik, E. Y. (2000). The Ste20 kinase misshapen regulates both photoreceptor axon targeting and dorsal closure, acting downstream of distinct signals. *Mol Cell Biol* **20**, 4736-44.

Su, Y. C., Treisman, J. E. and Skolnik, E. Y. (1998). The Drosophila Ste20-related kinase misshapen is required for embryonic dorsal closure and acts through a JNK MAPK module on an evolutionarily conserved signaling pathway. *Genes Dev* **12**, 2371-80.

Sweeton, D., Parks, S., Costa, M. and Wieschaus, E. (1991). Gastrulation in Drosophila: the formation of the ventral furrow and posterior midgut invaginations. *Development* **112**, 775-89.

Szidonya, J. and Reuter, G. (1988). Cytogenetic analysis of the echinoid (ed), dumpy (dp) and clot (cl) region in Drosophila melanogaster. *Genet. Res* **51**, 197-208.

Tautz, D. and Pfeifle, C. (1989). A non-radioactive in situ hybridization method for the localization of specific RNAs in Drosophila embryos reveals translational control of the segmentation gene hunchback. *Chromosoma* **98**, 81-5.

Thibault, S. T., Singer, M. A., Miyazaki, W. Y., Milash, B., Dompe, N. A., Singh, C. M., Buchholz, R., Demsky, M., Fawcett, R., Francis-Lang, H. L. et al. (2004). A complementary transposon tool kit for Drosophila melanogaster using P and piggyBac. *Nat Genet* **36**, 283-7.

Thisse, B., el Messal, M. and Perrin-Schmitt, F. (1987). The twist gene: isolation of a Drosophila zygotic gene necessary for the establishment of dorsoventral pattern. *Nucleic Acids Res* **15**, 3439-53.

Treisman, J. E., Ito, N. and Rubin, G. M. (1997). misshapen encodes a protein kinase involved in cell shape control in Drosophila. *Gene* **186**, 119-25.

Tseng, A. S. and Hariharan, I. K. (2002). An overexpression screen in Drosophila for genes that restrict growth or cell-cycle progression in the developing eye. *Genetics* **162**, 229-43.

Underwood, E. M., Briot, A. S., Doll, K. Z., Ludwiczak, R. L., Otteson, D. C., Tower, J., Vessey, K. B. and Yu, K. (1990). Genetics of 51D-52A, a region containing several maternal-effect genes and two maternal-specific transcripts in Drosophila. *Genetics* **126**, 639-50.

Varfolomeev, E. E. and Ashkenazi, A. (2004). Tumor necrosis factor: an apoptosis JuNKie? *Cell* **116**, 491-7.

Vincent, A., Blankenship, J. T. and Wieschaus, E. (1997). Integration of the head and trunk segmentation systems controls cephalic furrow formation in Drosophila. *Development* **124**, 3747-54.

Vincent, S., Wilson, R., Coelho, C., Affolter, M. and Leptin, M. (1998). The Drosophila protein Dof is specifically required for FGF signaling. *Mol Cell* **2**, 515-25.

Wajant, H., Henkler, F. and Scheurich, P. (2001). The TNF-receptor-associated factor family: scaffold molecules for cytokine receptors, kinases and their regulators. *Cell Signal* **13**, 389-400.

Wang, C. Y., Mayo, M. W., Korneluk, R. G., Goeddel, D. V. and Baldwin, A. S., Jr. (1998). NF-kappaB antiapoptosis: induction of TRAF1 and TRAF2 and c-IAP1 and c-IAP2 to suppress caspase-8 activation. *Science* **281**, 1680-3.

Wang, F., Dumstrei, K., Haag, T. and Hartenstein, V. (2004). The role of DE-cadherin during cellularization, germ layer formation and early neurogenesis in the Drosophila embryo. *Dev Biol* **270**, 350-63.

Weston, C. R. and Davis, R. J. (2002). The JNK signal transduction pathway. *Curr Opin Genet Dev* **12**, 14-21.

Wieschaus, E. and Sweeton, D. (1988). Requirements for X-linked zygotic gene activity during cellularization of early Drosophila embryos. *Development* **104**, 483-93.

Xia, Y. and Karin, M. (2004). The control of cell motility and epithelial morphogenesis by Jun kinases. *Trends Cell Biol* **14**, 94-101.

Xie, H. B. and Golic, K. G. (2004). Gene deletions by ends-in targeting in Drosophila melanogaster. *Genetics* **168**, 1477-89.

Xu, Y. C., Wu, R. F., Gu, Y., Yang, Y. S., Yang, M. C., Nwariaku, F. E. and Terada, L. S. (2002). Involvement of TRAF4 in oxidative activation of c-Jun N-terminal kinase. *J Biol Chem* **277**, 28051-7.

Xue, Y., Wang, X., Li, Z., Gotoh, N., Chapman, D. and Skolnik, E. Y. (2001). Mesodermal patterning defect in mice lacking the Ste20 NCK interacting kinase (NIK). *Development* **128**, 1559-72.

Zapata, J. M. (2003). TNF-receptor-associated factors as targets for drug development. *Expert Opin Ther Targets* **7**, 411-25.

Zapata, J. M., Matsuzawa, S., Godzik, A., Leo, E., Wasserman, S. A. and Reed, J. C. (2000). The Drosophila tumor necrosis factor receptor-associated factor-1 (DTRAF1) interacts with Pelle and regulates NFkappaB activity. *J Biol Chem* **275**, 12102-7.

Zusman, S. B. and Wieschaus, E. F. (1985). Requirements for zygotic gene activity during gastrulation in Drosophila melanogaster. *Dev Biol* **111**, 359-71.

6. Appendix

6.1 Molecular mapping of deficiencies by Single Embryo PCR

To precisely localize the break points of the deficiencies of interest, single embryo PCR, using embryos from the respective deficiencies were performed, with sequences from genes in the vicinity of the predicted break points used as primers. The protocol used for the single embryo PCR and the primer sequences used are given in the Materials and Methods section. The relative positions of the primer sequences are represented in Figure 33 by the blue arrowheads.

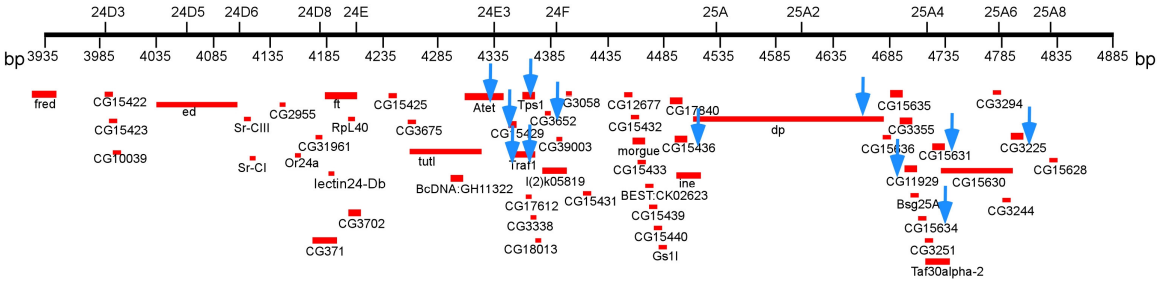

Figure 33: Detailed map of the region 24D-25B. This map is drawn to scale, representing both the cytogenetic divisions (24D3-25A8) and the nucleotide number (3935 – 4885) in terms of kilobase pairs from the beginning of the left arm of the second chromosome. The genes are represented as red bars with the respective name below and the relative positions of the primer pairs used for PCR mapping are marked by the position of the blue arrowheads.

In all of the agarose gel electrophoresis photographs shown henceforth, the 10kb DNA ladder is in the left most lane; the primer pairs used are labelled with white arrowheads towards the left of each picture and the horizontal lines above the picture, with a number, represents a single embryo, which was used as the template for the respective PCR. Also, the mapping has been restricted to the left, right or both break points of the respective deficiency, depending on whether the break point is of consequence in narrowing down the genomic stretch responsible for the phenotype described before.

The idea used here is that, a quarter of the embryos from a cross within a heterozygous deficiency fly stock will be homozygous for the deficiency. These embryos will not yield a PCR band, if the primers used lie within the deleted region. A positive control, which is a pair of primers lying outside the deficiency and a negative control, which is a pair of primers for a gene known to lie within the deficiency are also used to show that the PCR worked. Ideally, the positive control should give a band in every case and the negative control should not in approximately a quarter of the cases.

6.2.1 Df(2L)ed-dp

In the case of Df(2L)ed-dp, only the right break point was mapped by PCR since the left break was not near the region of interest.

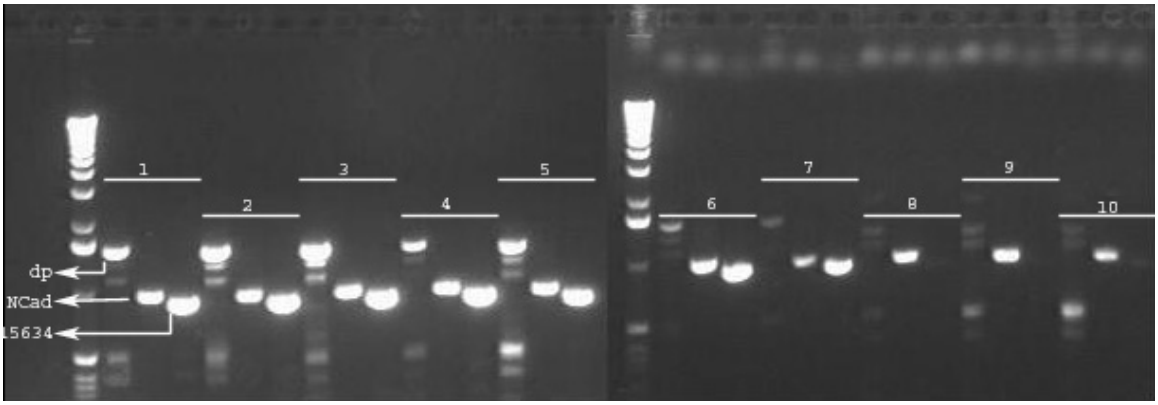

Figure 34: Single embryo PCR with primers for *dumpy* (dp), *N-Cadherin* (NCad) and CG15634 (15634), on Df(2L)ed-dp embryos. dp is the negative control here, NCad, the positive control and 15634 the candidate gene tested in this instance.

From Figure 34, it is clear that the deficiency Df(2L)ed-dp uncovers CG15634, as can be seen by an absence of PCR product in the case of embryos 8, 9 and 10, which generate no PCR products with primers for the gene dp but do for NCad, the positive control. It is evident from Figure 35 that Df(2L)ed-dp also uncovers CG15631 but not CG3225, as is the case in embryos 3 and 5 where the positive control (NCad) and CG3225 are PCR positive whereas the negative control(dp) and CG15631 are PCR negative. This shows that the right break point of the deficiency Df(2L)ed-dp maps to the genomic region between CG15631 and CG3225.

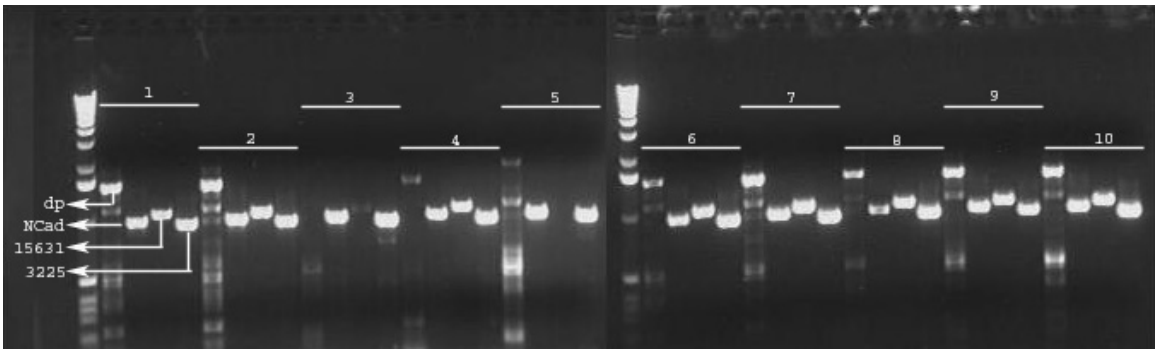

Figure 35: Single embryo PCR with primers for *dumpy* (dp), *N-Cadherin* (NCad), CG15631 (15631) and CG3225 (3225) on Df(2L)ed-dp embryos. dp is the negative control here, NCad, the positive control, 15631 and 3225 the candidate genes tested.

6.2.2 Df(2L)dp-h19

Both the right and left break points are of interest in the case of the deficiency Df(2L)dp-h19 as both break points might help in narrowing down the region where the gene of interest is located.

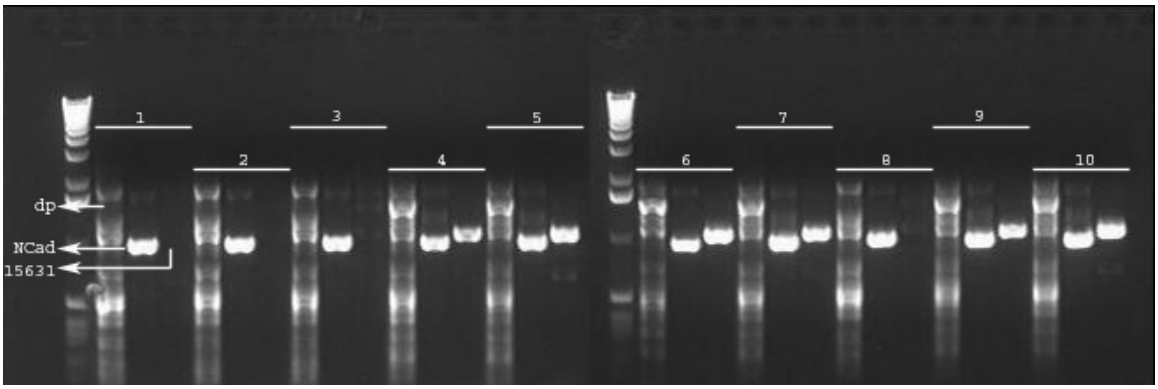

Figure 36: **Single embryo PCR with primers for *dumpy* (dp), *N-Cadherin* (NCad) and CG15631 (15631) on Df(2L)dp-h19 embryos.** dp is the negative control here, NCad, the positive control and 15631 the candidate gene tested.

From Figure 36 it is clear that the deficiency Df(2L)dp-h19 uncovers CG15631 from the absence of a PCR product in the case of embryos 1,2,3 and 8. It is also clear that Df(2L)dp-h19 is not uncovered for CG3225 as shown in Figure 37, embryos 2,6 and 9 where the negative control dp is PCR negative but CG3225 is positive. This shows that the right break point in the case of the deficiency Df(2L)dp-h19 also lies between CG15631 and CG3225.

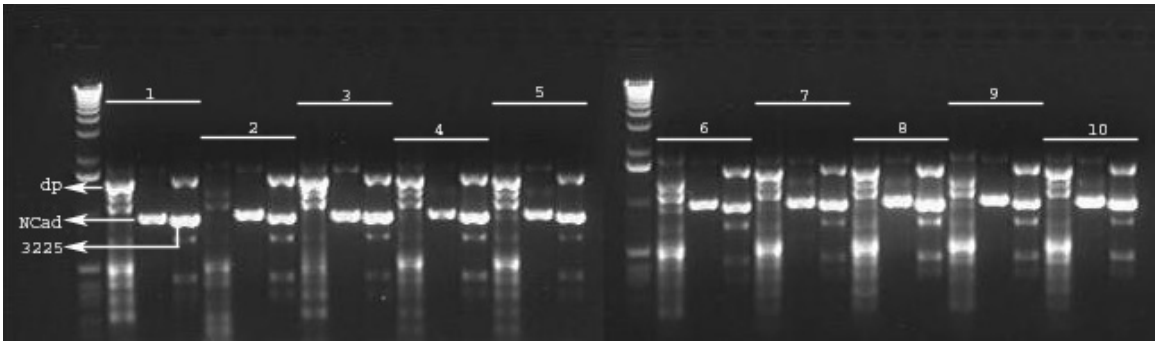

Figure 37: Single embryo PCR with primers for *dumpy* (dp), *N-Cadherin* (NCad) and CG3225 (3225) on Df(2L)dp-h19 embryos. dp is the negative control here, NCad, the positive control and 3225 the candidate gene tested.

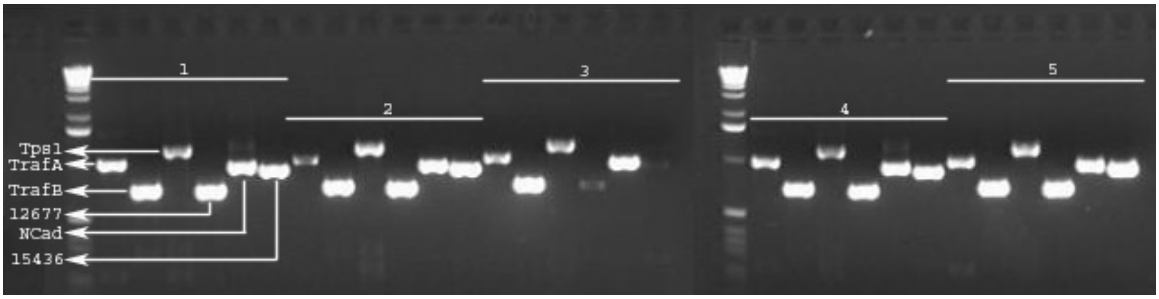

Figure 38: Single embryo PCR with primers for *Traf1* (TrafA and TrafB), Tps1 (Tps1), CG12677 (12677), *N-Cadherin* (NCad) and CG15436 (15436) on Df(2L)dp-h19 embryos. 15436 is the negative control here, NCad, the positive control, TrafA, TrafB, Tps1 and 12677 the candidate genes tested.

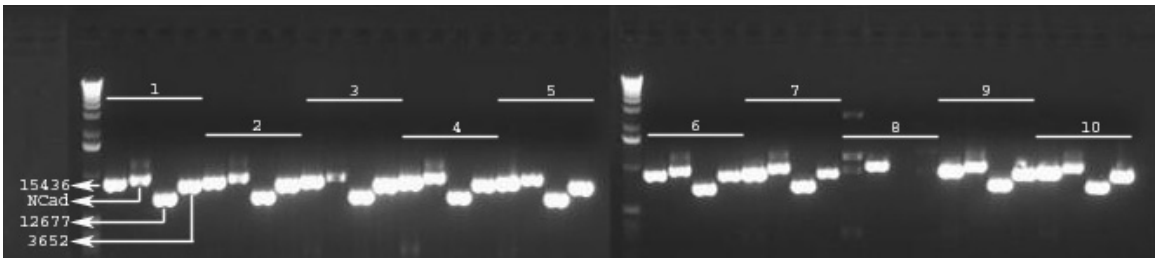

Figure 39: Single embryo PCR with primers for CG15436 (15436), *N-Cadherin* (NCad)), CG12677 (12677) and CG3652 (3652) on Df(2L)dp-h19 embryos. 15436 is the negative control here, NCad, the positive control, 12677 and 3652 the candidate genes tested.

From Figure 38, where single embryo PCR was performed on Df(2L)dp-h19 embryos with primers for the genes Traf1, Tps1, CG12677, predicted to be in close proximity to the left break point of this deficiency, positive (Ncad) and negative (15436) controls, it is clear that only CG12677 is deleted (Embryo 3). From Figure 39, where PCR was performed on the same embryos with primers for CG12677 and CG3652 along with the positive and negative controls, it is clear that CG3652 is also deleted in the deficiency Df(2L)dp-h19. This shows that the right break point of the deficiency Df(2L)dp-h19 lies in the interval between the genes CG3652 which is deleted and Tps1, which is not deleted.

6.2.3 Df(2L)dp-h25

The right break point of this deficiency was not of interest for narrowing down the region responsible for the phenotype, as this deficiency is known to extend beyond the right break point of the deficiencies described before, from genetic data (Bryant *et al.,* 1988). Single embryo PCRs were performed to confirm this and indeed the right break point of this deficiency extends beyond CG3225, which is a gene not deleted in the other deficiencies described so far.

The left break point of this deficiency is quite important in narrowing down the region responsible for the phenotype, as this is the smallest deficiency that shows the zygotic phenotype described before. The results of single embryo PCR performed with primers specific for the left break point region are shown in Figure 40.

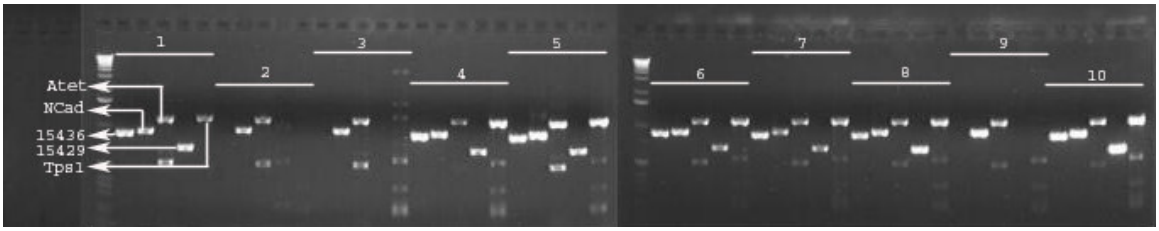

Figure 40: Single embryo PCR with primers for CG15436 (15436), *N-Cadherin* (NCad)), Atet (Atet), CG15429 (15429) and Tps1 (Tps1) on Df(2L)dp-h25 embryos. 15436 is the negative control here, NCad, the positive control, Atet, 15429 and Tps1 the candidate genes tested.

The primers for the genes Atet, CG15429 and Tps1, which lie close to the predicted left break point of the deficiency Df(2L)dp-h25 were used in this single embryo PCR (Figure 40), in conjunction with CG15436 as negative control and NCad as positive control. It can be seen in the case of embryos 2, 3 and 9 that when the negative control CG15436 does not give a product, CG15429 and Tps1 also fail to give a product showing that these two genes are deleted in this deficiency, whereas Atet gives a product in these three cases and is thus not deleted in this deficiency. This leads to the conclusion that the left break point of the deficiency Df(2L)dp-h25 lies between the genes CG15429 and Atet.

6.2.4 Df(2L)dp-h28

The left break point of this deficiency was not of interest in narrowing down the region responsible for the phenotype, as it extends beyond that of Df(2L)dp-h25, which is the shortest deficiency that exhibits the phenotype. The right breakpoint of this deficiency was also not of interest although experiments were done to confirm that the right break point was where it was predicted to be. Indeed the distal break point of Df(2L)dp-h28 was not uncovered for any of the genes for which primers were designed and single embryo PCR was performed, namely *dumpy*, CG11929 and CG3225, meaning that this break point is within *dumpy*, as this deficiency does not complement an allele of *dumpy*. Figure 41 shows PCR on single embryos of Df(2L)dp-h28 and is positive for primers for dumpy, positive control and CG15631. In embryos 9 and 10, CG15631 does not give a product but by further analysis, it was found that indeed this deficiency is not deleted for CG15631.

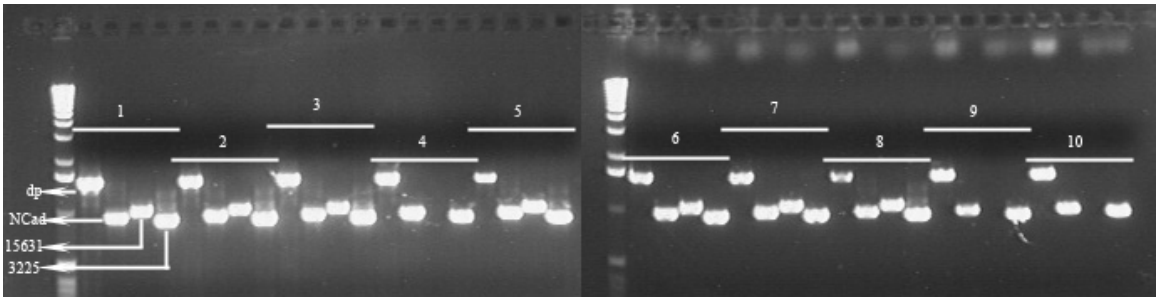

Figure 41: Single embryo PCR with primers for *dumpy* (dp), *N-Cadherin* (NCad) and CG15631 (15631), on Df(2L)dp-h28 embryos. dp is the negative control here, NCad, the positive control, 15631 and 3225 the candidate genes tested.

6.2.5 Df(2L)dp-h24

This was the smallest deficiency tested and was important initially, in order to exclude the region including and distal to *dumpy*, as being responsible for the phenotype. Both the left and right break points were mapped in the case of this deficiency, although, in final analysis, it was not important in narrowing down the phenotype as such, as Df(2L)dp-h19, uncovers the genomic stretch deleted in the case of Df(2L)dp-h24 and further proximally. The distal break point of Df(2L)dp-h24 was not uncovered for any of the genes for which primers were designed and single embryo PCR was performed, namely *dumpy*, CG11929 and CG3225 (data not shown). The proximal break point of this deficiency was narrowed down to between CG15436 which is uncovered and CG12677 which is not, as can be seen in embryos 3, 4 and 5 in Figure 42. The PCR bands for CG15436 in embryos 3, 4 and 5 do not correspond to the expected product size, which is exemplified in all the other cases.

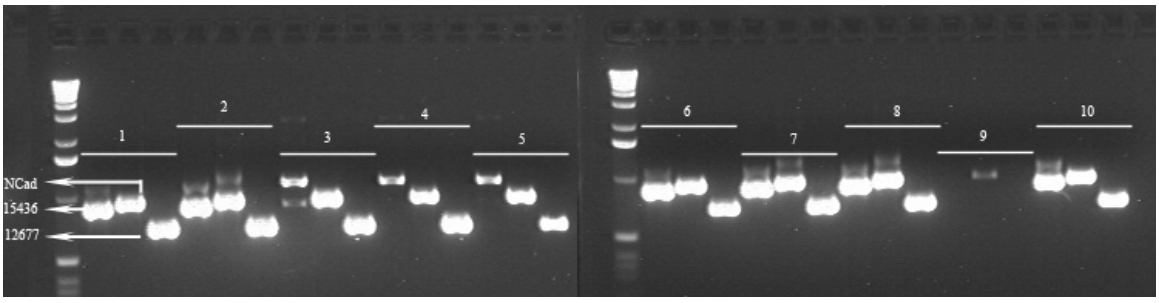

Figure 42: Single embryo PCR with primers for CG15436 (15436), *N-Cadherin* (NCad) and CG12677 (12677), on Df(2L)dp-h24 embryos. NCad, the positive control here, 15436 and 12677 the candidate genes tested. The PCR did not work for embryo 9.

Abbreviations

AEL	After Egg Laying
bp	base pairs
BDGP	Berkeley *Drosophila* Genome Project
BSA	Bovine Serum Albumen
bsk	*basket*
cta	*concertina*
C(2)V	Compound (2) vermilion
dNTP	deoxy nucleotide tri phosphate
EDTA	Ethylene Diamine Tetracetic acid
egr	*eiger*
fog	*folded gastrulation*
frs	*fruhstart*
g	gram
how	*held out wings*
hep	*hemipterous*
hkb	*huckebein*
JNK	Jun N-terminal Kinase
K	Kilo
Kb	Kilo base
M	mol per litre
m	milli
MAPK	Mitogen Activated Protein Kinase
Mat24F	Maternal effect locus at 24F
msn	*misshapen*
Mb	Mega base
µ	Micro
p	pico

Abbreviations

PCR	Polymerase Chain Reaction
puc	*puckered*
RhoGEF2	Rho Guanine Exchange Factor 2
RhoK	Rho Kinase
SEPCR	Single embryo PCR
sna	*snail*
stg	*string*
TNF	Tumour Necrotic Factor
TRAF	TNF Receptor Associated Factor
trbl	*tribbles*
twi	*twist*
wgn	*wengen*

Abstract

Gastrulation in Drosophila begins with ventral furrow formation. Although some genes required for ventral furrow formation have been known, it was evident that as yet unidentified genes were involved in this process. Thus, a screen to identify new loci involved in ventral furrow formation was performed previously, implicating the cytogenetic region 24-25 on the left arm of the second chromosome among other regions. In this study, further genetic analysis of this region was carried out to pinpoint and fine map the locus or loci in the 24-25 region that are responsible for the defect in ventral furrow formation. It was found that at least two genetically separable maternal loci and one zygotic locus were involved in the observed defects. Mapping of the different loci were carried out. The maternal loci were narrowed down to short genomic stretches of 15-20 Kb and a candidate gene for the zygotic effect, *Traf1* was identified. *Traf1* was identified based on the *Traf1* expression pattern. Later, it was found that *Traf1* is a Twist target and embryos from available hypomorphic alleles of *Traf1* exhibited defects in gastrulation. However, conclusive evidence in this regard requires a complete loss of function allele. Overexpression of Traf1 in the mesoderm also caused defective gastrulation, possibly mediated by the ability of Traf1 to activate the JNK signalling cascade. It was found that the gastrulation defects observed upon overexpression of Traf1 was not due to cell fate changes or abnormal cell division. Further investigations are required to identify the precise processes affected upon such overexpression that lead to gastrulation defects.

Zusammenfassung

Die Gastrulation in *Drosophila* beginnt mit der Bildung der Ventralfurche. Obgleich einige der an der Ventralfurchenbildung beteiligten Gene identifiziert werden konnten, müssen auch bisher noch nicht beschriebene Gene an diesem Prozess beteiligt sein. In einem vorangegangenen Screen zur Identifizierung weiterer an der Ventralfurchenbildung beteiligter Loci konnte neben anderen Regionen die zytogenetische Region 24-25 auf dem linken Arm des zweiten Chromosoms ermittelt werden. In der vorliegenden Arbeit wurden weitere genetische Analysen durchgeführt, um den Locus oder die Loci innerhalb der Region 24-25, die bei Verlust zu Defekten in der Ventralfurchenbildung führen, festzulegen und genau zu kartieren. Es konnte festgestellt werden, dass zumindest zwei genetisch unterschiedliche maternale Loci und ein zygotischer Locus an den beobachteten Defekten beteiligt sind. Es wurde eine detailierte Kartierung der unterschiedlichen Loci durchgeführt. Die maternalen Loci konnten auf einen genomischen Bereich von 15-20 Kb eingeengt werden. Für den zygotischen Effekt konnte als mögliches Gen *Traf1* ermittelt werden. *Traf1* wurde aufgrund des *Traf1*-Expressionsmusters, seiner transkriptionalen Regulation durch Twist und des Phänotyps, den Embryonen von hypomorphen *Traf1* Allelen aufweisen, identifiziert. Eine beweiskräftige Aussage erfordert jedoch den kompletten Verlust des funktionstragenden Allels. Überexpression von Traf1 im Mesoderm verursachte ebenfalls Defekte während der Gastrulation. Diese beruhen möglicherweise auf der Fähigkeit von Traf1 den JNK Signaltransduktionsweg zu aktivieren. Es konnte festgestellt werden, dass die durch Überexpression von Traf1 hervorgerufenen Defekte während der Gastrulation nicht auf Änderungen des Zellschicksals oder anormale Zellteilung zurückzuführen sind. Weitere Untersuchungen sind nötig, um den durch die Überexpression beeinflussten Prozess der zu Gastrulationsdefekten führt, zu identifizieren.

Acknowledgements

I would like to thank Prof. Maria Leptin in whose lab this work was carried out, for allowing me to work on an extremely interesting and challenging project. The constant support, inspiration and able guidance provided by Maria were of paramount importance during the course of the work. This project was initiated by a former graduate student, Thomas Seher and his help and insight during the early stages helped immensely. I would like to acknowledge all the members (present and several former) of the Leptin, Klein, Sprenger and Roth groups, who have been most forthcoming with reagents, technical expertise and suggestions, which helped no end. In addition, I thank Jayan Nair for his help with the manuscript, Cornelia Stein and Verena Koelsch for help in translation and Lisa Vogelsang, who generated several of the transgenic stocks which were used in the study. Further, I am grateful to the large number of scientists who provided reagents which were used in the study.

I would also like to acknowledge members (students, faculty and staff) of the Graduate School in Genetics and Functional Genomics, University of Cologne. A special word of thanks to my friends and colleagues from the first (2001) batch with whom I had a thoroughly enjoyable four years. I would also like to thank Dr. Brigitte von Wilcken Bergmann who spent a lot of her time and energy towards making things easier for many of us.

Finally, I thank my family and friends for their endless support and prayers which kept me motivated throughout.

Eidesstattliche Erklärung

Ich versichere, daß ich die von mir vorgelegte Dissertation selbständig angefertigt, die benutzten Quellen und Hilfsmittel vollständig angegeben und die Stellen der Arbeit - einschließlich Tabellen, Karten und Abbildungen -, die anderen Werken im Wortlaut oder dem Sinn nach entnommen sind, in jedem Einzelfall als Entlehnung kenntlich gemacht habe; daß diese Dissertation noch keiner anderen Fakultät oder Universität zur Prüfung vorgelegen hat; daß sie - abgesehen von unten angegebenen Teilpublikationen - noch nicht veröffentlicht worden ist sowie, daß ich eine solche Veröffentlichung vor Abschluß des Promotionsverfahrens nicht vornehmen werde. Die Bestimmungen dieser Promotionsordnung sind mir bekannt. Die von mir vorgelegte Dissertation ist von Prof. Dr. Maria Leptin betreut worden.

Keine Teilpublikationen

Köln,
Dezember 2005. **Sam Jacob Mathew**

Lebenslauf

Name:	Sam Jacob Mathew
Geburtsdatum:	28.03.1976
Geburtsort:	Kochi, Indien
Staatsangehoerigkeit:	Indisch

1990-1991	Gymnasium (ICSE), Kerala, Indien
1991-1993	Abitur (Pre Degree), Kerala, Indien
1993-1996	Bachelor of Science (B.Sc), Kerala University, Indien
1996-1998	(Diplom) Master of Science (M.Sc), M.G University, Indien
2000-2001	Junior Research Fellow Evolutionary and Organismal Biology Unit Jawaharlal Nehru Centre for Advanced Scientific Research Bangalore, Indien
2001-2005	Doktorarbeit bei Prof. Dr. Maria Leptin am Institut fuer genetik Universitaet zu Koeln Titel: “Identification and characterization of a genomic region involved in *Drosophila* gastrulation”.

Koeln

Dezember 2005 Unterschrift